Supporting Information

Self-assembly of Diphenylalanine-Peptide Nucleic Acid-conjugates

Dhrubajyoti Datta[a†]*, Omshanker Tiwari[a†] and Manoj Kumar Gupta[a]

[a]Department of Chemistry, Chemical Biology Unit, Indian Institute of Science Education and Research Pune, Dr. Homi Bhabha Road, Pune 411008, India

*Corresponding author
[†]Equal Contribution

Table of Contents

CF= Carboxyfluorescein; **Dox** = Doxorubicin; **SPPS** = Solid Phase Peptide Synthesis

Synthesis of PNA monomer for amide / click conjugation with Phe-Phe moiety in solution phase:

Boc protected aminoethylglycyl (*aeg*) backbones **1S** and **2S** were synthesized first following known literature procedure[1]. Compound **2S** was treated with nucleobase adenine (A), 2-amino-6-chloropurine (6-Cl-G), and thymine (T) under heating condition in presence of K_2CO_3 to afford intermediates **3S**, **4S** and **5S** in good yields. Again, **1S** was coupled with N^2-(Isobutyryl)-9-(carboxymethyl)guanine to afford compound **6S** in moderate yield. The spectroscopic data matched perfectly with the literature values[1]. The exocyclic amino groups at N^6 and N^2 positions of **3S** and **4S** were protected by Cbz and isobutyl groups to obtain **7S** and **8S** respectively in good yields. Finally, the Boc groups were removed from **5S**, **6S**, **7S** and **8S** in presence of 5% TFA in DCM to obtain **2a-d** (Scheme S1). After removal of volatile materials from the respective reaction mixtures and without further purification these PNA backbones were subjected for amide coupling with Boc-Phe-Phe-OH (**1**).

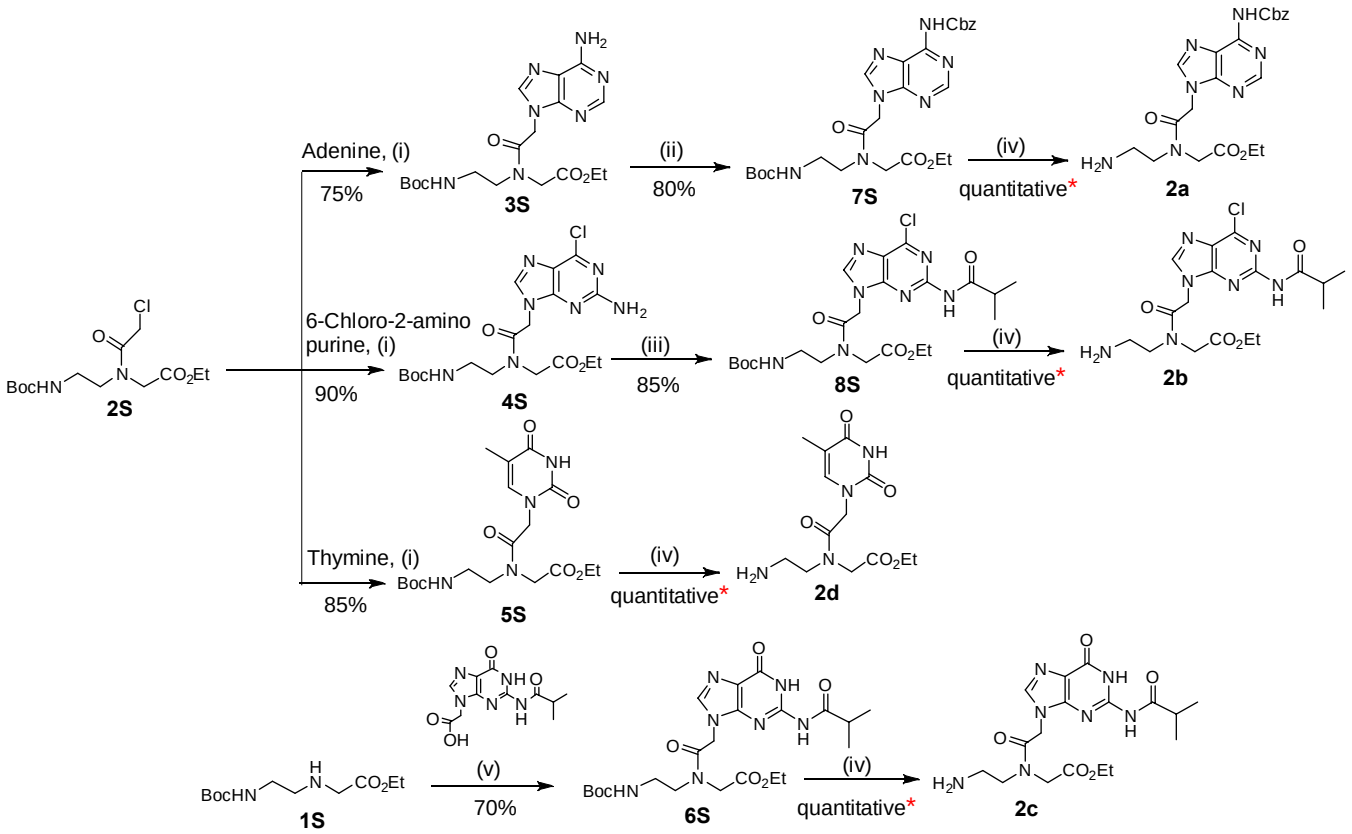

*According to converstion observed in TLC

Reagents and conditions: (i) K_2CO_3, DMF, 75°C, 3 h; (ii) Cbz-Cl, $NaHCO_3$, rt, 8 h; (iii) Isobutyrylchloride, dry Py, 12.5 h; (iv) 50% TFA in DCM, 0 °C-rt, 4-6 h; (v) EDC.HCl, HOBt, DIPEA, dry DMF, 0°C-rt, 36 h

Scheme S1: Synthesis of PNA monomers for amide coupling

To conjugate PNA motifs with Boc-Phe-Phe-Propyne (**4**), azidoethylglycyl backbone **9S**[2] was synthesized first following the literature procedure. Compound **9S** was coupled with N^6-Bis(*tert*butyloxycarbonyl)-9-(carboxymethyl)adenine, N^6-(Benzyloxycarbonyl)-9-(carboxymethyl)adenine, N^2-(Isobutyryl)-9-(carboxymethyl)guanine and, thymine-1-ylacetic acid in presence of isobutyl chloroformate (IBCF) and N-methylmorpholine (NMM) to afford **5a-d** respectively (Scheme S2).

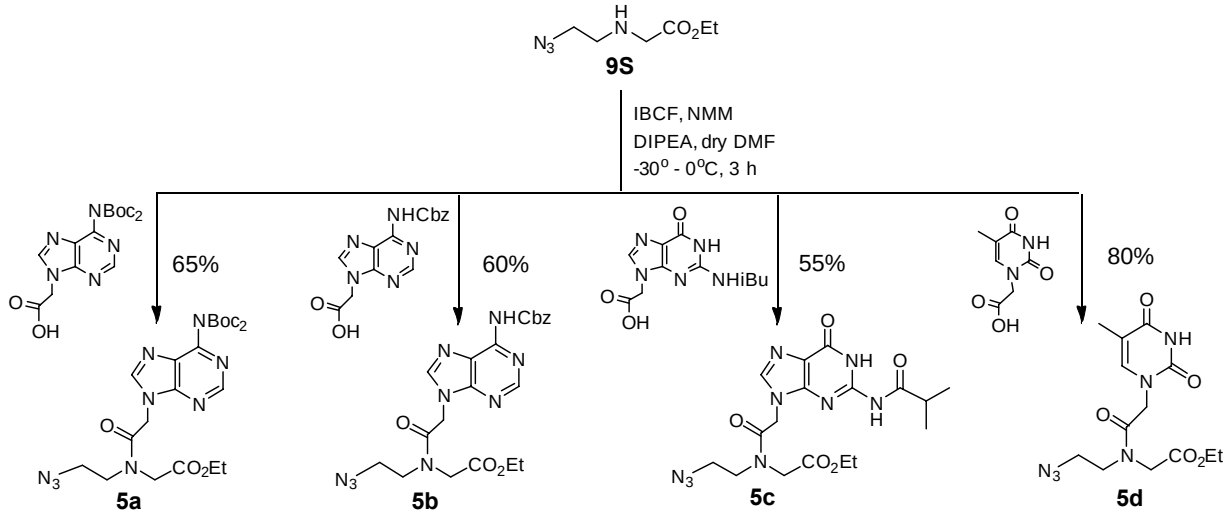

Scheme S2: Synthesis of PNA monomers for 'Click' conjugation

Spectroscopic data:

Compound **1S**: Compound **1S** was prepared following the known literature procedure[1]. ^{1}H NMR, (400 MHz, $CDCl_3$, 25°C, TMS) δ = 5.10 (s, 1H), 4.19 (q, J = 7.1 Hz, 2H), 3.40 (s, 2H), 3.22 (d, J = 5.2 Hz, 2H), 2.74 (t, J = 5.6 Hz, 2H), 1.44 (s, 9H), 1.28 ppm (td, J = 7.1, 1.2 Hz, 3H); ^{13}C NMR (100 MHz, $CDCl_3$) δ = 172.7, 156.3, 79.4, 61.0, 50.6, 48.9, 40.3, 28.6, 14.4 ppm. HRMS (ESI^+), m/z calculated for $(M+H)^+$ $C_{11}H_{23}N_2O_4$: 247.1658, found: 247.1666.

Compound **2S**: Compound **2S** was synthesized following the known literature procedure[1]. ^{1}H NMR, (400 MHz, $CDCl_3$, 25°C, TMS) δ = 5.60 (s, 1H), 4.28 – 4.17 (m, 4H), 4.05 (s, 2H), 3.54 (t, J = 5.8 Hz, 2H), 3.29 (dd, J = 11.7, 5.9 Hz, 2H), 1.50 – 1.38 (m, 9H), 1.35 – 1.21 ppm (m, 3H); ^{13}C NMR (100 MHz, $CDCl_3$) δ = 169.6, 169.1, 167.7, 167.6, 156.2, 156.1, 79.7, 79.3, 62.1, 61.6, 50.5, 49.5, 49.0, 48.2, 41.2, 40.8, 38.6, 38.3, 28.3, 14.1 ppm. HRMS (ESI^+), m/z calculated for $(M+Na)^+$ $C_{13}H_{23}ClN_2O_5Na$: 345.1192, found: 345.1198.

Compound **3S**: Compound **3S** was synthesized following the known procedure[1]. ^{1}H NMR, (400 MHz, $CDCl_3$, 25°C, TMS) δ = 8.28 (d, J = 5.2 Hz, 1H), 7.92 (d, J = 16.5 Hz, 1H), 6.22 (d, J = 17.1 Hz, 2H), 5.84 (s, 0.75H), 5.23 (s, 0.25H), 5.07 (d, J = 8.1 Hz, 1.5H), 4.93 (s, 0.5H), 4.27 (s, 0.5H), 4.23 (dd, J = 14.3, 7.2 Hz, 0.5H), 4.16 (q, J = 7.2 Hz, 1.5H), 4.03 (s, 1.5H), 3.60 (t, J = 5.4 Hz, 1.5H), 3.52 (d, J = 5.5 Hz, 0.5H), 3.36 (d, J = 5.4 Hz,

1.5H), 3.25 (d, J = 5.8 Hz, 0.5H), 1.39 (s, 9H), 1.29 (t, J = 7.1 Hz, 1H), 1.23 ppm (t, J = 7.1 Hz, 2H); ^{13}C NMR (100 MHz, $CDCl_3$) δ = 169.6, 169.2, 167.4, 167.0, 156.2, 155.7, 153.1, 150.3, 141.6, 119.0, 80.1, 79.6, 62.4, 61.8, 50.6, 49.2, 48.8, 43.9, 43.6, 38.8, 38.5, 28.5, 14.2, 14.2 ppm. HRMS (ESI^+), m/z calculated for $(M+H)^+$ $C_{18}H_{28}N_7O_5$: 422.2152, found: 422.2148.

Compound **4S**: Compound **4S** was synthesized following the known literature procedure[1]. ^{1}H NMR, (400 MHz, $CDCl_3$, 25°C, TMS) δ = 7.82 (s, 1H), 5.75 (s, 1H), 5.41 (dd, J = 38.2, 19.2 Hz, 2H), 4.96 (s, 1.5H), 4.80 (s, 0.5H), 4.27 – 4.12 (m, 2H), 4.03 (s, 2H), 3.55 (dt, J = 28.7, 5.8 Hz, 2H), 3.39 – 3.19 (m, 2H), 1.38 (s, 9H), 1.22 ppm (td, J = 7.2, 1.8 Hz, 3H); ^{13}C NMR (100 MHz, $CDCl_3$) δ = 171.3, 169.6, 167.1, 166.7, 159.3, 156.2, 154.1, 151.2, 143.3, 124.5, 80.2, 62.5, 61.9, 60.5, 49.2, 49.1, 48.8, 43.6, 38.8, 28.5, 21.1, 14.2, 14.2, 14.1 ppm. HRMS (ESI^+), m/z calculated for $(M+H)^+$ $C_{18}H_{27}ClN_7O_5$: 456.1762, found: 456.1762.

Compound **5S**: ^{1}H NMR, (400 MHz, $CDCl_3$, 25°C, TMS) δ = 8.88 (s, 1H), 7.02 (s, 0.35H), 6.96 (s, 0.65H), 5.61 (s, 1H), 4.56 (s, 1.5H), 4.41 (s, 0.5H), 4.29 – 4.14 (m, 4H), 4.03 (d, J = 3.5 Hz, 2H), 3.51 (dt, J = 12.2, 6.3 Hz, 2H), 3.31 (ddd, J = 18.3, 12.7, 6.7 Hz, 2H), 1.93 – 1.90 (m, 3H), 1.46 – 1.39 (m, 9H), 1.31 – 1.23 ppm (m, 3H); ^{13}C NMR (100 MHz, $CDCl_3$) δ = 169.8, 169.5, 168.0, 167.6, 164.6, 156.2, 151.4, 141.1, 110.8, 79.9, 79.5, 62.3, 61.7, 50.5, 49.1, 48.8, 47.9, 47.8, 38.8, 28.5, 14.2, 12.4 ppm. HRMS (ESI^+), m/z calculated for $(M+Na)^+$ $C_{18}H_{28}N_4O_7Na$: 435.1856, found: 435.1860.

Compound **6S**: Compound **6S** was synthesized following the known literature procedure[3]. ^{1}H NMR, (400 MHz, DMSO-d_6, 25°C) δ = 12.08 (d, J = 5.5 Hz, 1H), 11.65 (d, J = 7.6 Hz, 1H), 7.83 (s, 0.7H), 7.82 (s, 0.3H), 7.03 (t, J = 5.5 Hz, 0.7H), 6.76 (s, 0.3H), 5.13 (s, 1.4H), 4.97 (s, 0.6H), 4.42 (s, 0.6H), 4.22 (q, J = 7.1 Hz, 0.6H), 4.08 (q, J = 7.0 Hz, 2.8H), 3.50 (t, J = 6.5 Hz, 1.4H), 3.32 (d, J = 11.9 Hz, 0.6H), 3.24 (d, J = 6.1 Hz, 1.4H), 3.02 (d, J = 6.1 Hz, 0.6H), 2.84 – 2.71 (m, 1H), 1.37 (d, J = 6.5 Hz, 9H), 1.27 (t, J = 7.1 Hz, 1H), 1.17 (t, J = 7.1 Hz, 2H), 1.11 ppm (d, J = 6.7 Hz, 6H); ^{13}C NMR (100 MHz, DMSO-d_6, 25°C) δ = 180.2, 180.1, 169.5, 169.0, 167.0, 166.6, 155.8, 155.6, 154.9, 149.1, 149.2, 147.9, 147.9, 140.5, 140.4, 119.6, 78.2, 77.8, 61.3, 60.6, 49.1, 47.8, 46.9, 44.1, 43.9, 38.3, 37.7, 34.7, 34.7, 28.2, 18.9, 14.0 ppm. HRMS (ESI^+), m/z calculated for $(M+H)^+$ $C_{22}H_{34}N_7O_7$: 508.2520, found: 508.2535.

Compound **7S**: To a suspension of **3S** (0.42g, 1.00 mmol) in satd $NaHCO_3$ solution (30 mL) at 0°C was added Cbz-Cl (0.20 g, 1.2 mmol). The resulting mixture was stirred at room temperature for 8 h at. EtOAc (20 mL) was added to the reaction mixture and the organic layer was separated. Aqueous layer was further extracted with EtOAc (25x2 mL). The combined organic layer was dried over anhyd Na_2SO_4, filtered and the filtrate was evaporated to dryness in vacuo. The crude residue was purified by column chromatography [Eluent: 20-90%

EtOAc in hexane] to afford compound **7S** (0.44 g, 80%) as hygroscopic solid. ^{1}H NMR, (400 MHz, $CDCl_3$, 25°C, TMS) δ = 8.97 (s, 1H), 8.16 (s, 1H), 7.36 – 7.18 (m, 8H), 6.36 (d, *J* = 11.2 Hz, 1H), 5.61 – 5.25 (m, 0.6H), 5.10 (s, 2H), 5.07 (d, *J* = 4.8 Hz, 2H), 4.93 (d, *J* = 5.4 Hz, 0.3H), 4.27 – 4.09 (m, 4H), 4.08 – 3.94 (m, 2H), 3.45 (dd, *J* = 24.5, 5.4 Hz, 2H), 3.29 – 3.16 (m, 2H), 1.38 – 1.29 (m, 9H), 1.25 – 1.16 ppm (m, 3H); ^{13}C NMR (100 MHz, $CDCl_3$) δ = 169.9, 169.6, 169.5, 169.0, 159.8, 156.1, 155.6, 154.4, 153.9, 151.0, 136.1, 136.1, 135.5, 128.7, 128.6, 128.6, 128.6, 128.4, 128.3, 128.2, 128.1, 105.9, 80.0, 79.6, 68.1, 67.7, 67.6, 62.2, 61.8, 49.7, 48.9, 48.8, 48.3, 42.9, 38.7, 28.5, 14.2 ppm. HRMS (ESI^+), m/z calculated for $(M+H)^+$ $C_{26}H_{34}N_7O_7$: 556.2520, found: 556.2511.

Compound **8S**: Compound **4S** was converted to **8S** following the procedure described in the *Eur. Pat. Appl*. **2001**, EP 1085020 A1 20010321. To a solution of **4S** (0.45 g, 1.00 mmol) in dry pyridine (10 mL) at 0°C was added isobutyrylchloride (0.13 g, 1.2 mmol). The resulting mixture was stirred at 0°C for 30 min, followed by 12 h at room temperature. Satd $NaHCO_3$ solution (20 mL) was added to the reaction mixture and extracted with EtOAc (25x3 mL). The combined organic layer was dried over anhyd Na_2SO_4, filtered and the filtrate was evaporated to dryness in vacuo. The crude residue was purified by flash column chromatography [Eluent: 20-70% EtOAc in hexane] to afford compound **6S** (0.44 g, 85%) as hygroscopic solid. ^{1}H NMR, (400 MHz, $CDCl_3$, 25°C, TMS) δ = 8.31 (s, 1H), 8.21 (s, 0.7H), 8.13 (s, 0.3H), 6.29 (s, 0.75H), 5.30 (d, *J* = 16.6 Hz, 0.25H), 5.14 (s, 1.7H), 4.98 (d, *J* = 12.4 Hz, 0.3H), 4.36 (s, 0.3H), 4.27 (q, *J* = 7.1 Hz, 0.3H), 4.17 (q, *J* = 7.1 Hz, 1.7H), 4.14 – 4.08 (m, 1.7H), 3.67 (t, *J* = 5.8 Hz, 1.7H), 3.55 (t, *J* = 5.8 Hz, 0.3H), 3.43 (dd, *J* = 11.9, 5.9 Hz, 1.7H), 3.29 – 3.21 (m, 0.3H), 2.77 - 2.71 (m, 1H), 1.40 (s, 2H), 1.32 (dd, *J* = 13.7, 6.6 Hz, 1H), 1.27 (d, *J* = 3.5 Hz, 4H), 1.25 (d, *J* = 1.0 Hz, 5H), 1.22 ppm (s, 6H); ^{13}C NMR (100 MHz, $CDCl_3$) δ = 175.4, 169.4, 166.5, 156.6, 152.9, 151.9, 151.1, 146.0, 127.8, 79.5, 62.5, 61.7, 60.5, 50.9, 49.1, 48.8, 44.3, 43.6, 38.5, 36.7, 28.5, 28.4, 19.4, 14.3, 14.2 ppm. HRMS (ESI^+), m/z calculated for $(M+H)^+$ $C_{22}H_{33}ClN_7O_6$: 526.2181, found: 526.2173.

General procedure of Boc deprotection: To an ice-cold mixture of compound (0.5 mmol in 5 mL), 2 mL TFA was added slowly and stirred for 4-6 h at rt. Completion of reaction was monitored by TLC. The volatile part of the reaction mixture was completely removed by co-evaporation with toluene and carbontetrachloride to afford TFA salts of compound **2a-d** as brown oil which were used for amide coupling reaction without further purification.

Compound **2a**: HRMS (ESI^+), m/z calculated for $(M+H)^+$ $C_{21}H_{26}N_7O_5$: 456.1995, found: 456.1985.
Compound **2b**: HRMS (ESI^+), m/z calculated for $(M+H)^+$ $C_{17}H_{25}ClN_7O_4$: 426.1656, found: 426.1642.

Compound **2c:** White solid. M.p. 97-100°C; ^{1}H NMR, (400 MHz, DMSO-d_6, 25°C): δ = 12.09 (d, J = 5.1 Hz, 1H), 11.63 (d, J = 6.1 Hz, 1H), 8.04 (s, 1H), 7.87 (s, 0.5H), 7.82 (s, 0.5H), 7.78 (s, 1H), 5.17 (s, 1H), 4.98 (s, 1H), 4.46 (s, 1H), 4.22 (q, J = 7.1 Hz, 1H), 4.10 (dd, J = 12.2, 4.9 Hz, 2H), 3.70 (t, J = 6.7 Hz, 1H), 3.52 (t, J = 6.3 Hz, 1H), 3.17 (d, J = 5.4 Hz, 1H), 2.97 (dd, J = 10.9, 5.1 Hz, 1H), 2.86 – 2.68 (m, 1H), 1.27 (t, J = 7.1 Hz, 1.5H), 1.18 (t, J = 7.1 Hz, 1.5H), 1.11 ppm (d, J = 6.8 Hz, 6H); ^{13}C NMR (100 MHz, DMSO-d_6, 25°C): δ = 180.2, 180.1, 169.5, 169.3, 168.0, 166.8, 158.9, 158.6, 158.3, 154.9, 149.3, 148.0, 147.9, 140.6, 119.4, 61.4, 60.9, 48.6, 47.7, 44.9, 44.8, 44.2, 44.1, 36.9, 36.7, 34.7, 34.7, 18.9, 18.9, 14.0, 14.0 ppm; HRMS (ESI$^+$), m/z calculated for $(M+H)^+$ $C_{17}H_{26}N_7O_5$: 408.1995, found: 408.1992.

Compound **2d**: HRMS (ESI$^+$), m/z calculated for $(M+H)^+$ $C_{13}H_{21}N_4O_5$: 313.1512, found: 313.1514.

Compound **9S**: Compound **9S** was synthesized following previously mentioned literature[2].^{1}H NMR, (400 MHz, $CDCl_3$, 25°C, TMS) δ = 4.20 (q, J = 7.2 Hz, 2H), 3.46 – 3.39 (m, 4H), 2.88 – 2.79 (m, 2H), 2.00 (s, 1H), 1.32 – 1.24 ppm (m, 3H); ^{13}C NMR (100 MHz, $CDCl_3$) δ = 172.2, 60.9, 51.5, 50.6, 48.2, 14.3 ppm; IR: ν_{N3} = 2101 cm^{-1}; HRMS (ESI$^+$), m/z calculated for $(M+H)^+$ $C_6H_{13}N_4O_2$: 173.1038, found: 173.1044.

Compound **4**: Compound **4** was synthesized following the reported procedure.[4] ^{1}H NMR, (400 MHz, $CDCl_3$, 25°C, TMS) δ = 7.24 (dt, J = 6.4, 4.1 Hz, 3H), 7.18 – 7.02 (m, 6H), 6.91 (t, J = 18.1 Hz, 2H), 6.54 (s, 1H), 6.28 (s, 1H), 4.84 (d, J = 5.9 Hz, 1H), 4.72 – 4.54 (m, 1H), 4.20 (d, J = 6.0 Hz, 1H), 3.92 (ddd, J = 21.0, 11.9, 9.0 Hz, 1H), 3.77 (dd, J = 17.5, 2.4 Hz, 1H), 3.14 (s, 1H), 2.99 – 2.76 (m, 3H), 2.08 (t, J = 2.5 Hz, 1H), 1.25 ppm (s, 9H); ^{13}C NMR (100 MHz, $CDCl_3$) δ = 171.0, 170.3, 155.9, 136.0, 129.4, 129.3, 129.0, 128.8, 81.02, 79.2, 71.3, 56.3, 53.4, 37.8, 37.5, 29.2, 28.3, 28.2 ppm. HRMS (ESI$^+$), m/z calculated for $(M+Na)^+$ $C_{26}H_{31}N_3O_4Na$: 472.2212, found: 472.2213.

General procedure of coupling azide backbone with nucleobase acetic acid:

1. To a mixture of nucleobase acetic acid (0.5 mmol) in dry DMF (5mL), NMM (0.5 mmol) and IBCF (0.5 mmol) were added slowly and cooled to −50 ^{o}C. To the white semisolid mass obtained after 0.5 h, compound **9S** (0.4 mmol) dissolved in dry DMF (1.5 mL) and disopropylethylamine (DIPEA) (2.0 mmol) were slowly added at 0 ^{o}C. Reaction mixture was maintained at 0 ^{o}C for 0.5 h and then kept at rt for 6 h. Brine solution was added and extracted with EtOAc (3x50 mL). Combined organic layer was dried over anhyd Na_2SO_4 and evaporated to dryness. Crude mass thus obtained was purified by column chromatography.
2. N^2-(Isobutyryl)-9-(carboxymethyl)guanine was coupled with the azide backbone **9S** following the procedure mentioned for compound **3a-d** (main manuscript) to afford **5c** in good yield (75%).

Compound **5a**: ^{1}H NMR, (400 MHz, $CDCl_3$, 25°C, TMS) δ = 8.83 (d, J = 3.0 Hz, 1H), 8.24 (s, 1H), 5.32 (s, 1H), 5.09 (s, 1H), 4.37 (s, 1H), 4.32 (q, J = 7.2 Hz, 1H), 4.20 (q, J = 7.1 Hz, 1H), 4.14 (s, 1H), 3.74 – 3.70 (m, 1H), 3.67 (d, J = 4.8 Hz, 1H), 3.60 – 3.52 (m, 2H), 1.43 (d, J = 2.7 Hz, 18H), 1.36 (t, J = 7.1 Hz, 1.5H), 1.26 ppm (t, J = 7.1 Hz, 1.5H); ^{13}C NMR (100 MHz, $CDCl_3$) δ = 168.9, 168.7, 166.7, 166.5, 153.58, 153.5, 152.1, 150.4, 150.3, 150.3, 146.1, 145.9, 128.3, 83.8, 83.8, 62.5, 61.7, 51.1, 50.0, 49.9, 48.7, 48.4, 48.1, 44.0, 43.9, 27.8, 14.3, 14.2 ppm; IR: ν_{N3} = 2103 cm^{-1}; HRMS (ESI$^+$), m/z calculated for $(M+H)^+$ $C_{23}H_{34}N_9O_7$: 548.2581, found: 548.2587.

Compound **5b**: ^{1}H NMR, (400 MHz, CD_3OD + DMSO-d_6, 2:1, 25°C) δ = 8.22 (t, J = 12.7 Hz, 1H), 7.39 (d, J = 7.4 Hz, 1H), 7.31 (ddd, J = 22.2, 21.7, 7.0 Hz, 5H), 5.36 (s, 1H), 5.19 (s, 1H), 5.12 (d, J = 17.3 Hz, 1H), 4.20 (dd, J = 14.3, 7.1 Hz, 1H), 4.12 – 3.93 (m, 3H), 3.66 (d, J = 11.7 Hz, 3H), 3.53 – 3.42 (m, 1H), 3.38 (dd, J = 13.7, 8.0 Hz, 1H), 1.25 (dd, J = 14.3, 7.2 Hz, 1H), 1.13 ppm (t, J = 7.1 Hz, 2H); ^{13}C NMR (100 MHz, CD_3OD + DMSO-d_6, 2:1) δ = 170.1, 168.8, 168.4, 153.2, 153.1, 152.8, 150.4, 146.2, 137.3, 129.4, 129.1, 129.0, 67.8, 62.7, 61.9, 61.0, 50.7, 50.6, 49.9, 49.4, 45.1, 45.1, 14.4 ppm; IR: ν_{N3} = 2102 cm^{-1}; HRMS (ESI$^+$), m/z calculated for $(M+H)^+$ $C_{21}H_{24}N_9O_5$: 482.1900, found: 482.1897.

Compound **5c**: ^{1}H NMR (400 MHz, DMSO-d_6, 25°C) δ = 12.08 (s, 1H), 11.65 (s, 0.3H), 11.62 (s, 0.7H), 7.88 (s, 0.6H), 7.83 (s, 0.4H), 5.20 (s, 1.3H), 4.99 (s, 0.7H), 4.48 (s, 0.7H), 4.22 (q, J = 7.1 Hz, 0.7H), 4.13 – 4.05 (m, 2.6H), 3.73 – 3.62 (m, 2.5H), 3.50 – 3.41 (m, 1.5H), 2.82 – 2.71 (m, 1H), 1.27 (t, J = 7.2 Hz, 1H), 1.17 (t, J = 7.1 Hz, 2H), 1.12 (s, 3H), 1.10 ppm (s, 3H); ^{13}C NMR (400 MHz, DMSO-d_6, 25°C) δ = 180.1, 169.5, 168.9, 167.3, 166.9, 154.9, 149.3, 147.9, 140.7, 140.5, 119.6, 61.3, 60.6, 49.0, 48.3, 48.0, 46.8, 46.4, 44.2, 34.6, 18.9, 14.0 ppm; IR: ν_{N3} = 2105 cm^{-1}; HRMS (ESI$^+$), m/z calculated for $(M+H)^+$ $C_{17}H_{24}N_9O_5$: 434.1900, found: 434.1903.

Compound **5d**: ^{1}H NMR, (400 MHz, DMSO-d_6, 25°C): δ = 11.29 (s, 1H), 7.36 (d, J = 1.2 Hz, 0.7H), 7.29 (d, J = 1.2 Hz, 0.3H), 4.71 (s, 1.3H), 4.50 (s, 0.7H), 4.37 (s, 0.7H), 4.18 (q, J = 7.1 Hz, 0.8H), 4.13 – 4.03 (m, 2.5H), 3.63 (t, J = 5.4 Hz, 1.3H), 3.56 (t, J = 5.5 Hz, 1.3H), 3.50 – 3.46 (m, 0.7H), 3.43 (t, J = 5.3 Hz, 0.7H), 1.75 (d, J = 1.1 Hz, 3H), 1.25 (t, J = 7.1 Hz, 1H), 1.18 ppm (t, J = 7.1 Hz, 2H); ^{13}C NMR (100 MHz, DMSO-d_6, 25°C): δ = 169.3, 168.9, 168.0, 167.6, 164.4, 164.4, 151.0, 142.2, 142.0, 108.2, 108.1, 61.2, 60.6, 49.1, 48.3, 48.1, 47.9, 46.8, 46.3, 14.0, 14.0, 11.9 ppm; IR: ν_{N3} = 2103 cm^{-1}; HRMS (ESI$^+$), m/z calculated for $(M+H)^+$ $C_{13}H_{17}N_6O_5$: 339.1417, found: 339.1420.

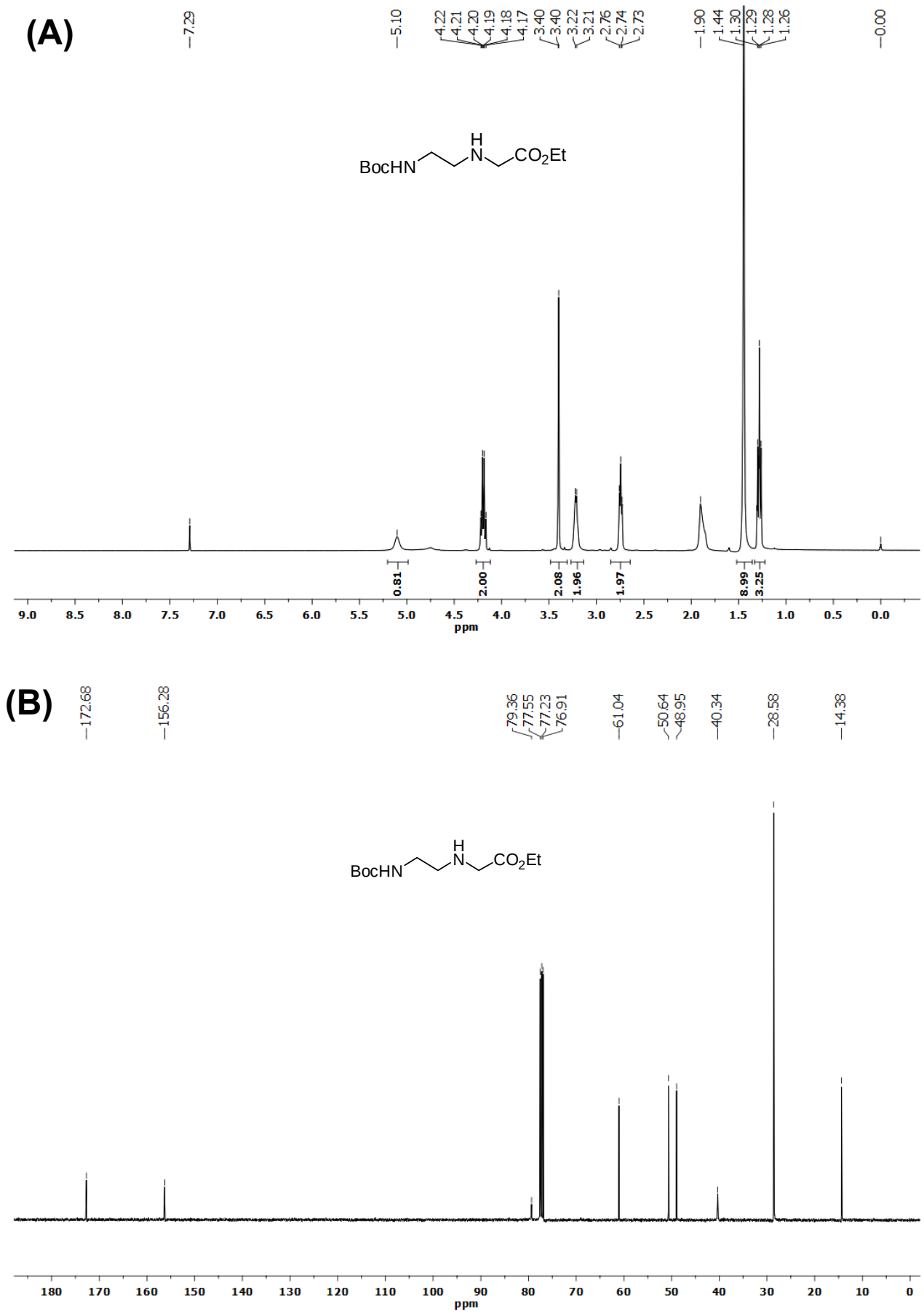

Figure S1: (A) ^{1}H-NMR and (B) ^{13}C-NMR spectra of **1S**.

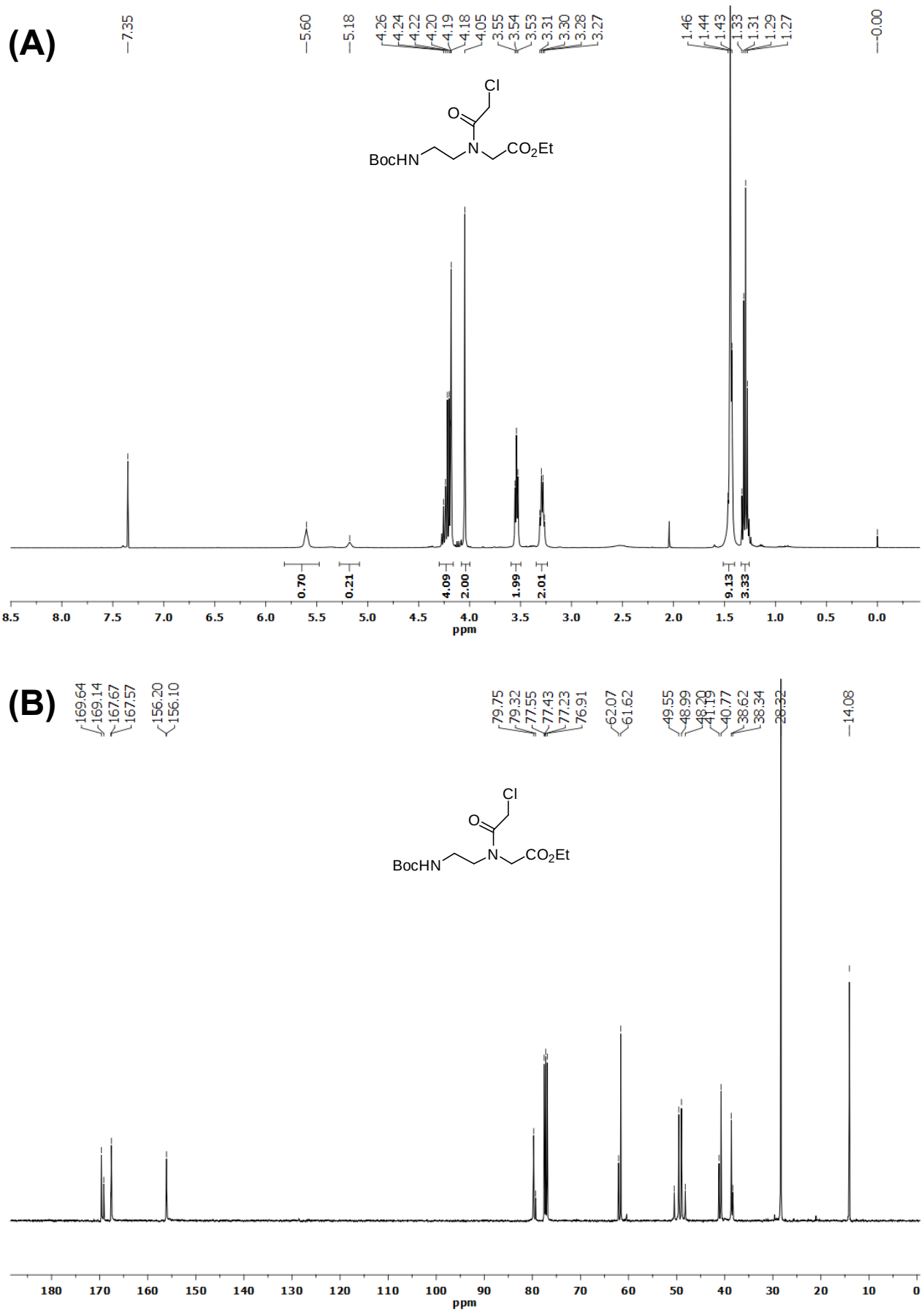

Figure S2: (A) ^{1}H-NMR and (B) ^{13}C-NMR spectra of **2S**

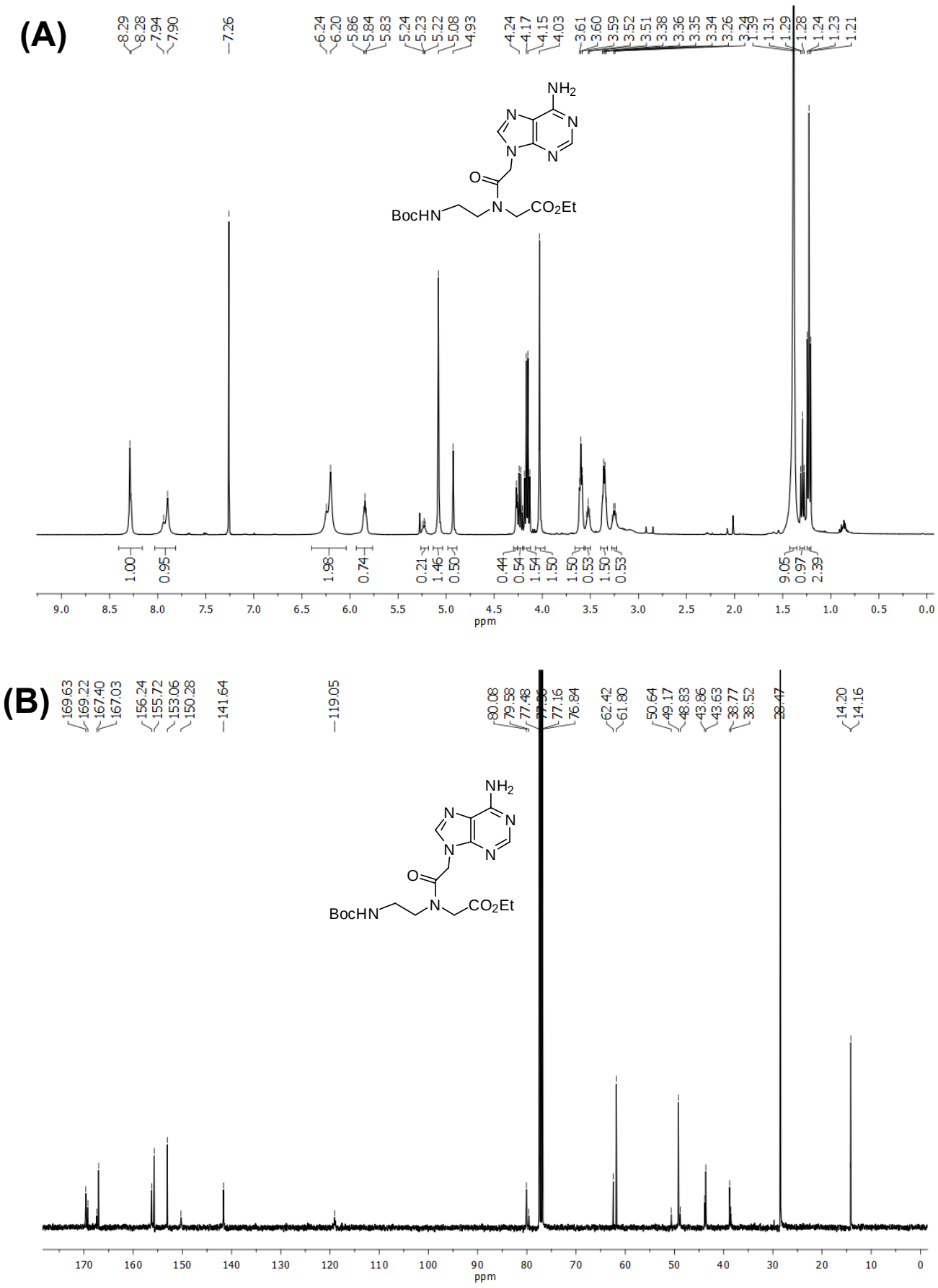

Figure S3: (A) ^{1}H-NMR and (B) ^{13}C-NMR spectra of **3S**

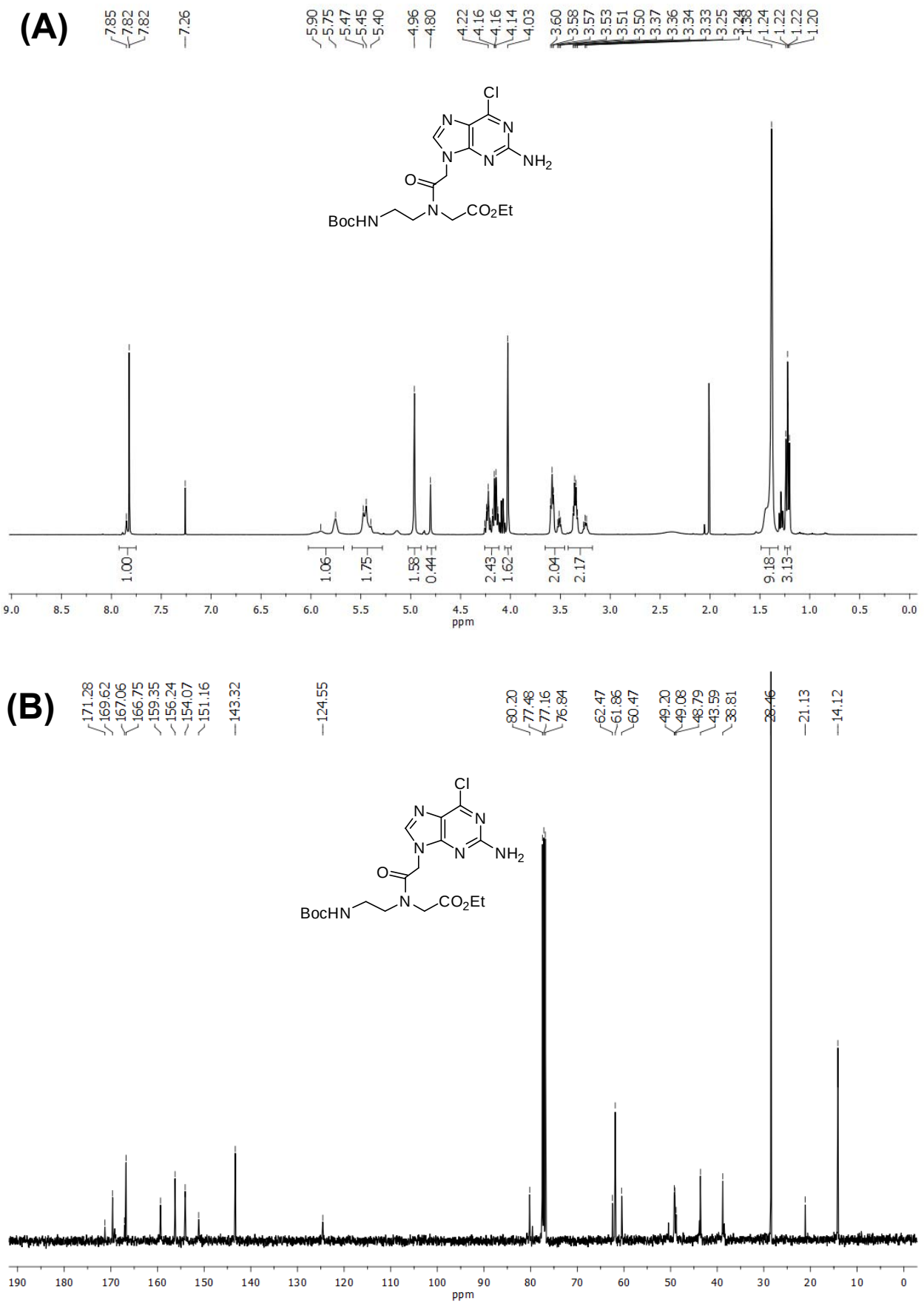

Figure S4: (A) ^{1}H-NMR and (B) ^{13}C-NMR spectra of **4S**

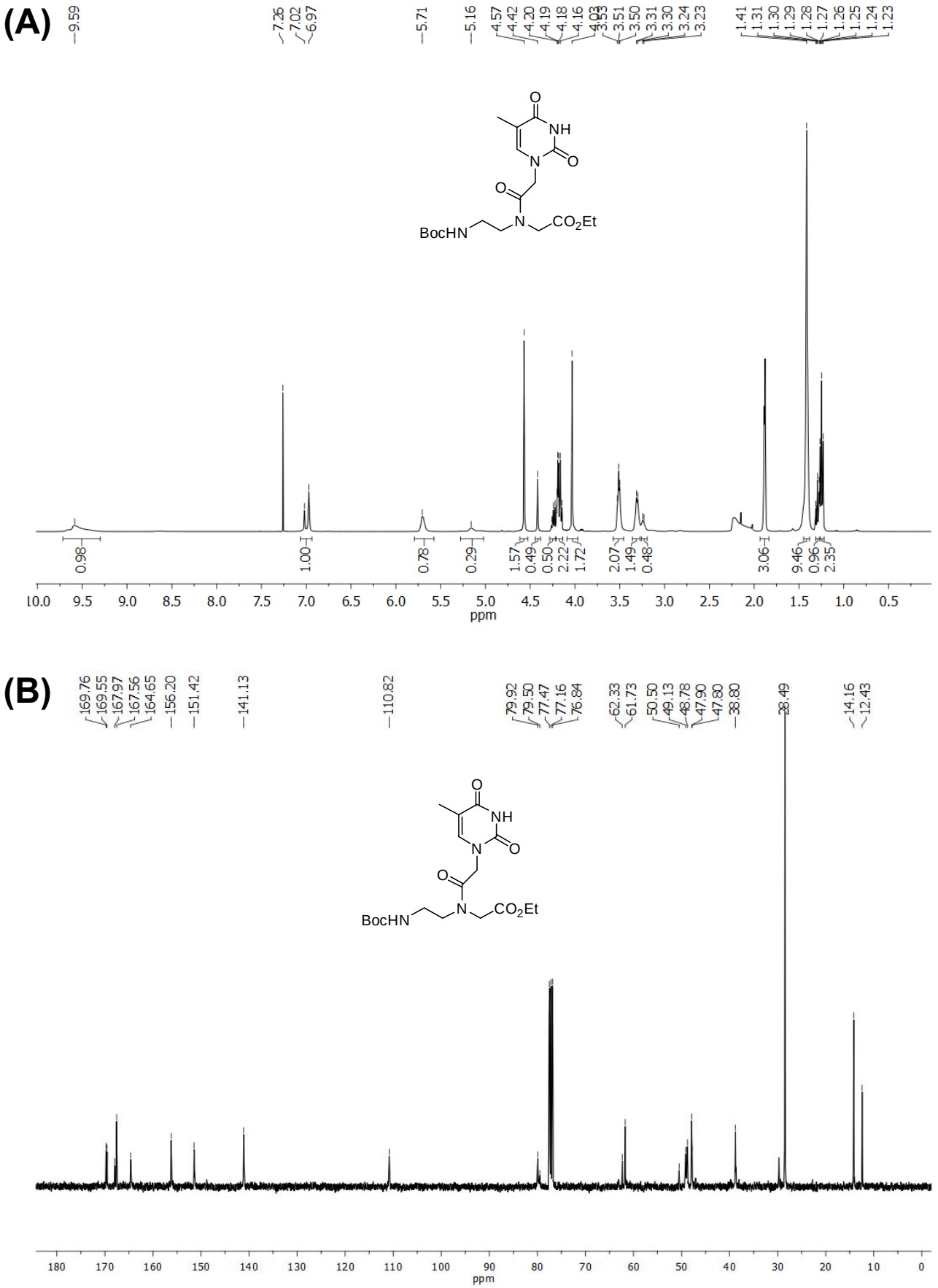

Figure S5: (A) ^{1}H-NMR and (B) ^{13}C-NMR spectra of **5S**

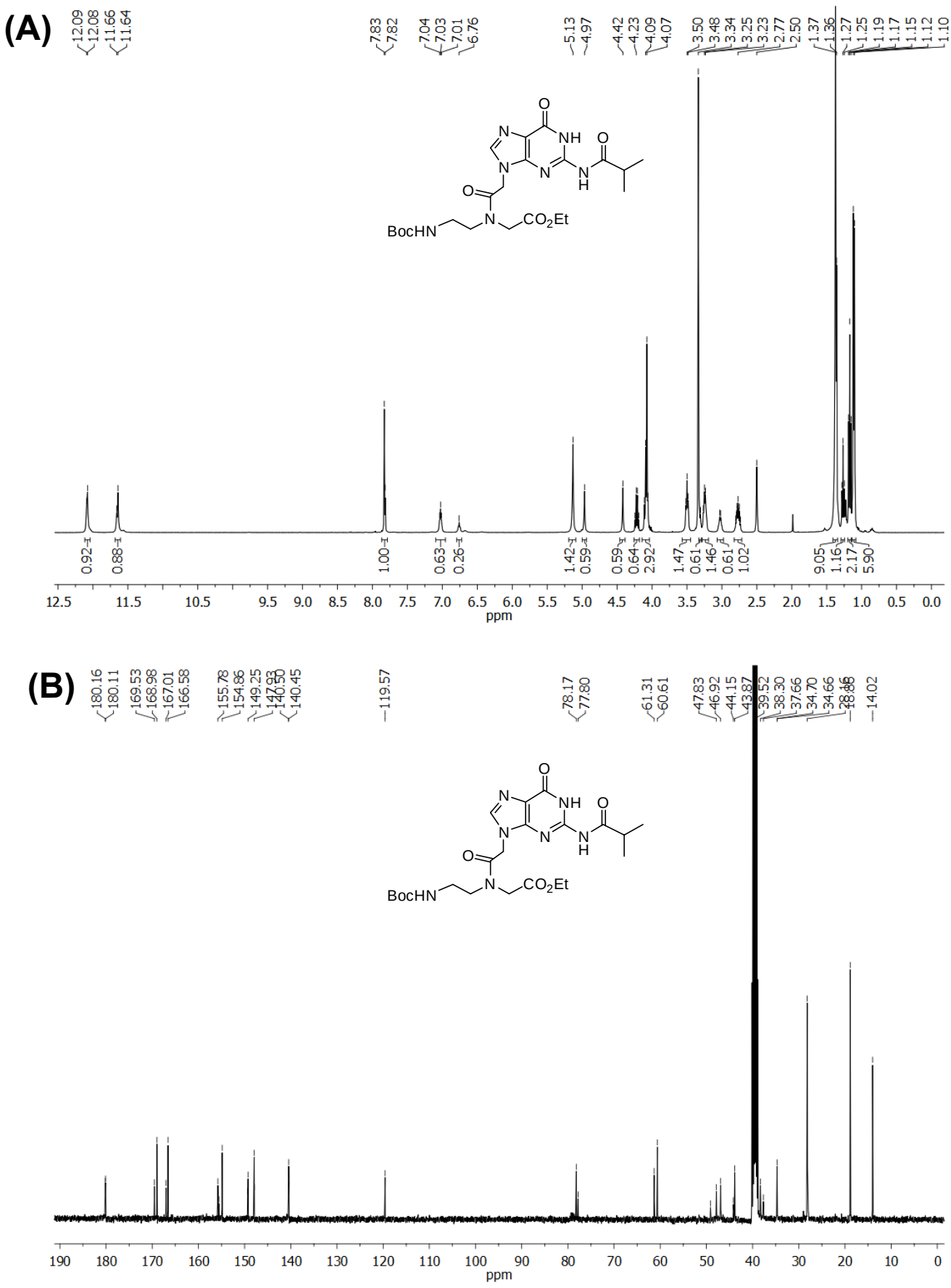

Figure S6: (A) ^{1}H-NMR and (B) ^{13}C-NMR spectra of **6S**

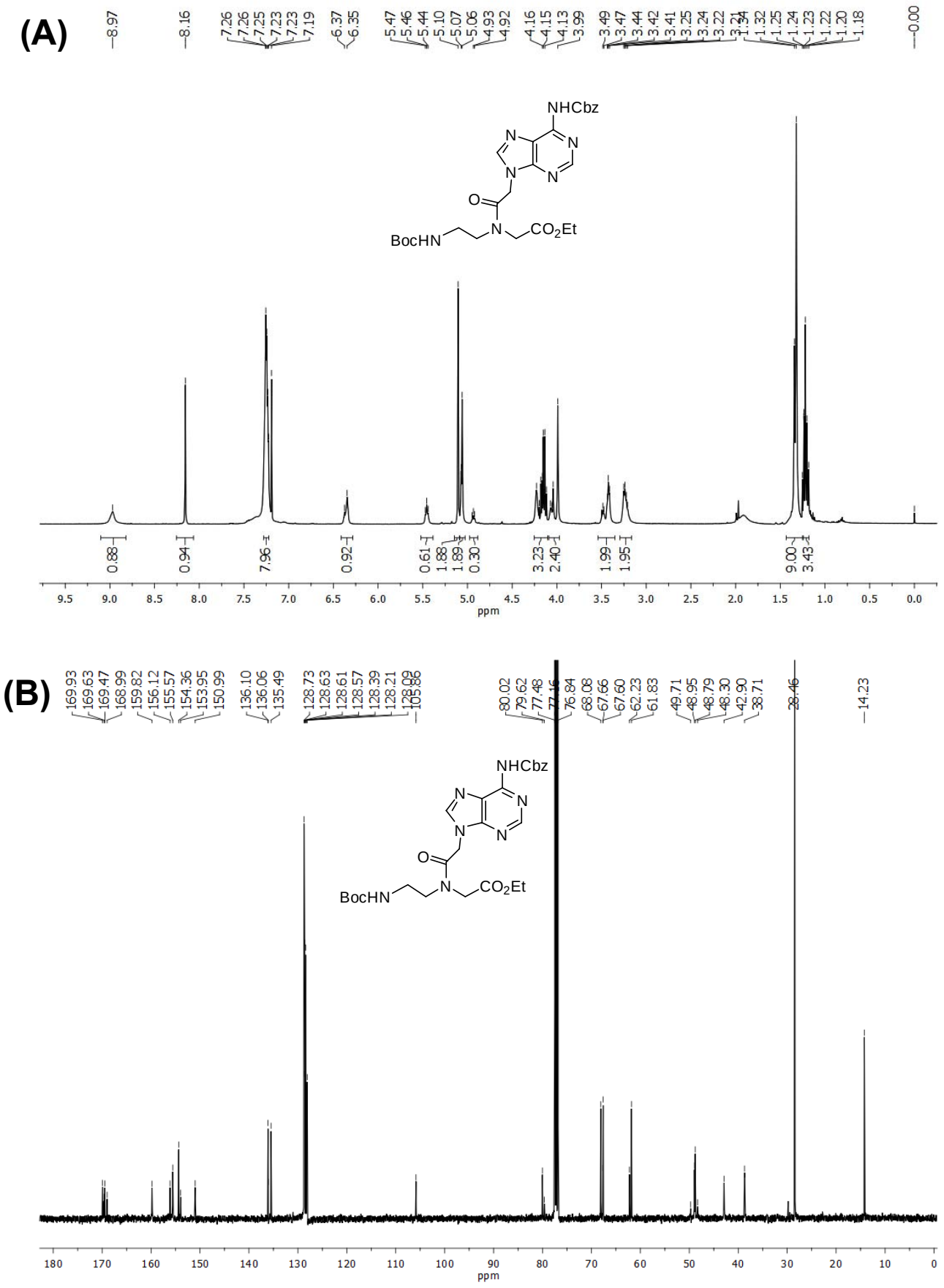

Figure S7: (A) ^{1}H-NMR and (B) ^{13}C-NMR spectra of **7S**

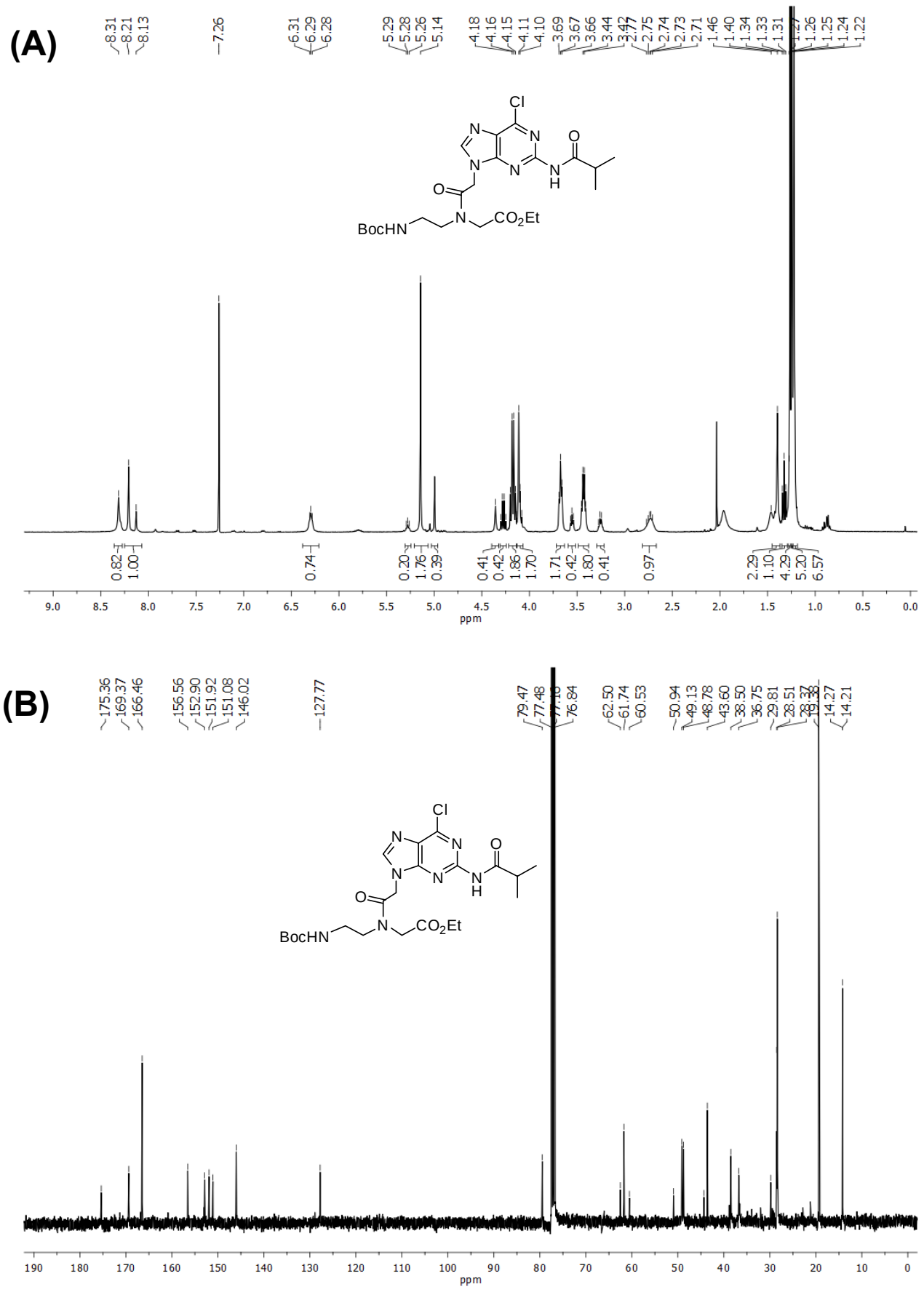

Figure S8: (A) ^{1}H-NMR and (B) ^{13}C-NMR spectra of **8S**

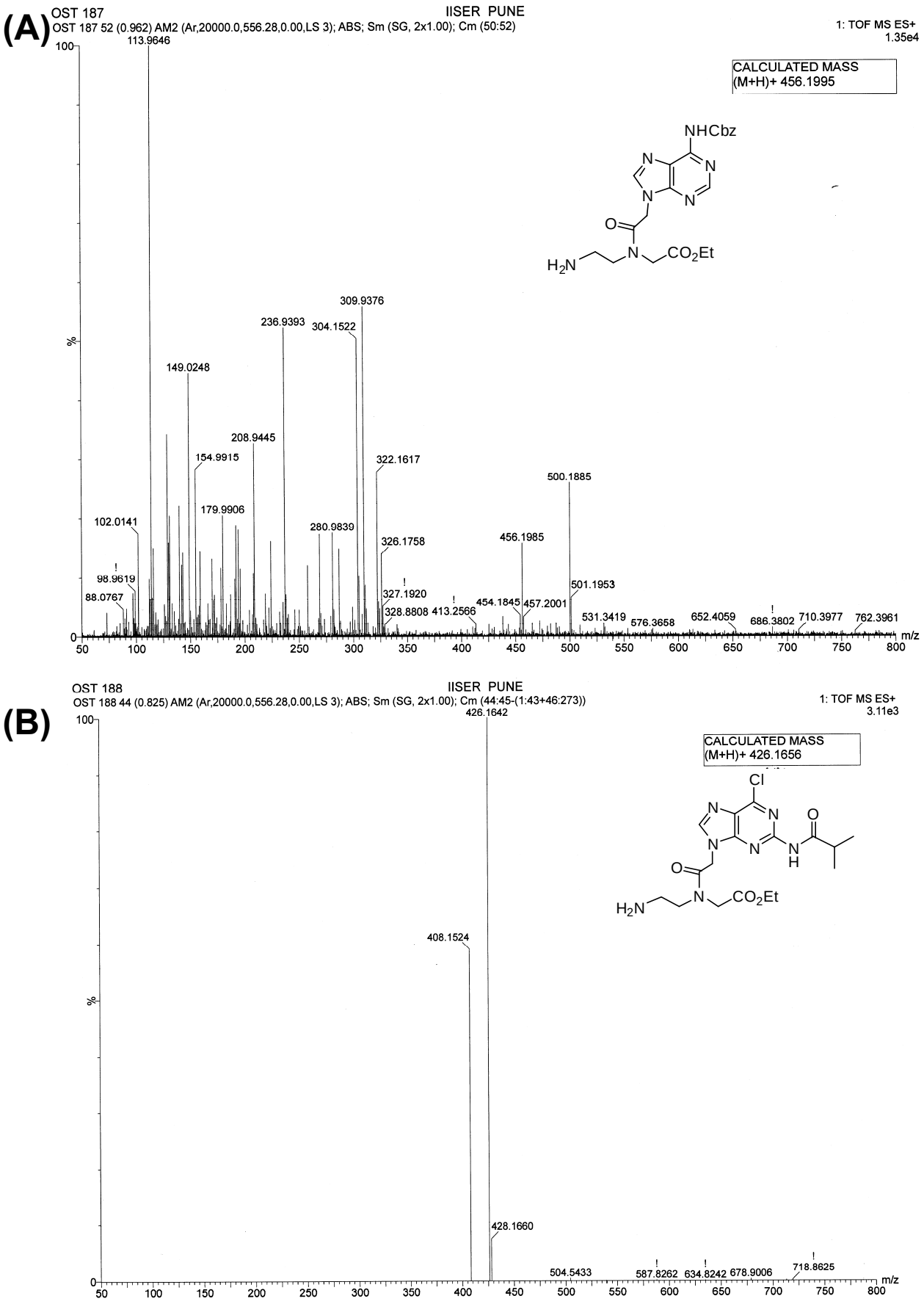

Figure S9: HRMS of crude intermediates (A) **2a** and (B) **2b**

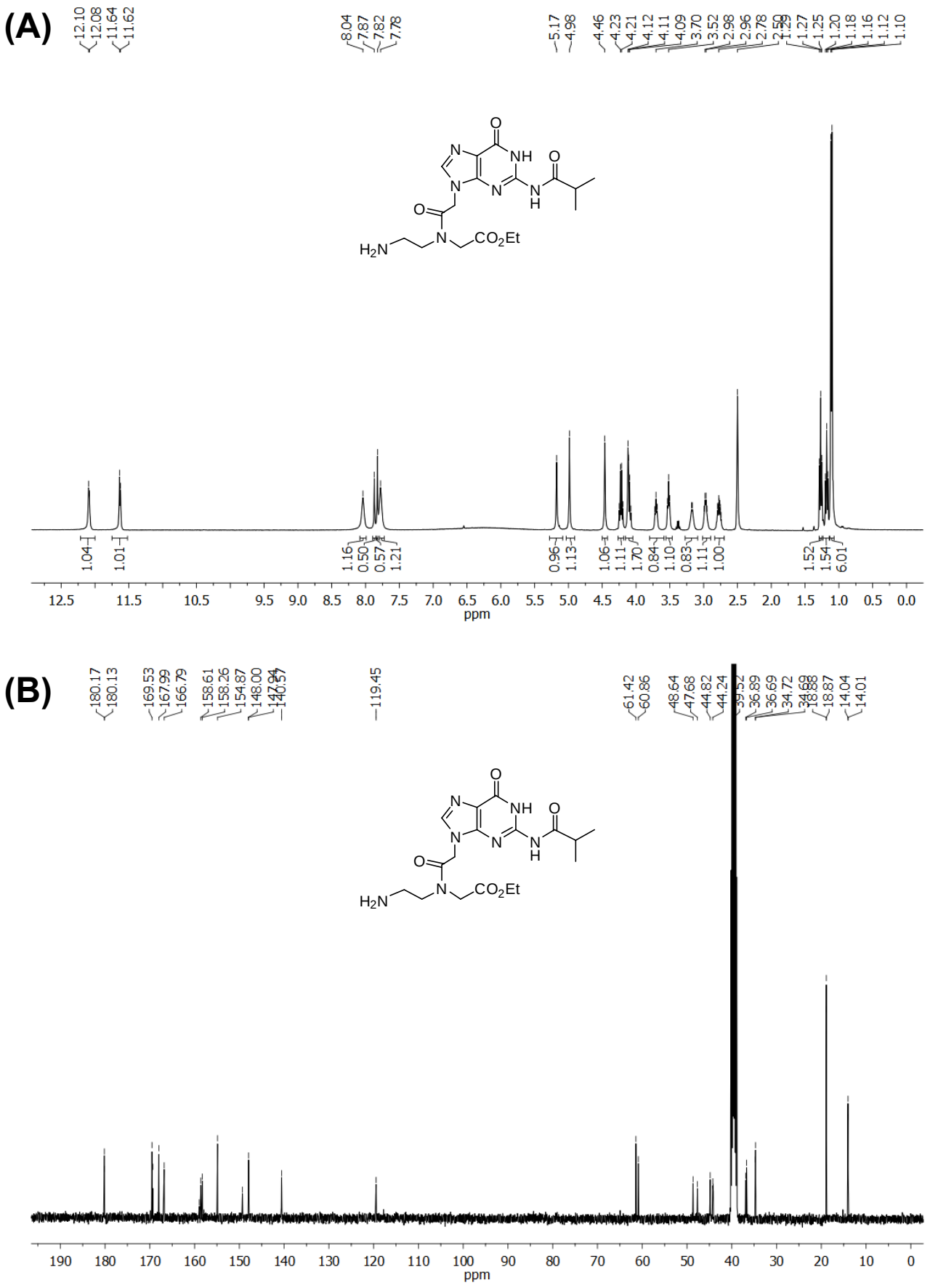

Figure S10: (A) ^{1}H-NMR and (B) ^{13}C-NMR spectra of **2c**

(A)

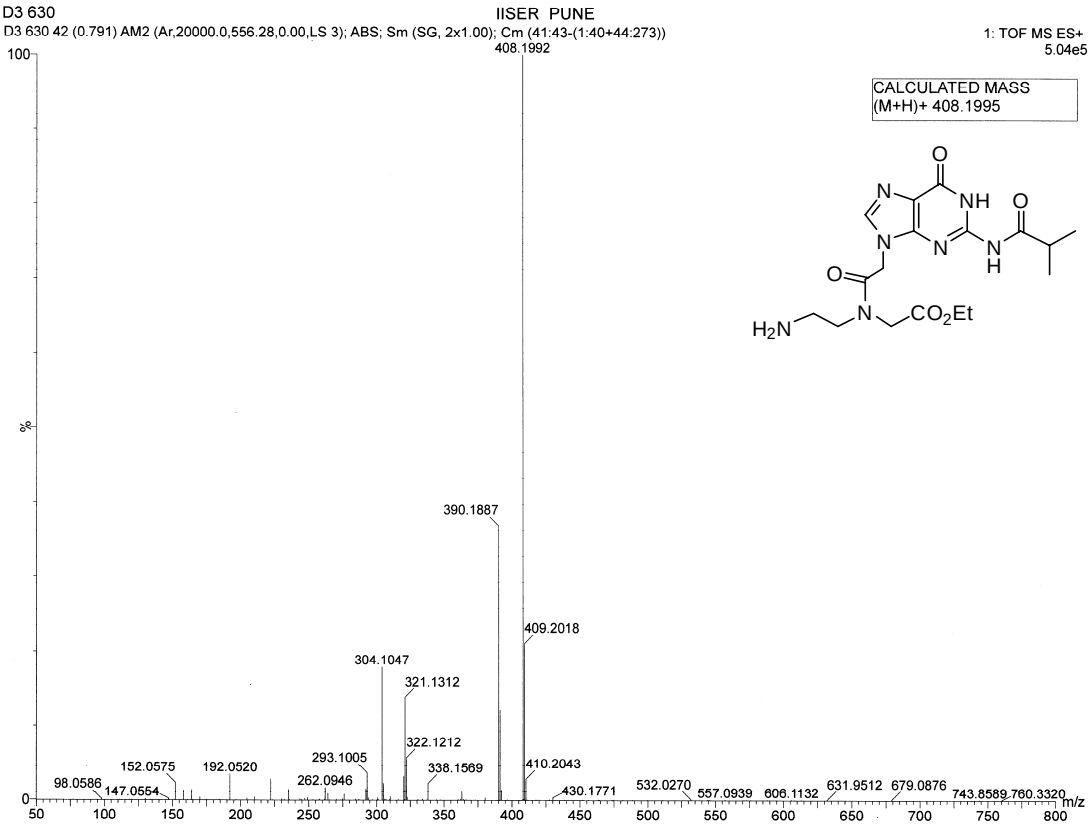

(B)

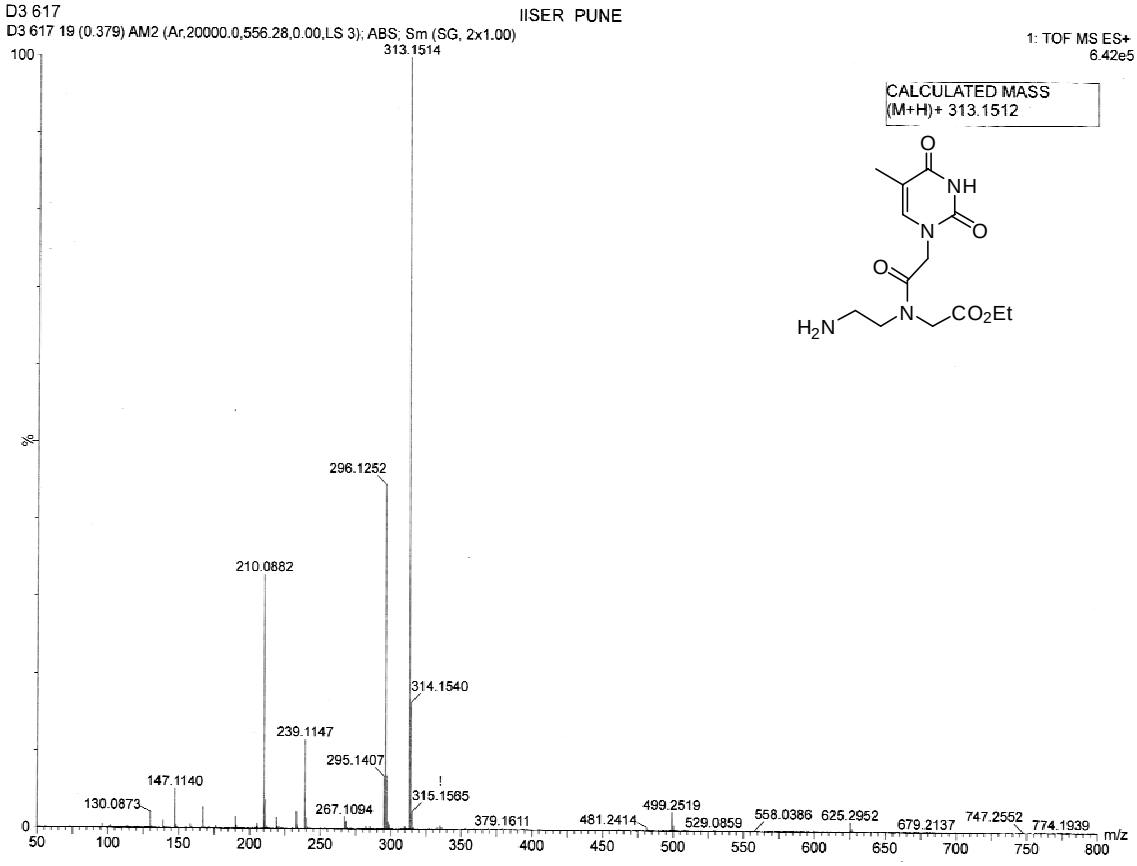

Figure S11: HRMS of intermediates (A) **2c** and (B) crude **2d**

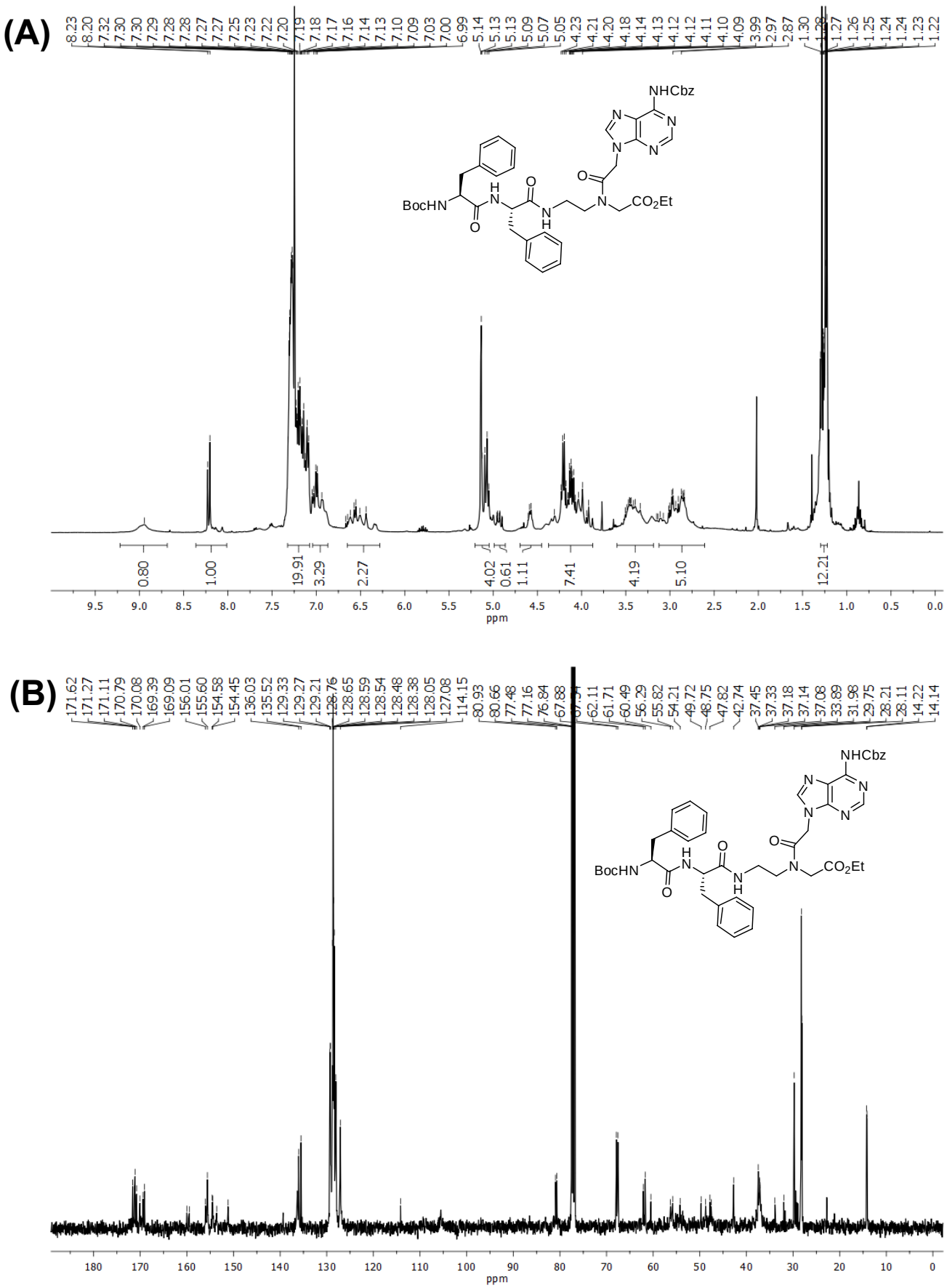

Figure S12: (A) ^{1}H-NMR and (B) ^{13}C-NMR spectra of peptide **3a**

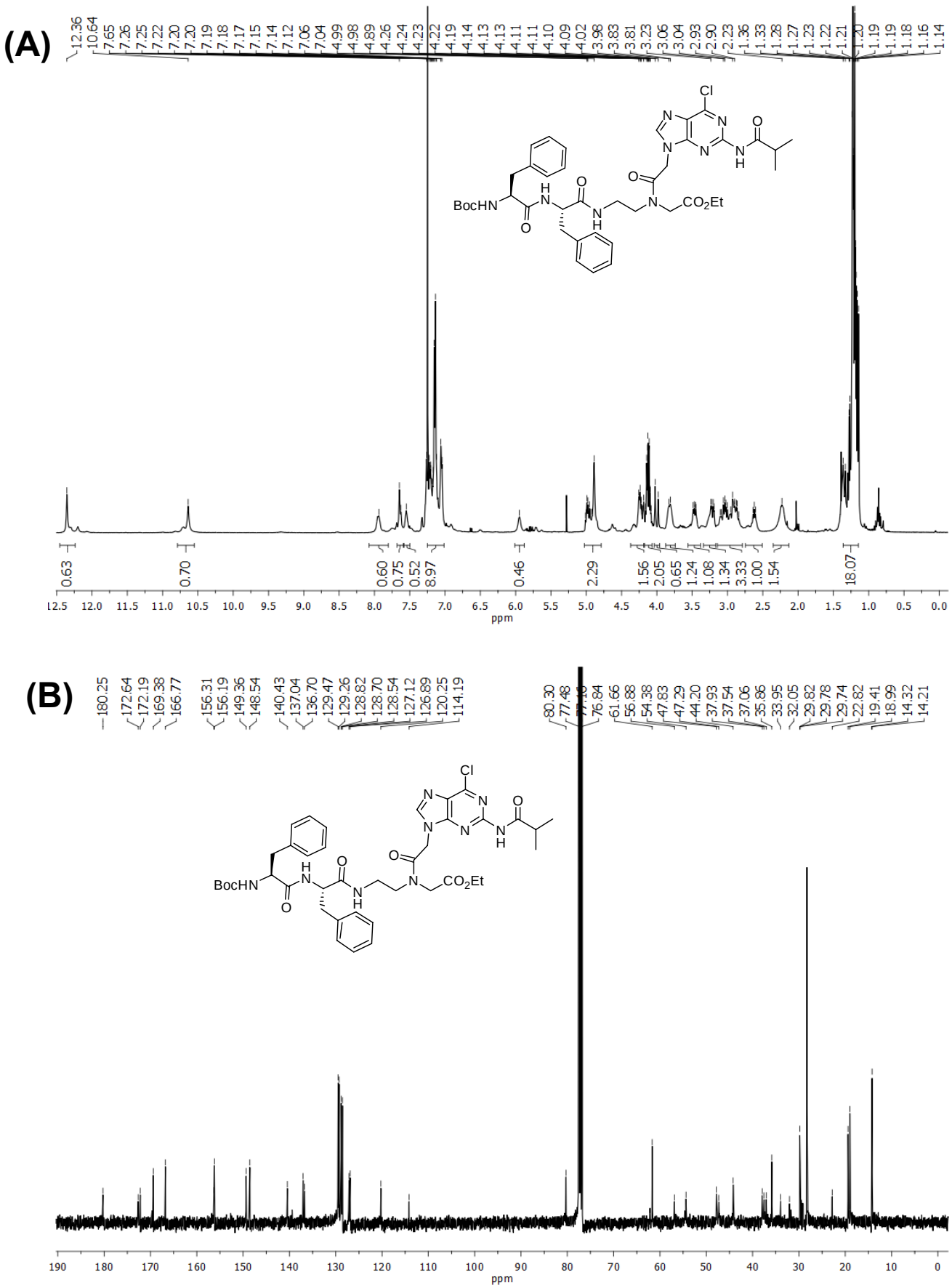

Figure S13: (A) ^{1}H-NMR and (B) ^{13}C-NMR spectra of peptide **3b**

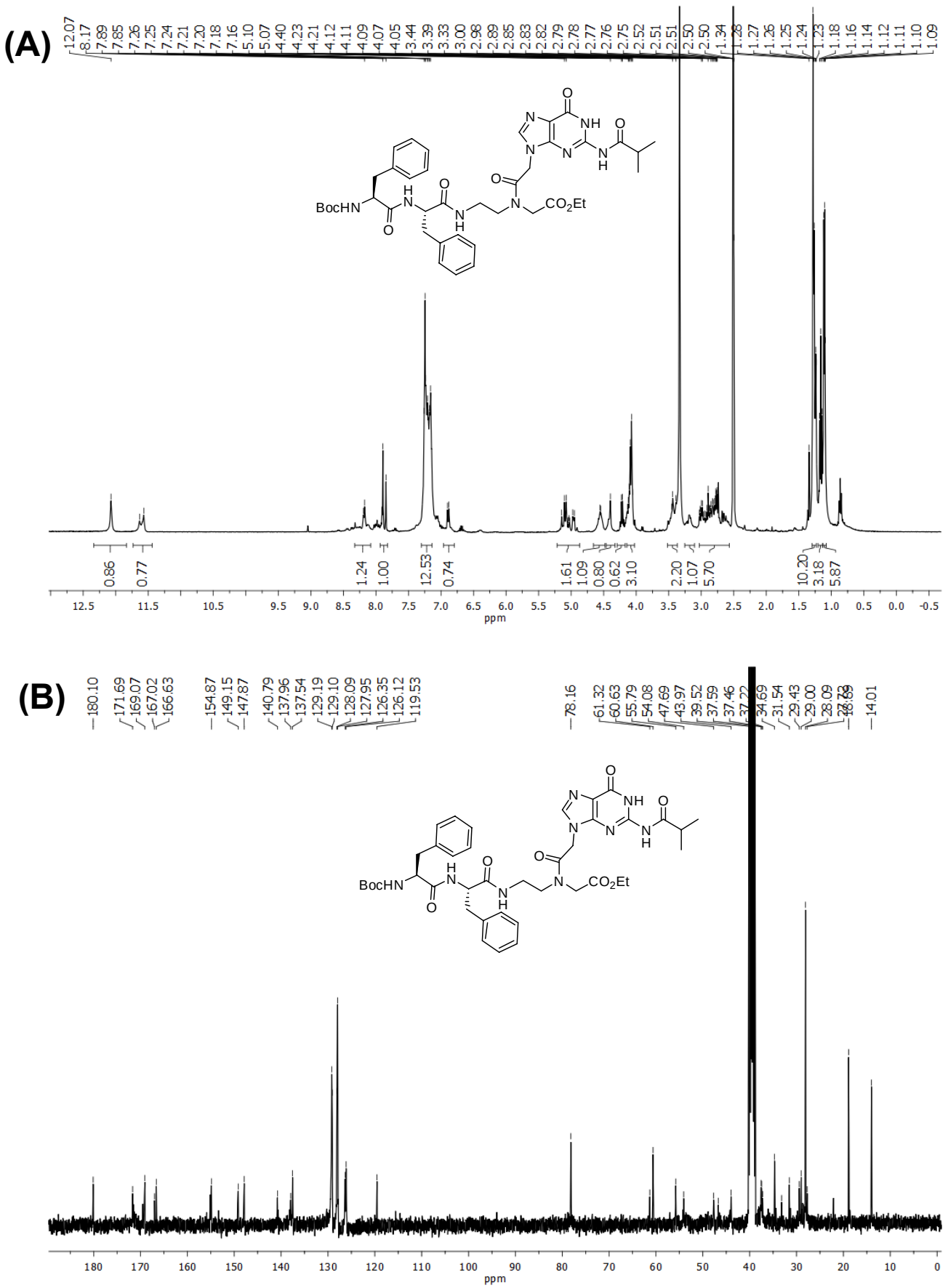

Figure S14: (A) ^{1}H-NMR and (B) ^{13}C-NMR spectra of peptide **3c**

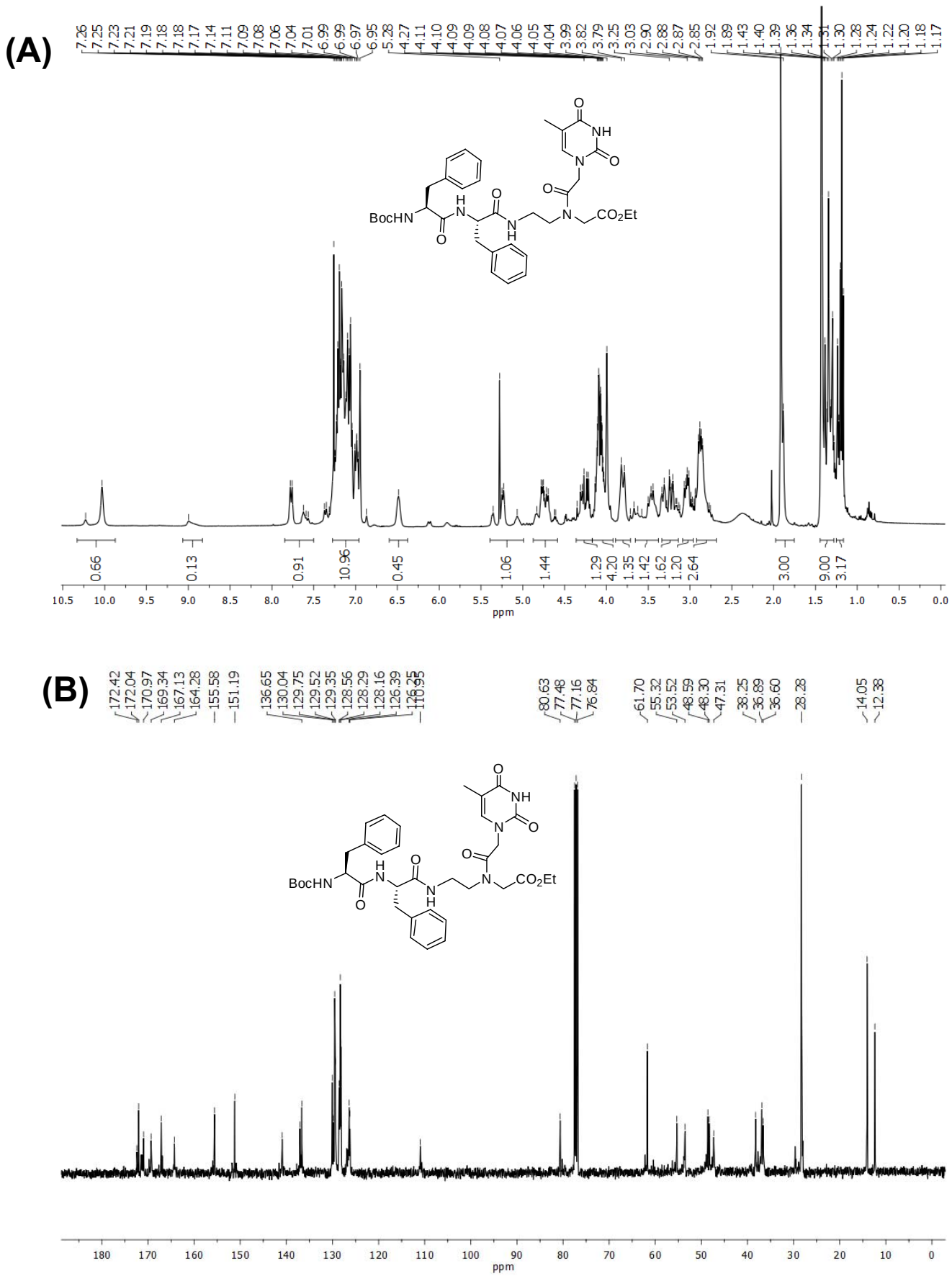

Figure S15: (A) ^{1}H-NMR and (B) ^{13}C-NMR spectra of peptide **3d**

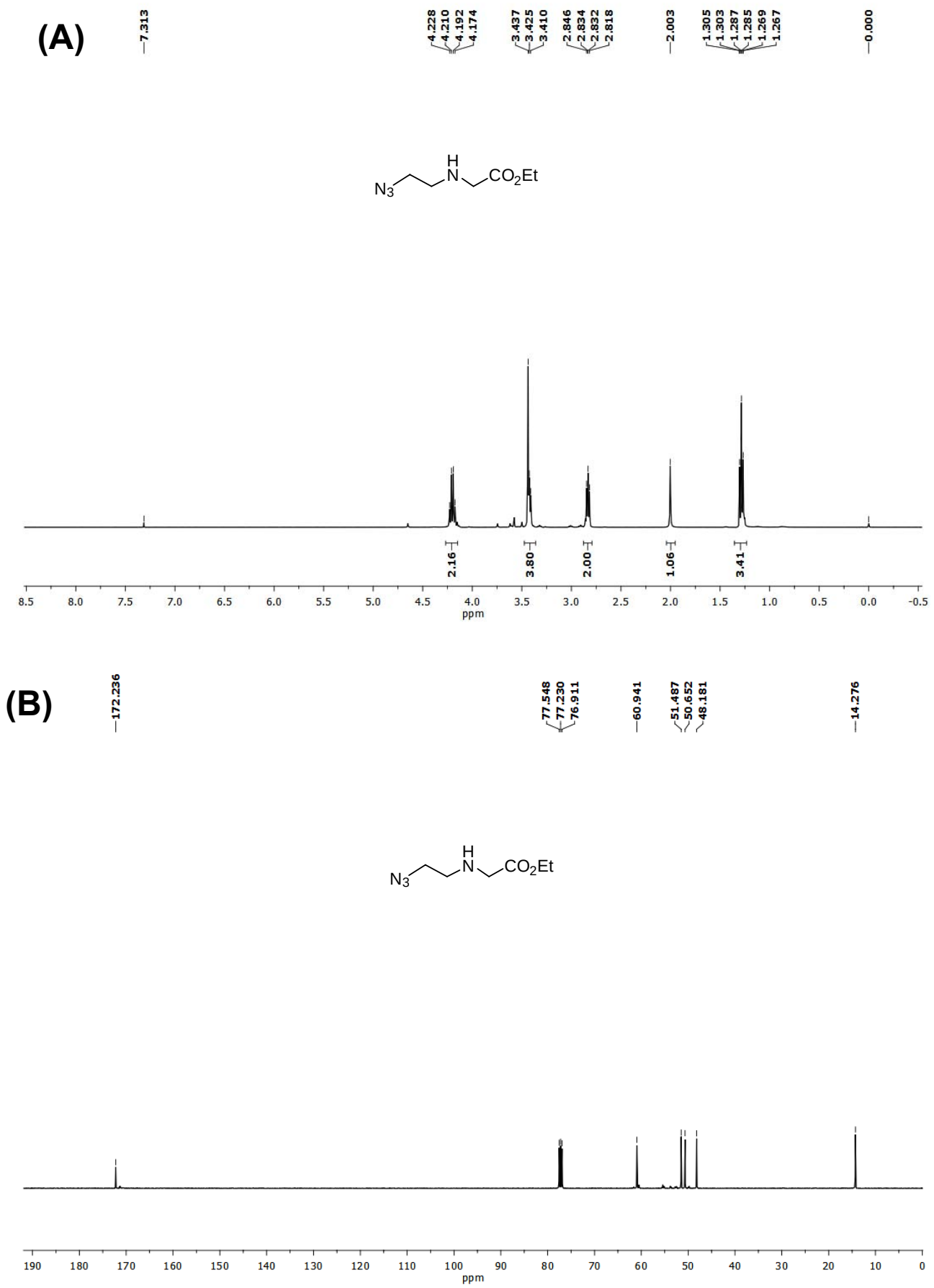

Figure S16: (A) ^{1}H-NMR and (B) ^{13}C-NMR spectra of **9S**

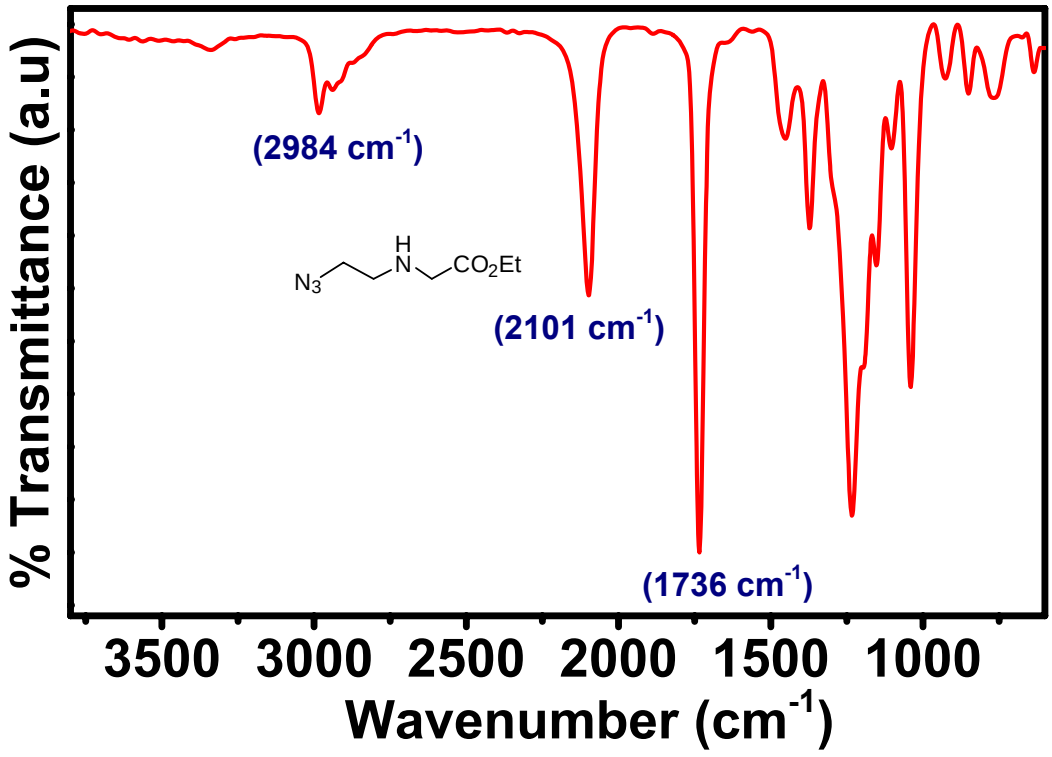

Figure S17: FTIR spectrum of **9S**

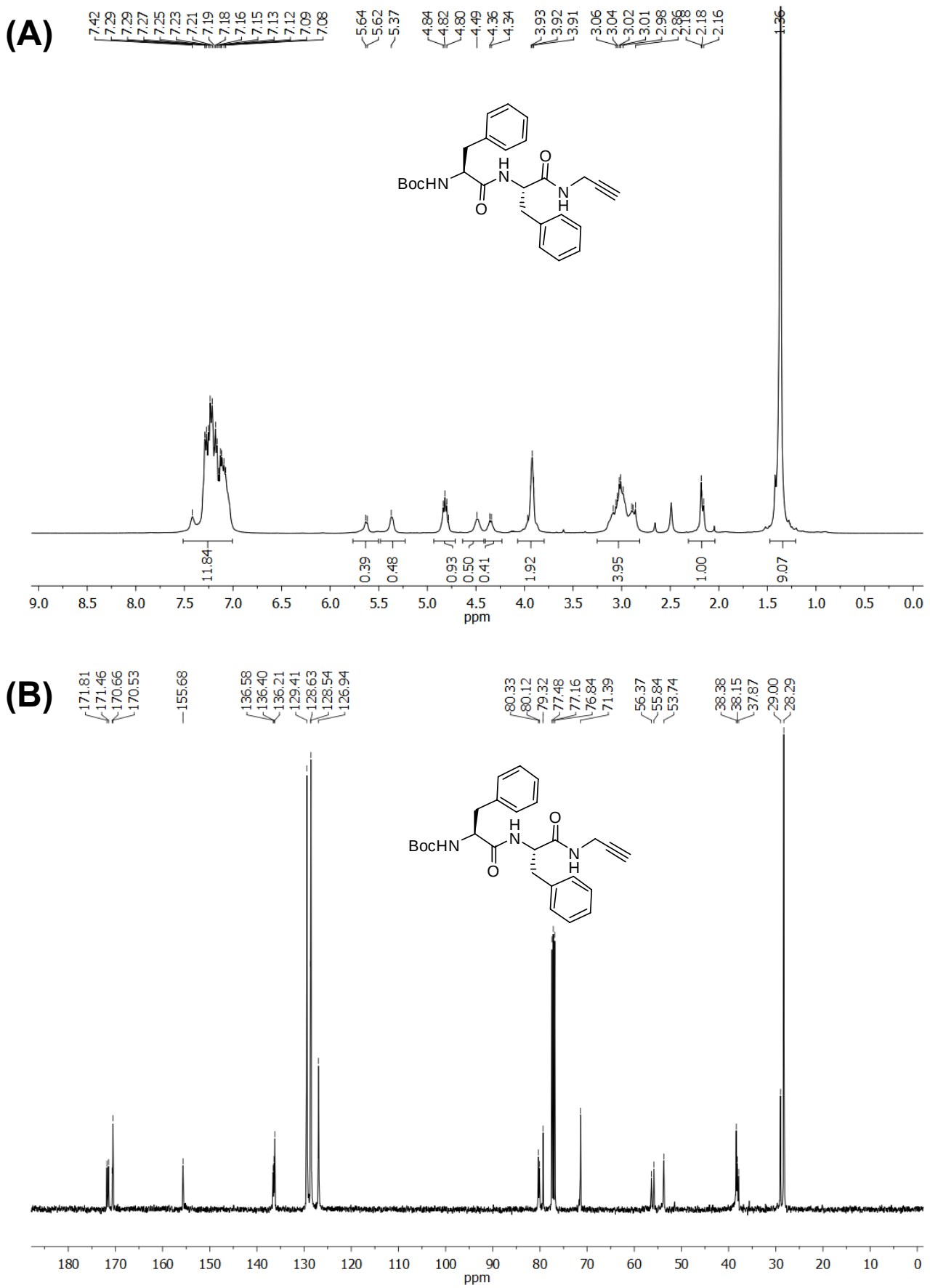

Figure S18: (A) ^{1}H-NMR and (B) ^{13}C-NMR spectra of peptide **4**

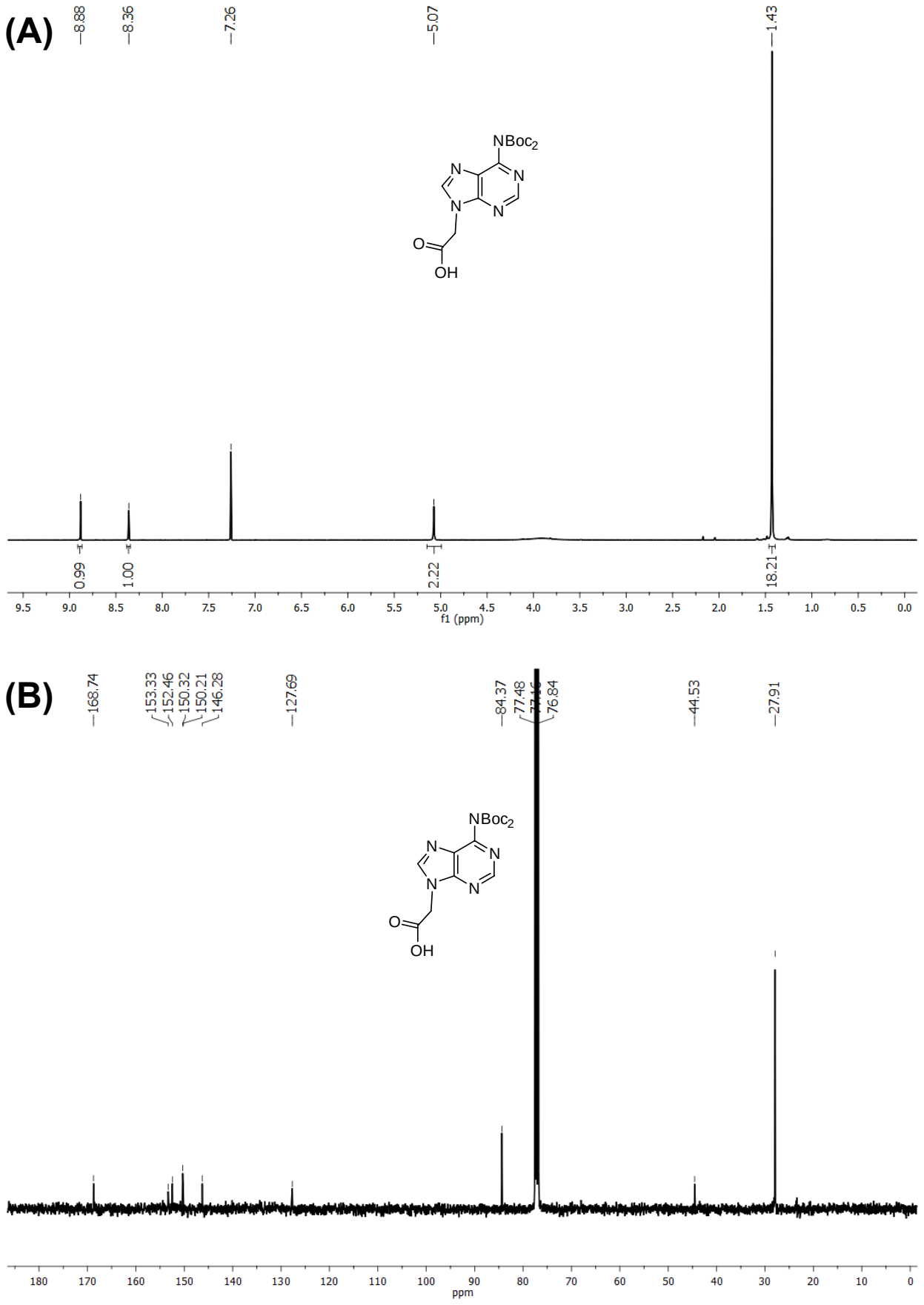

Figure S19: (A) ^{1}H-NMR and (B) ^{13}C-NMR spectra of $\mathbf{A^{N(Boc)_2}}$**-*N*^{9}-acetic acid**

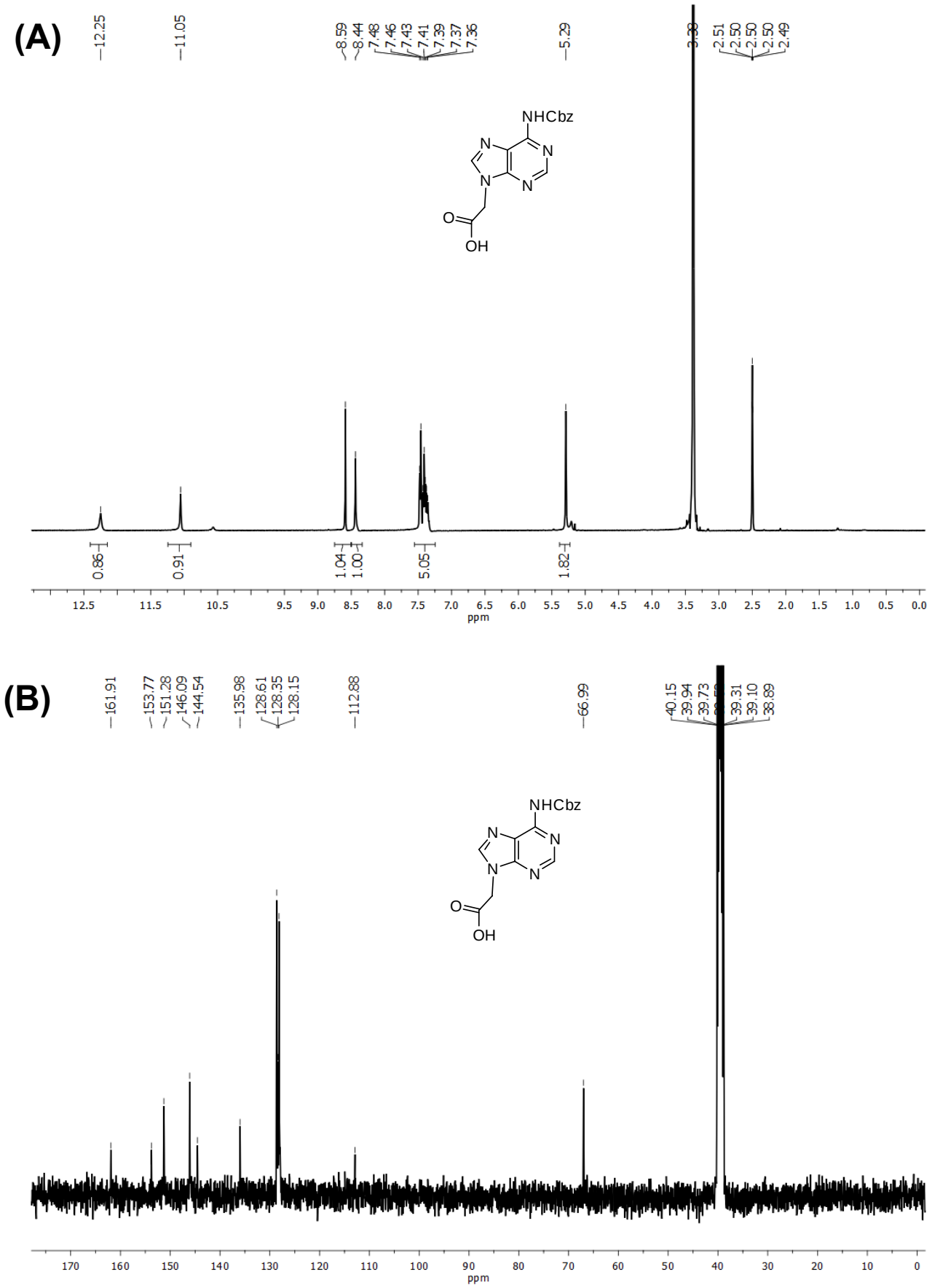

Figure S20: (A) ^{1}H-NMR and (B) ^{13}C-NMR spectra of $\mathbf{A^{NHCbz}}$**-*N*^{9}-acetic acid**

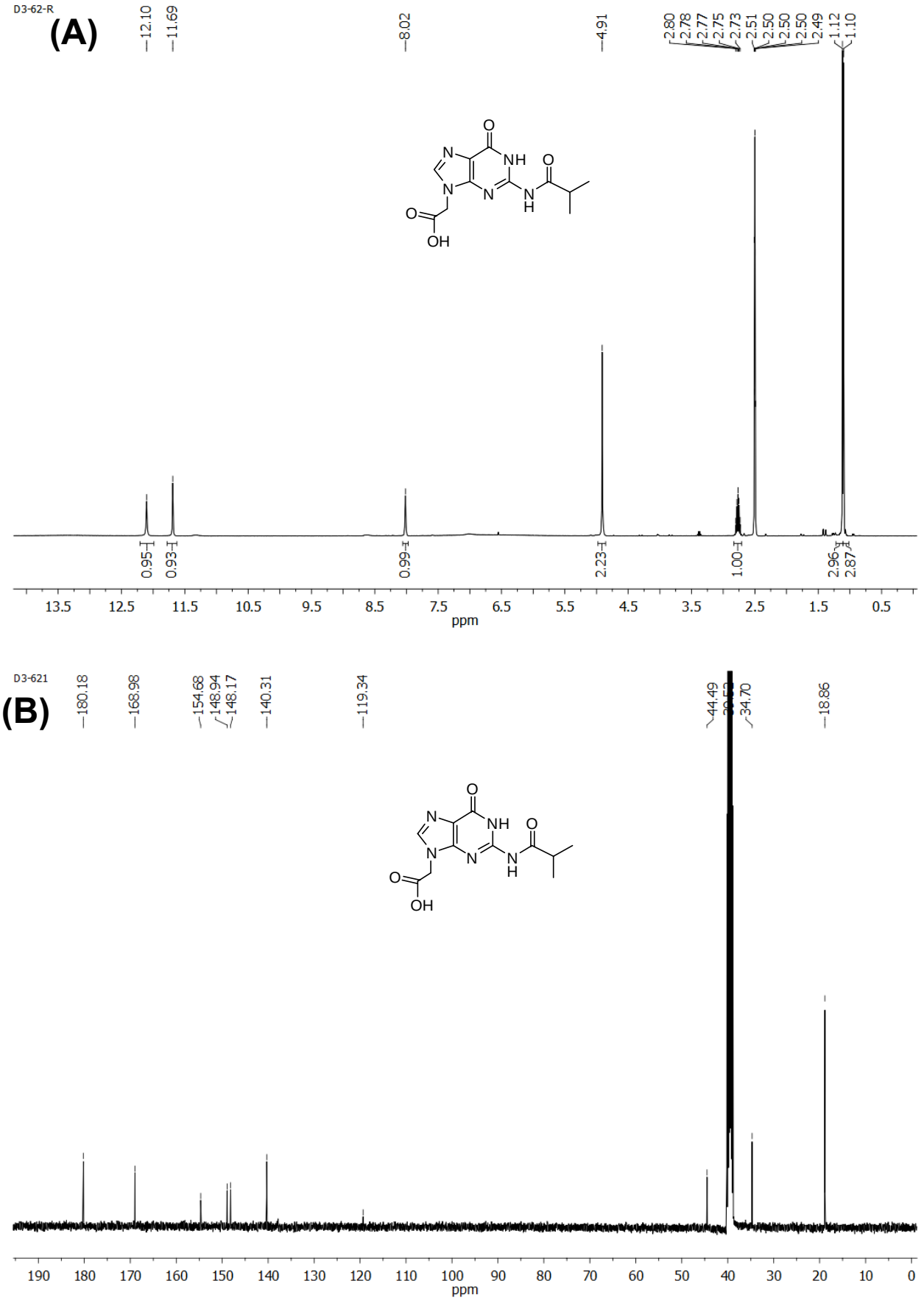

Figure S21: (A) ^{1}H-NMR and (B) ^{13}C-NMR spectra of **G^{ibu}-*N*^{9}-acetic acid**

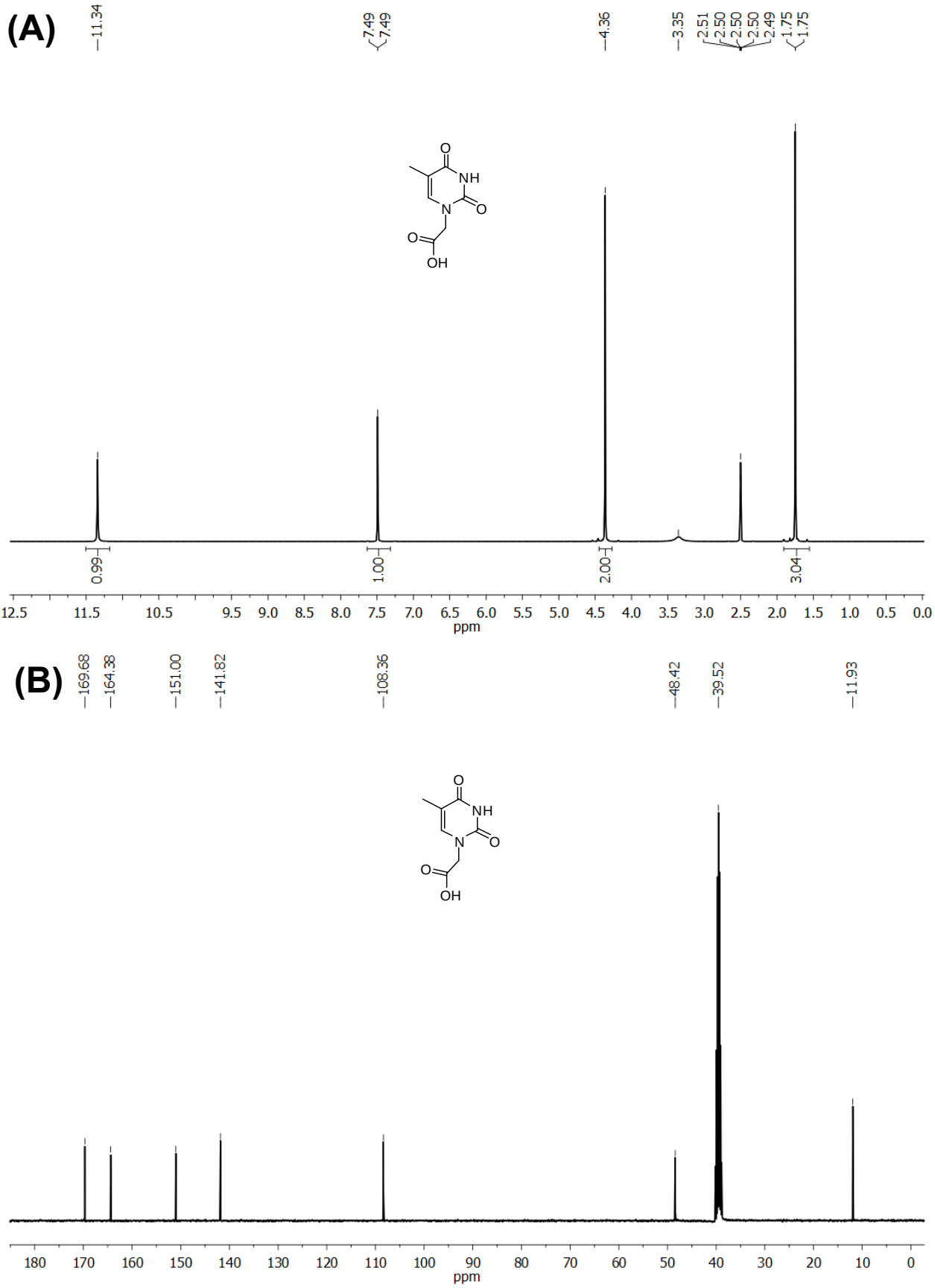

Figure S22: (A) ^{1}H-NMR and (B) ^{13}C-NMR spectra of **Thymine-1-acetic acid**

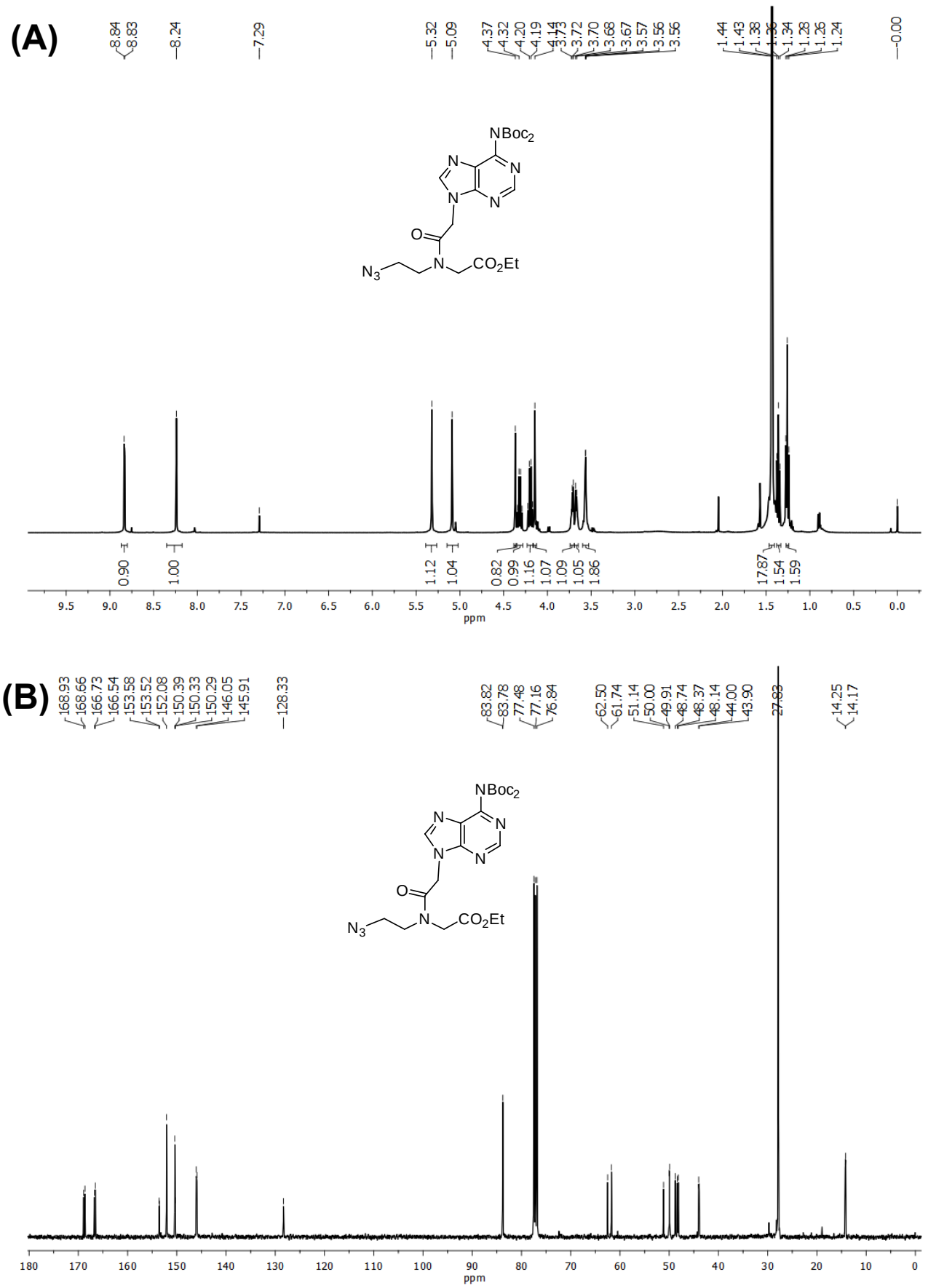

Figure S23: (A) ^{1}H-NMR and (B) ^{13}C-NMR spectra of **5a**

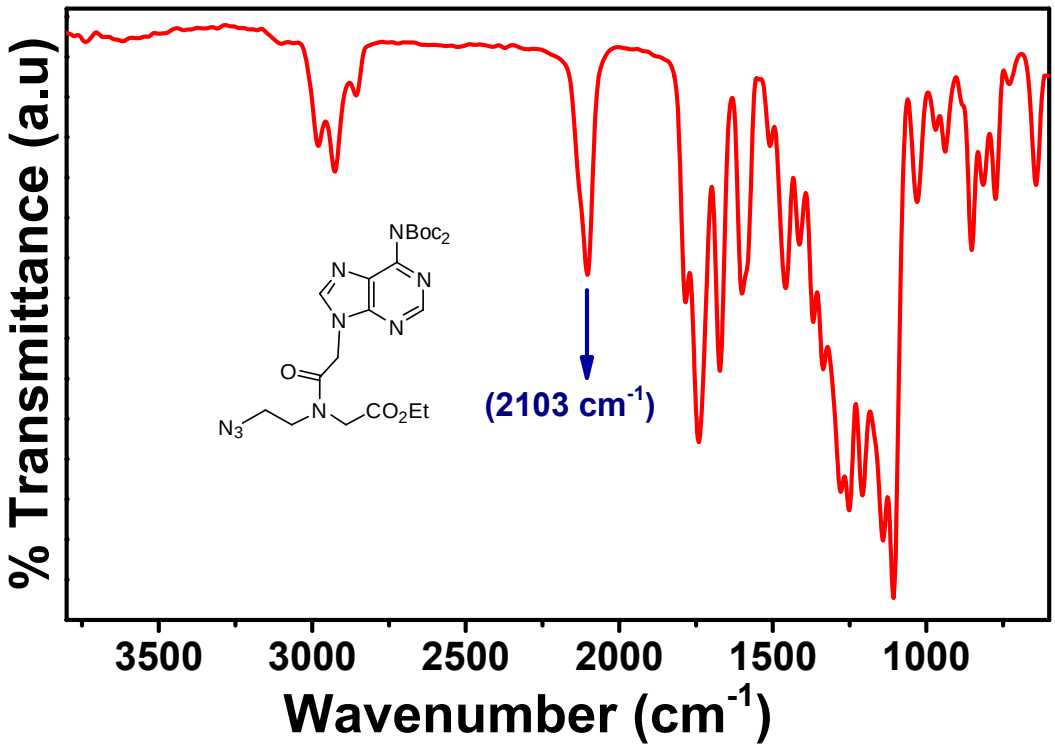

Figure S24: FTIR spectrum of **5a**

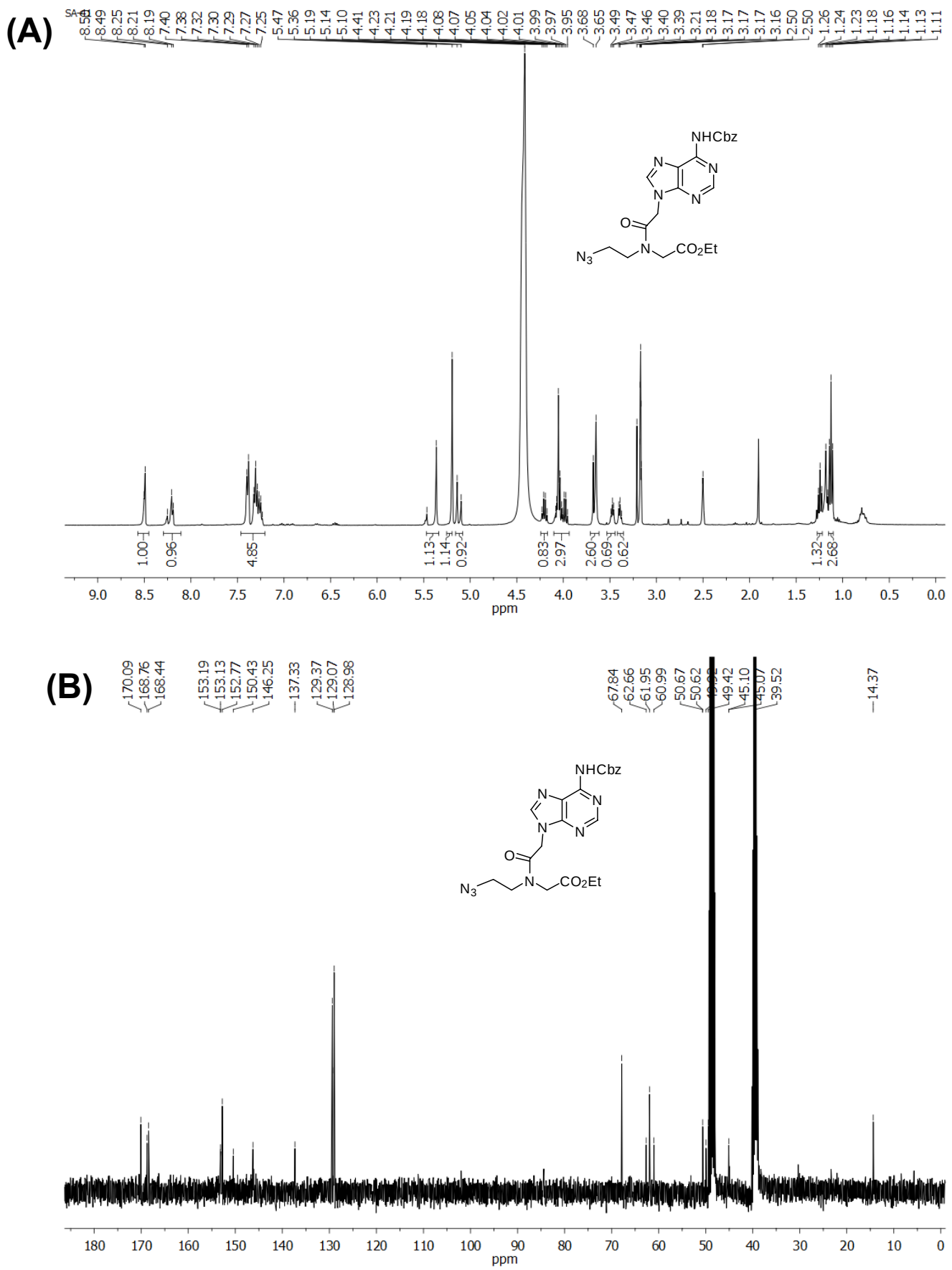

Figure S25: (A) ^{1}H-NMR and (B) ^{13}C-NMR spectra of **5b**

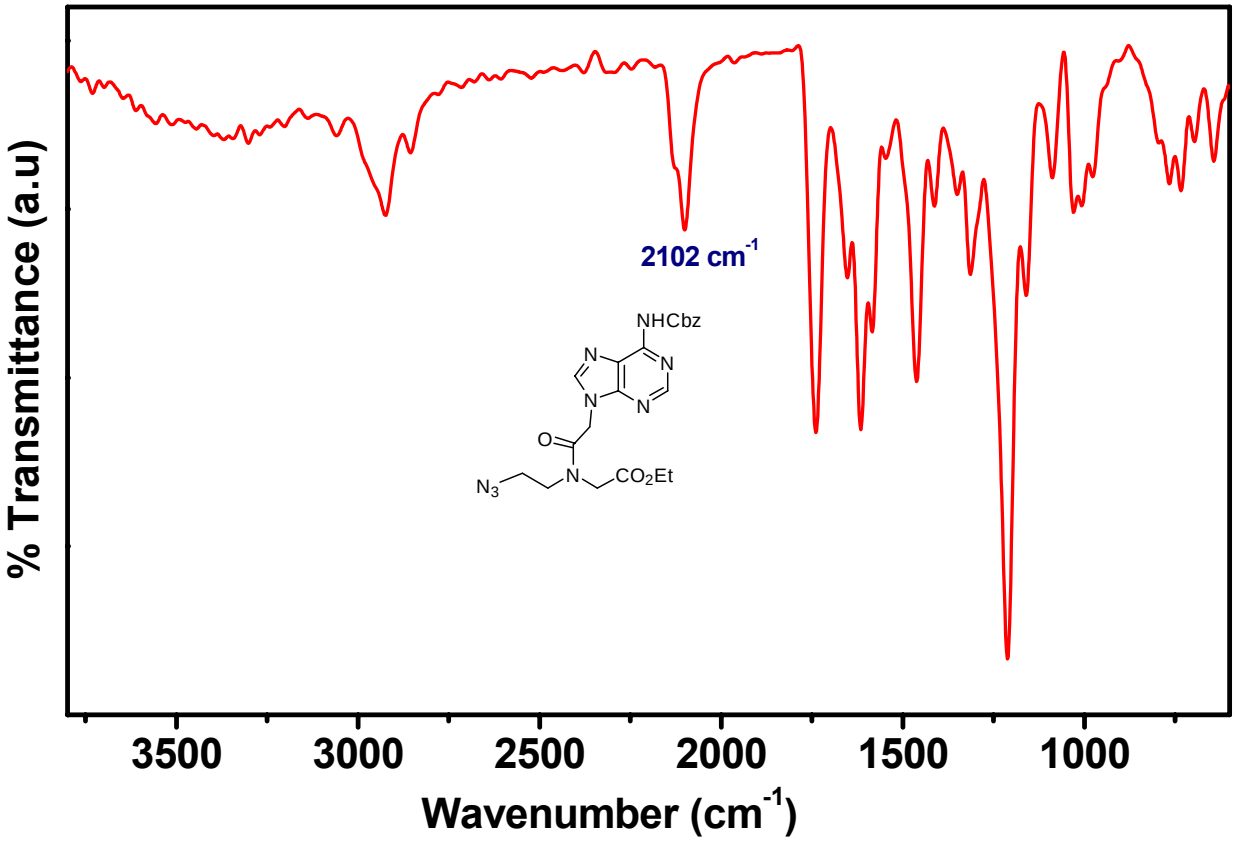

Figure S26: FTIR spectrum of **5b**

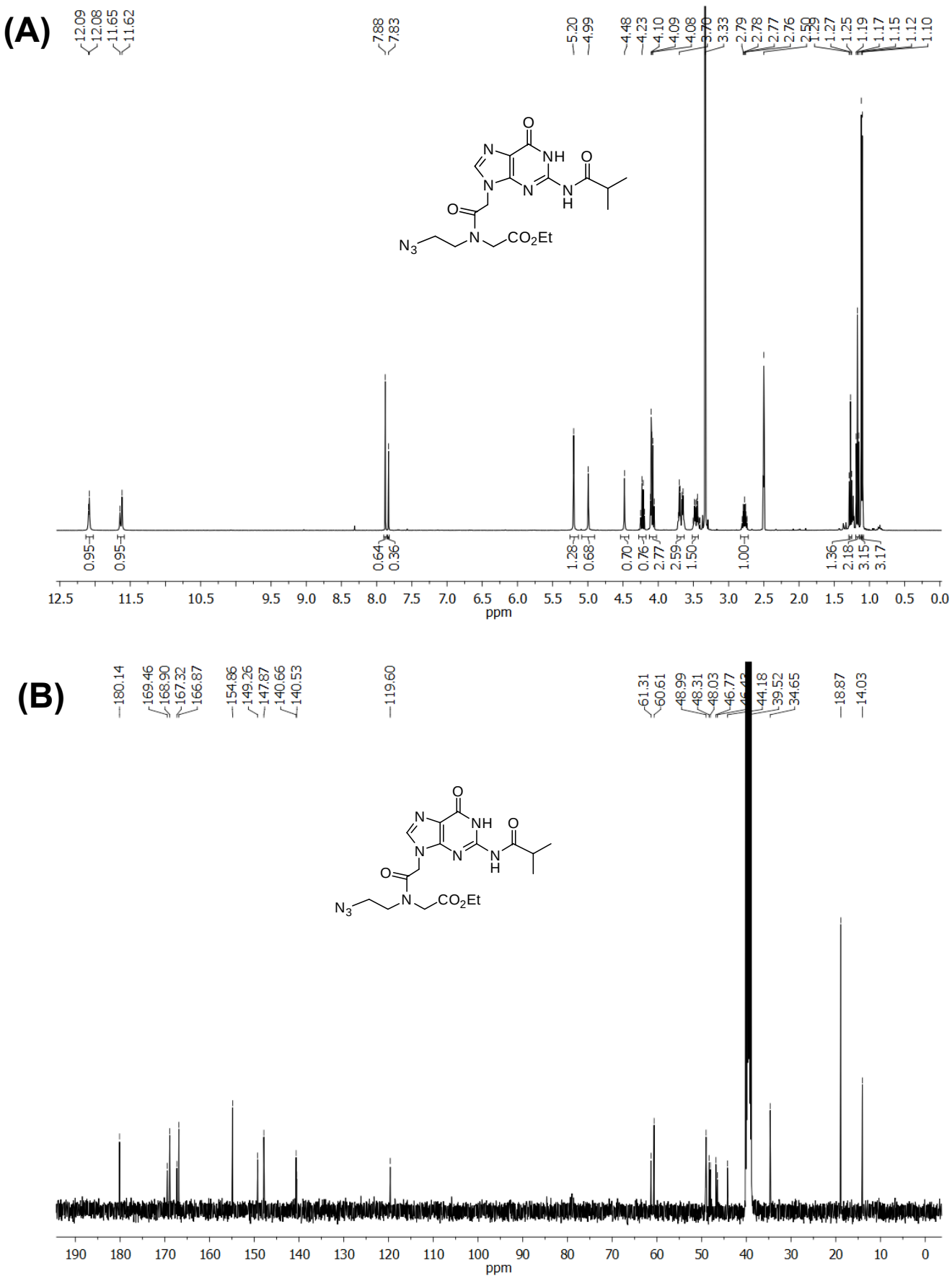

Figure S27: (A) ^{1}H-NMR and (B) ^{13}C-NMR spectra of **5c**

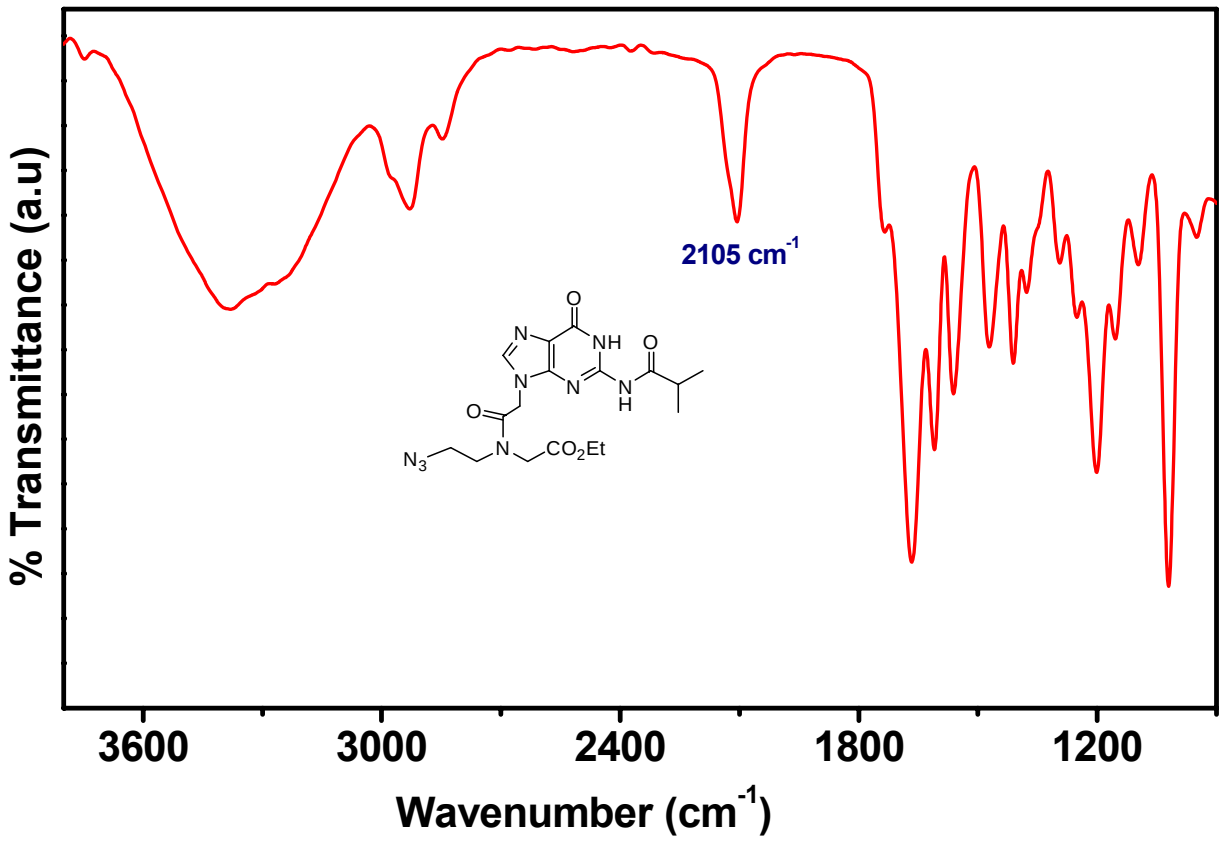

Figure S28: FTIR spectrum of **5c**

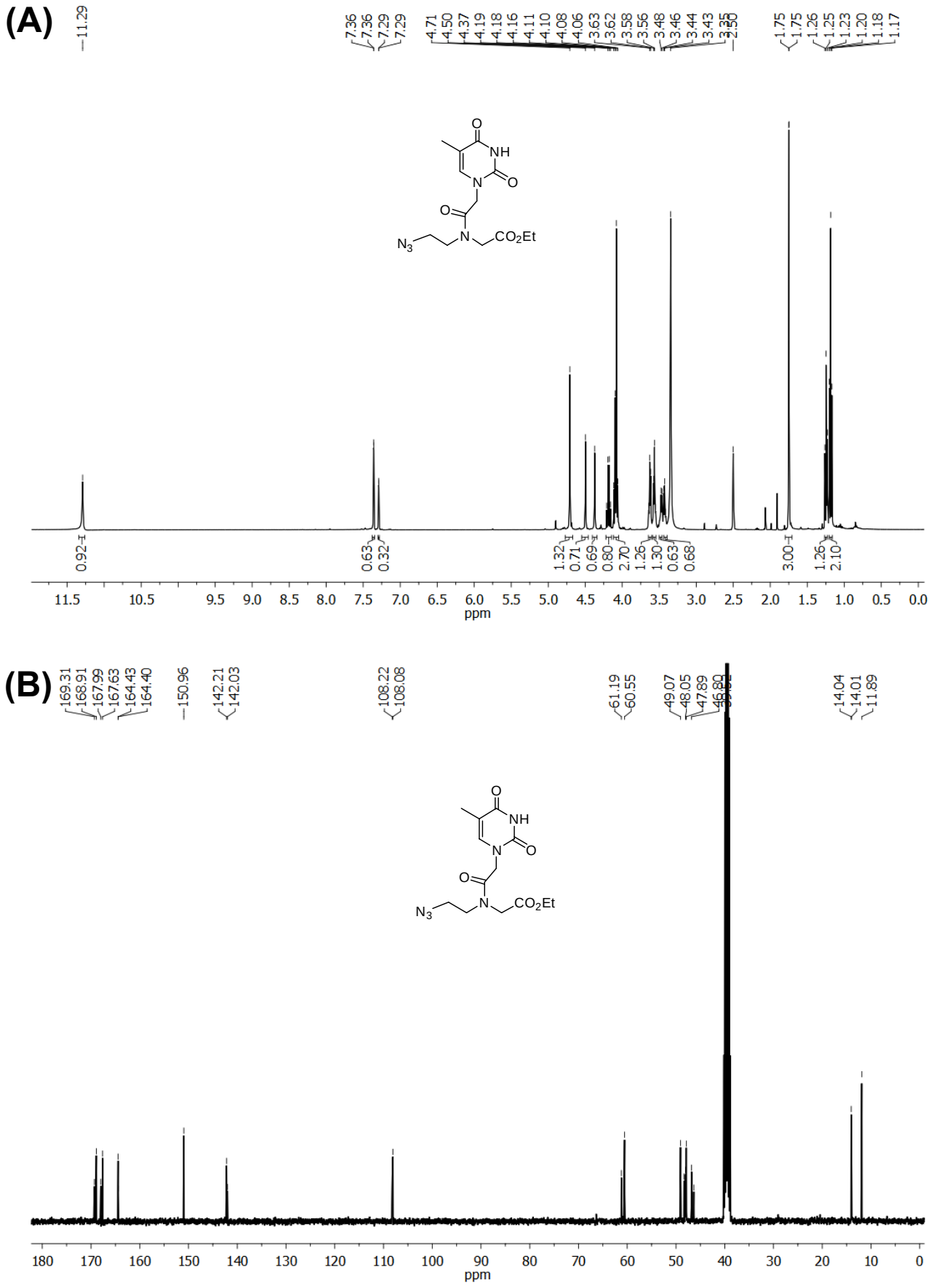

Figure S29: (A) ^{1}H-NMR and (B) ^{13}C-NMR spectra of **5d**

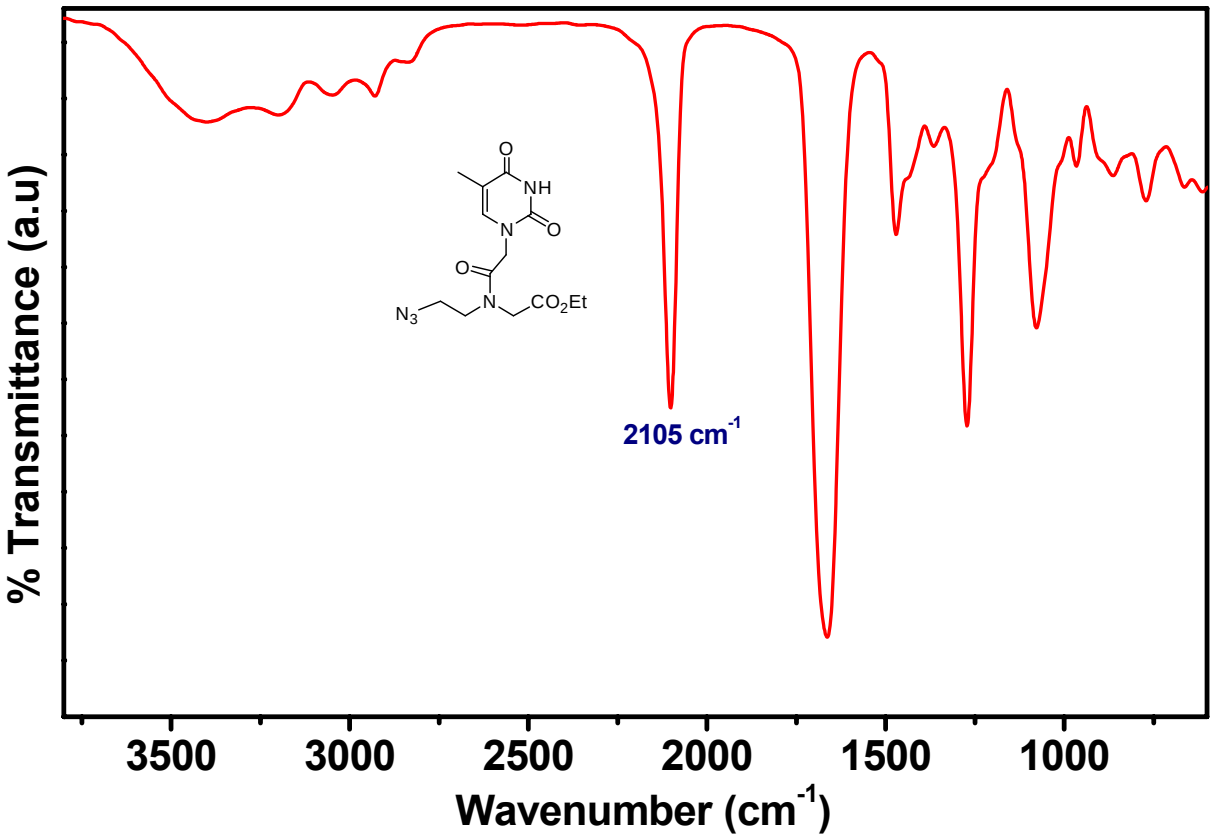

Figure S30: FTIR spectrum of **5d**

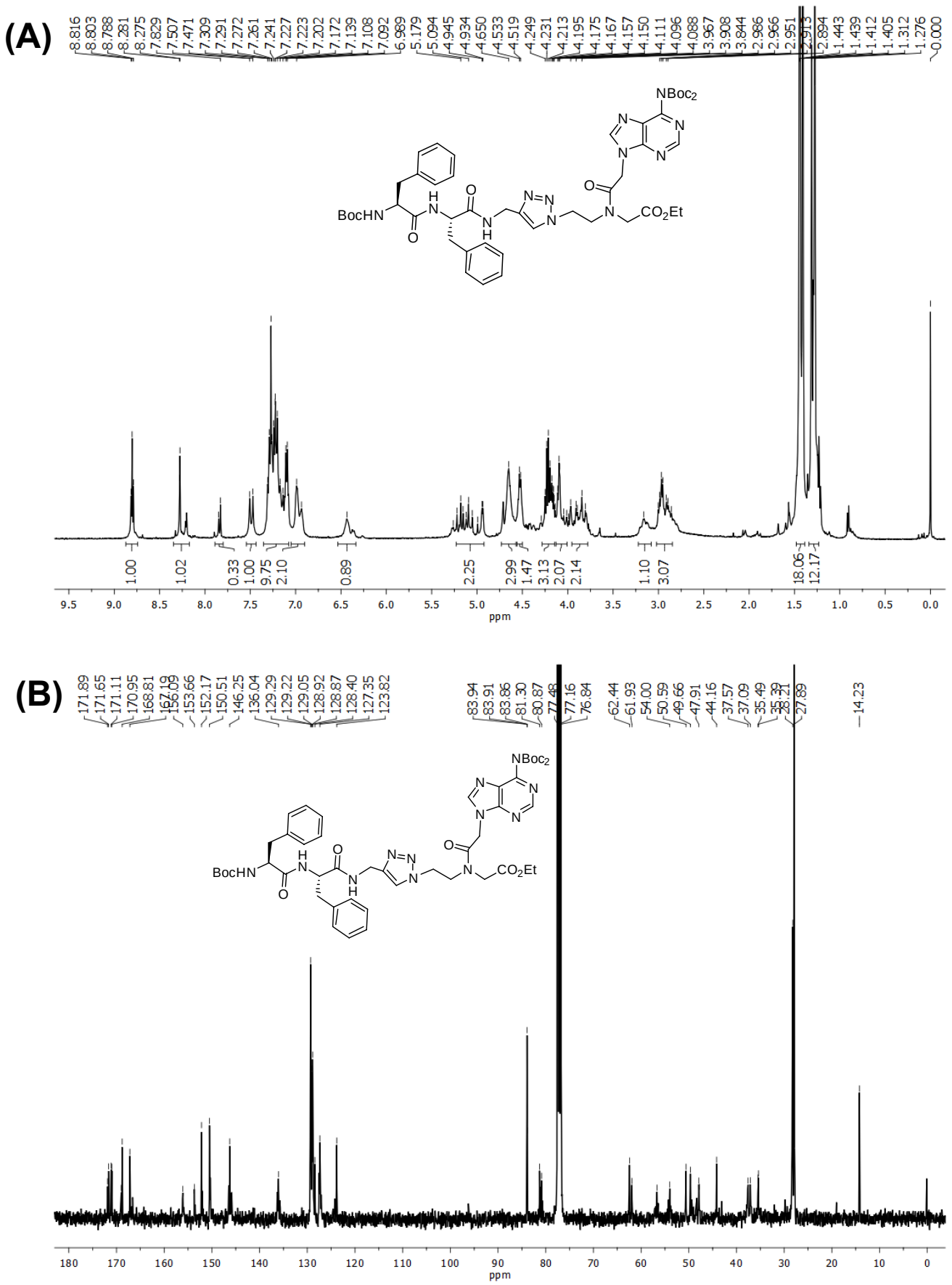

Figure S31: (A) ^{1}H-NMR and (B) ^{13}C-NMR spectra of peptide **6a**

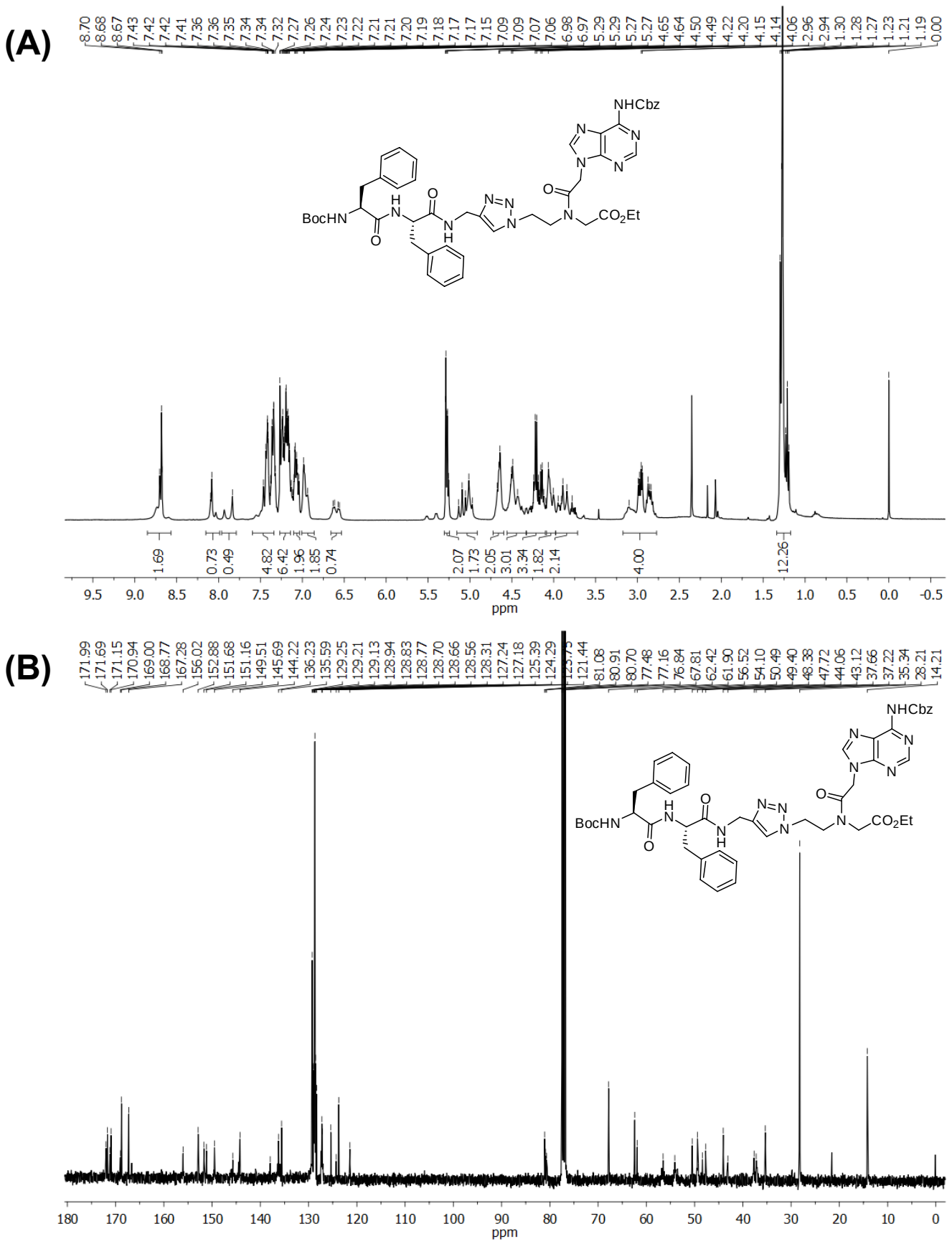

Figure S32: (A) ^{1}H-NMR and (B) ^{13}C-NMR spectra of peptide **6b**

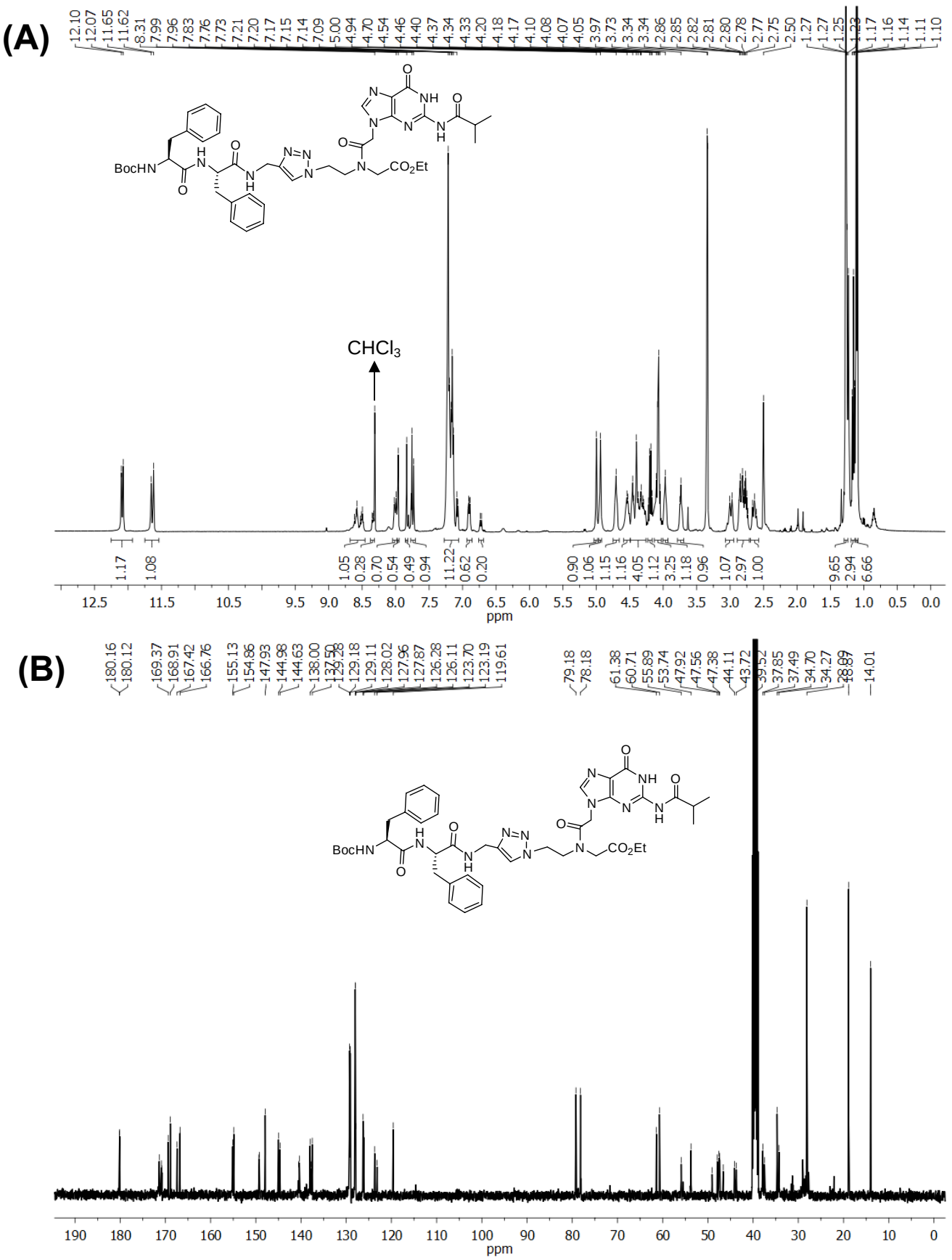

Figure S33: (A) ^{1}H-NMR and (B) ^{13}C-NMR spectra of peptide **6c**

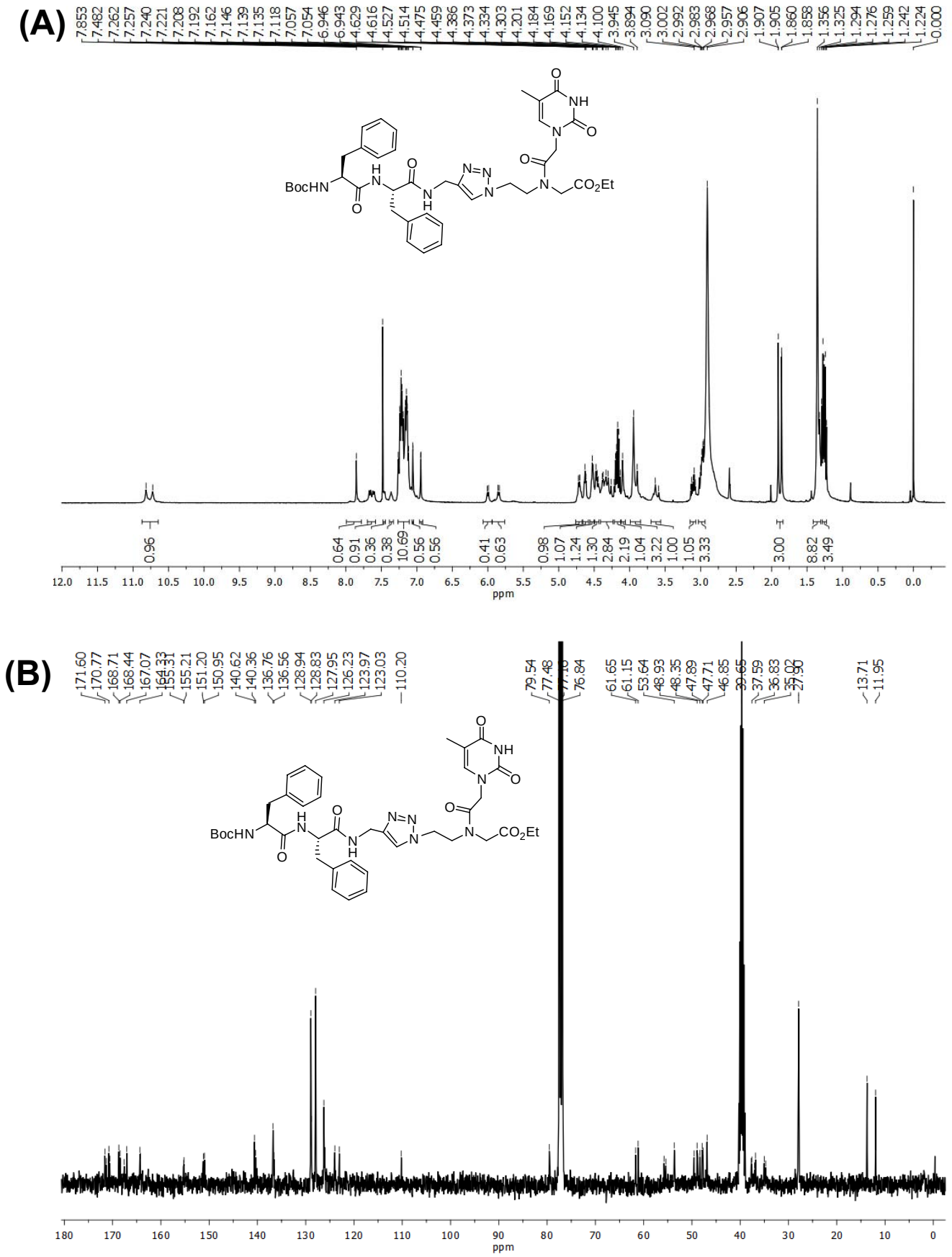

Figure S34: (A) ^{1}H-NMR and (B) ^{13}C-NMR spectra of peptide **6d**

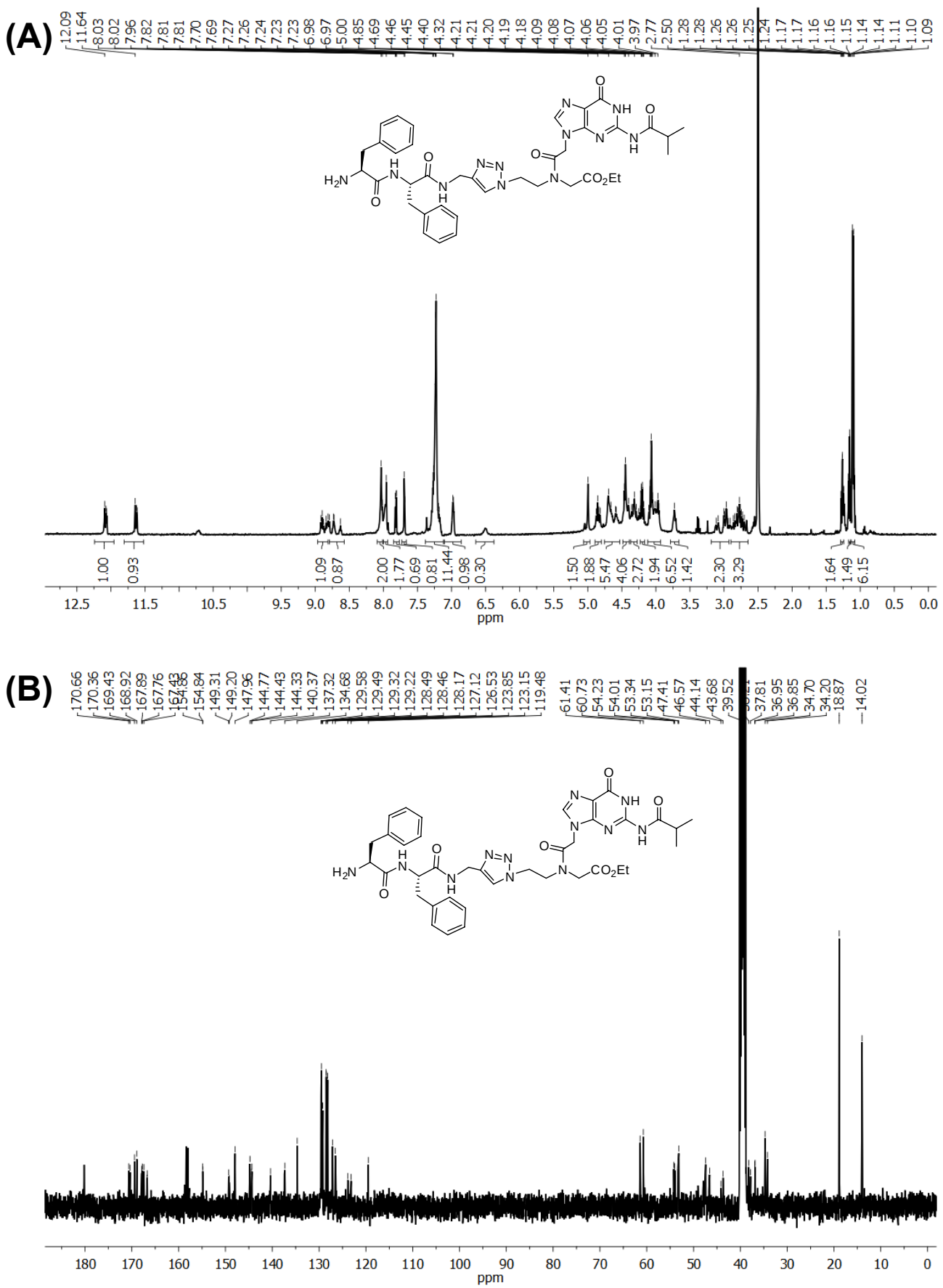

Figure S35: (A) ^{1}H-NMR and (B) ^{13}C-NMR spectra of peptide **7c**

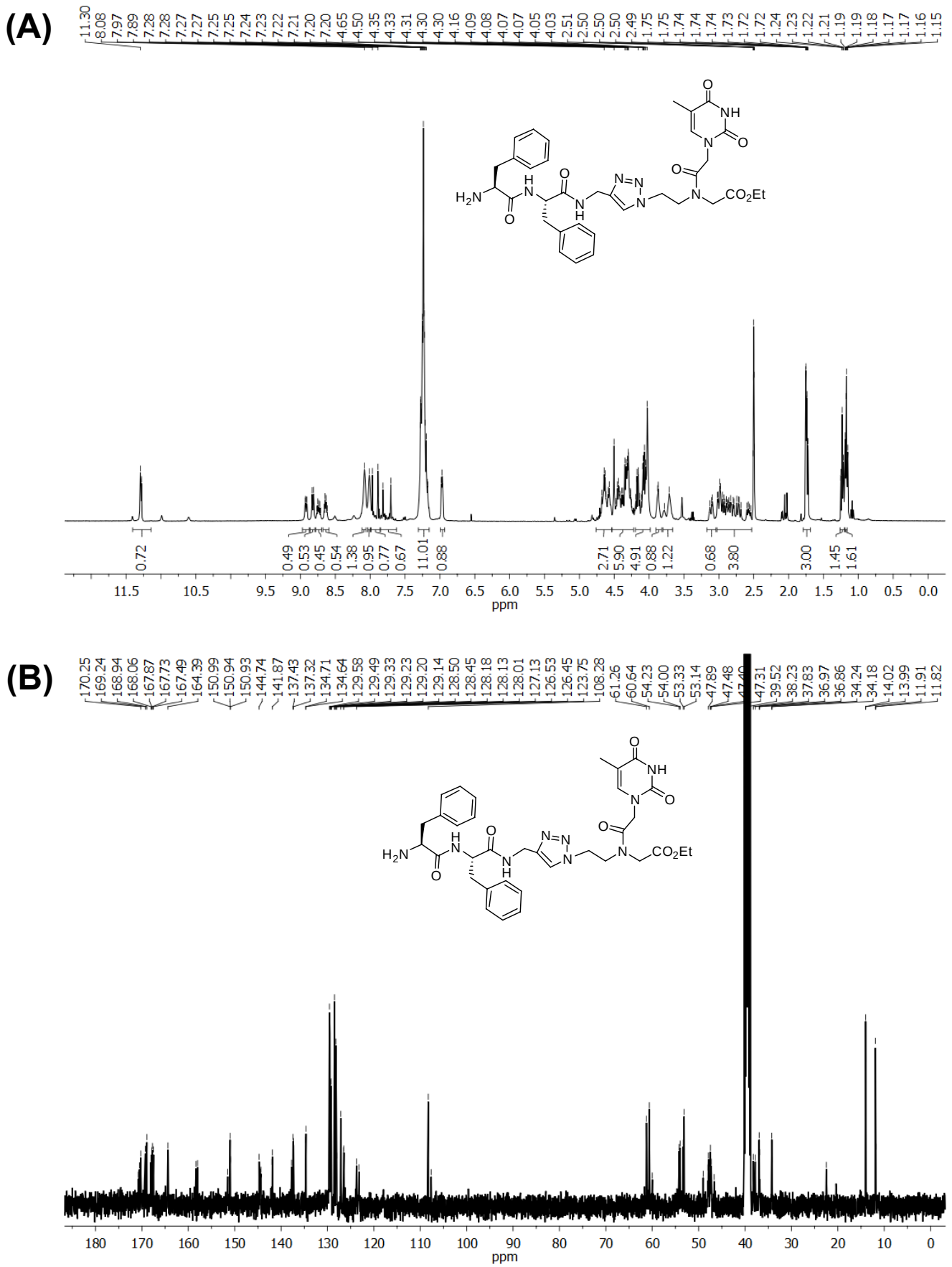

Figure S36: (A) ^{1}H-NMR and (B) ^{13}C-NMR spectra of nucleopeptide **7d**

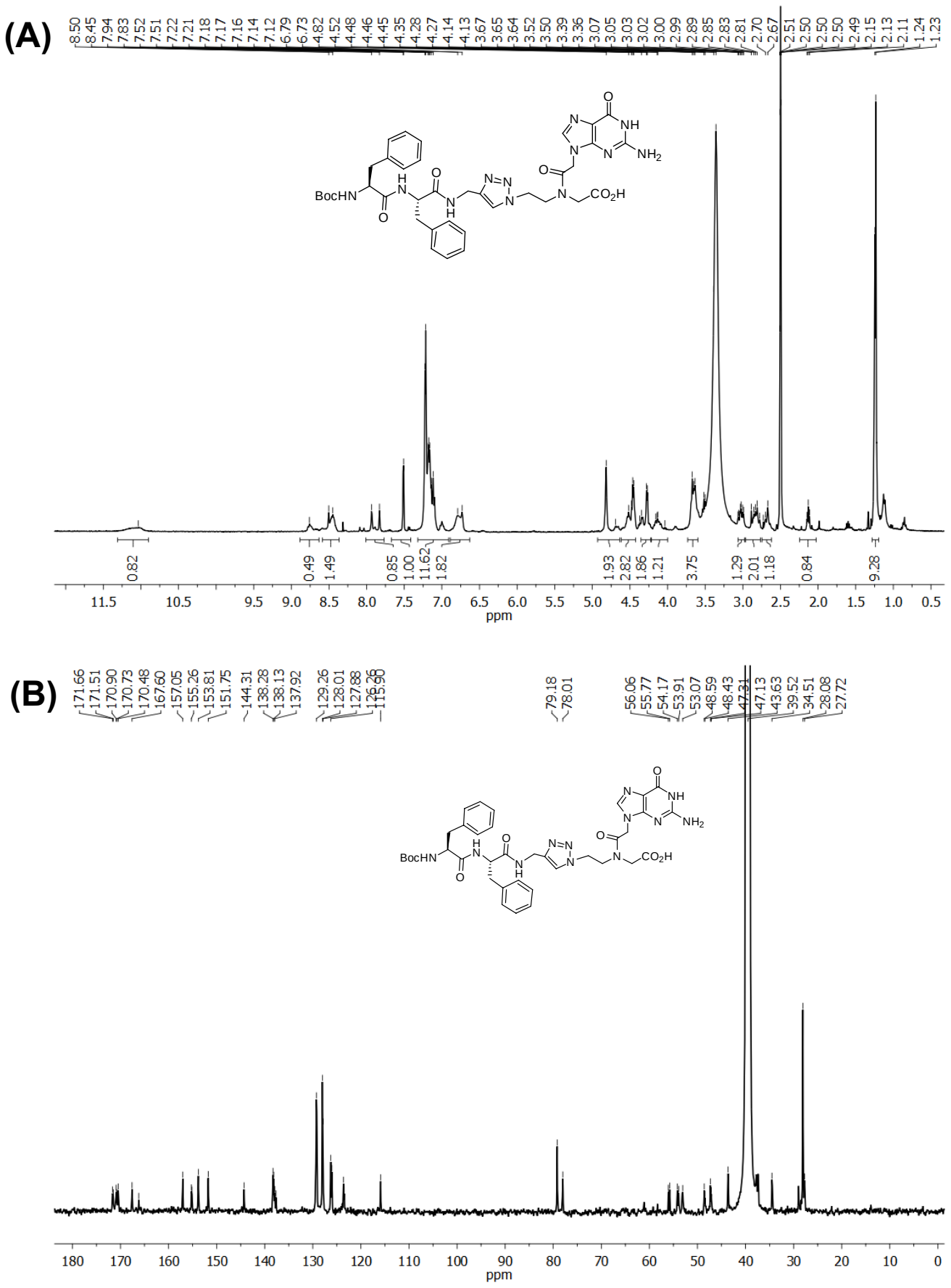

Figure S37: (A) ^{1}H-NMR and (B) ^{13}C-NMR spectra of nucleopeptide **8c**

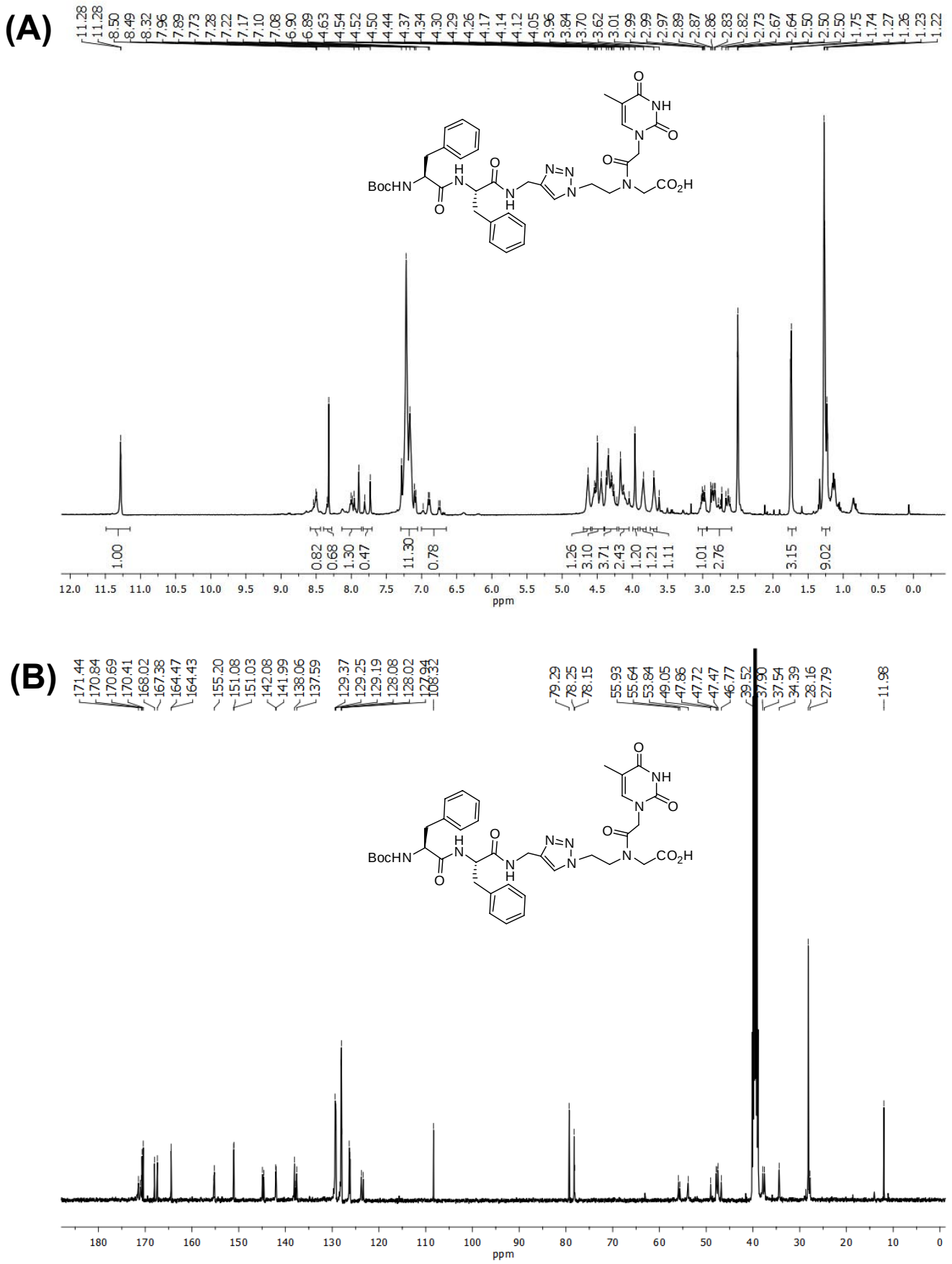

Figure S38: (A) ^{1}H-NMR and (B) ^{13}C-NMR spectra of peptide **8d**

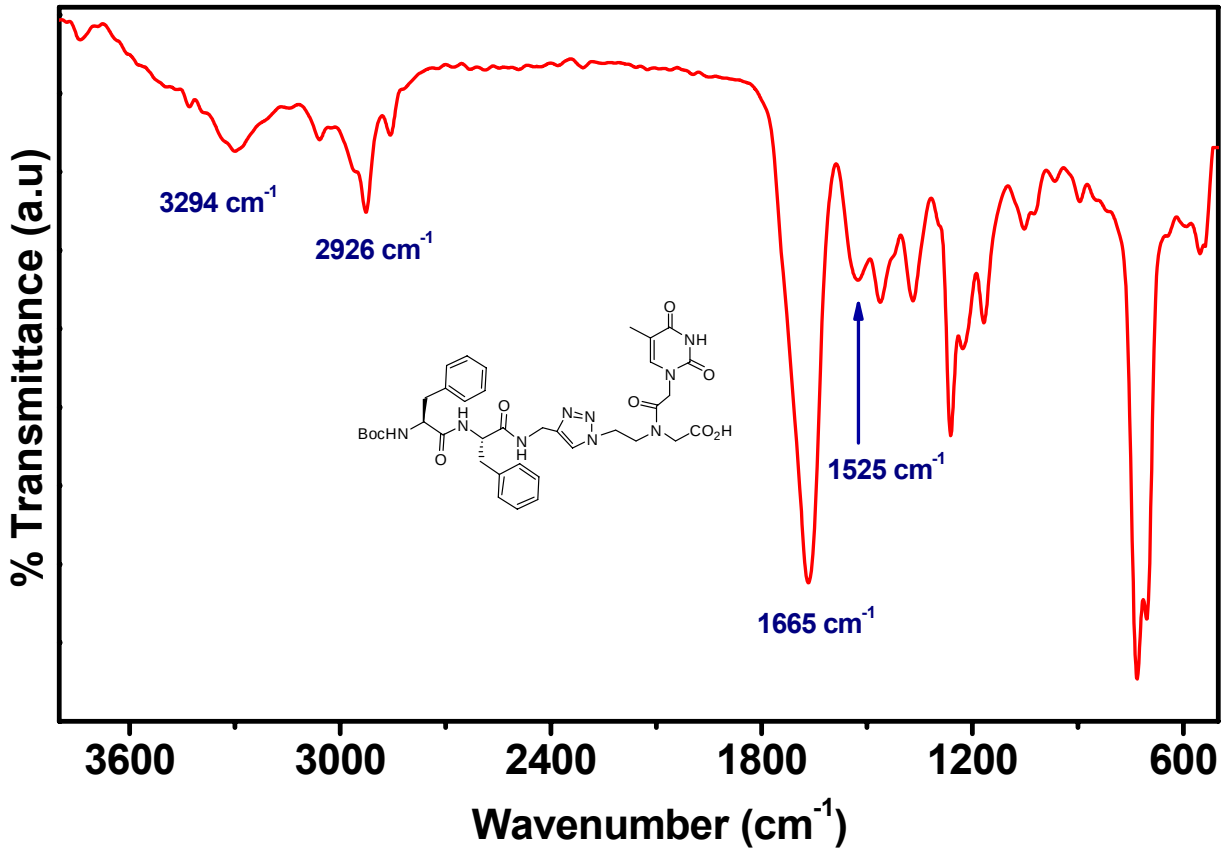

Figure S39: FTIR spectrum of **8d**

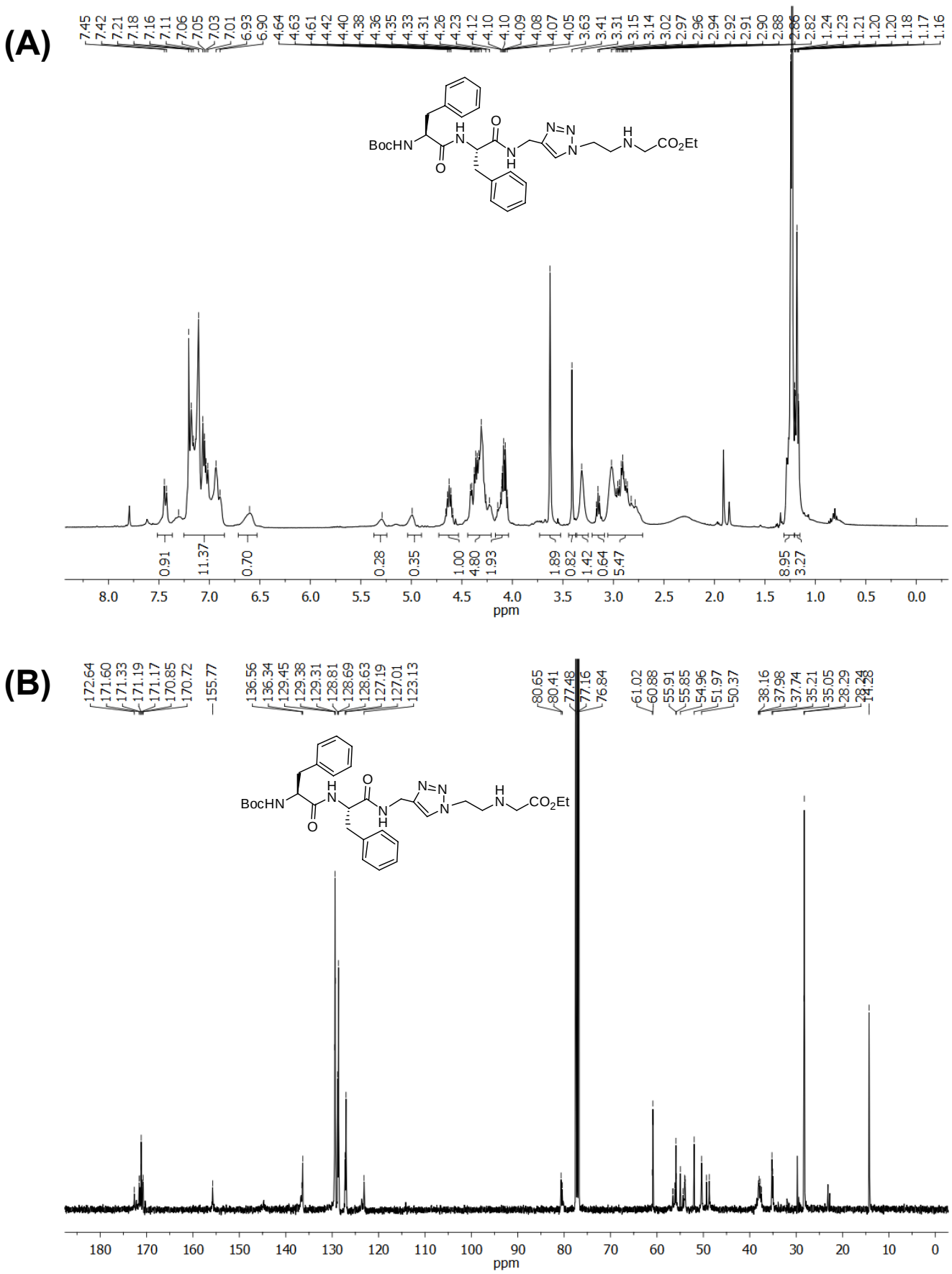

Figure S40: (A) ^{1}H-NMR and (B) ^{13}C-NMR spectra of **9**

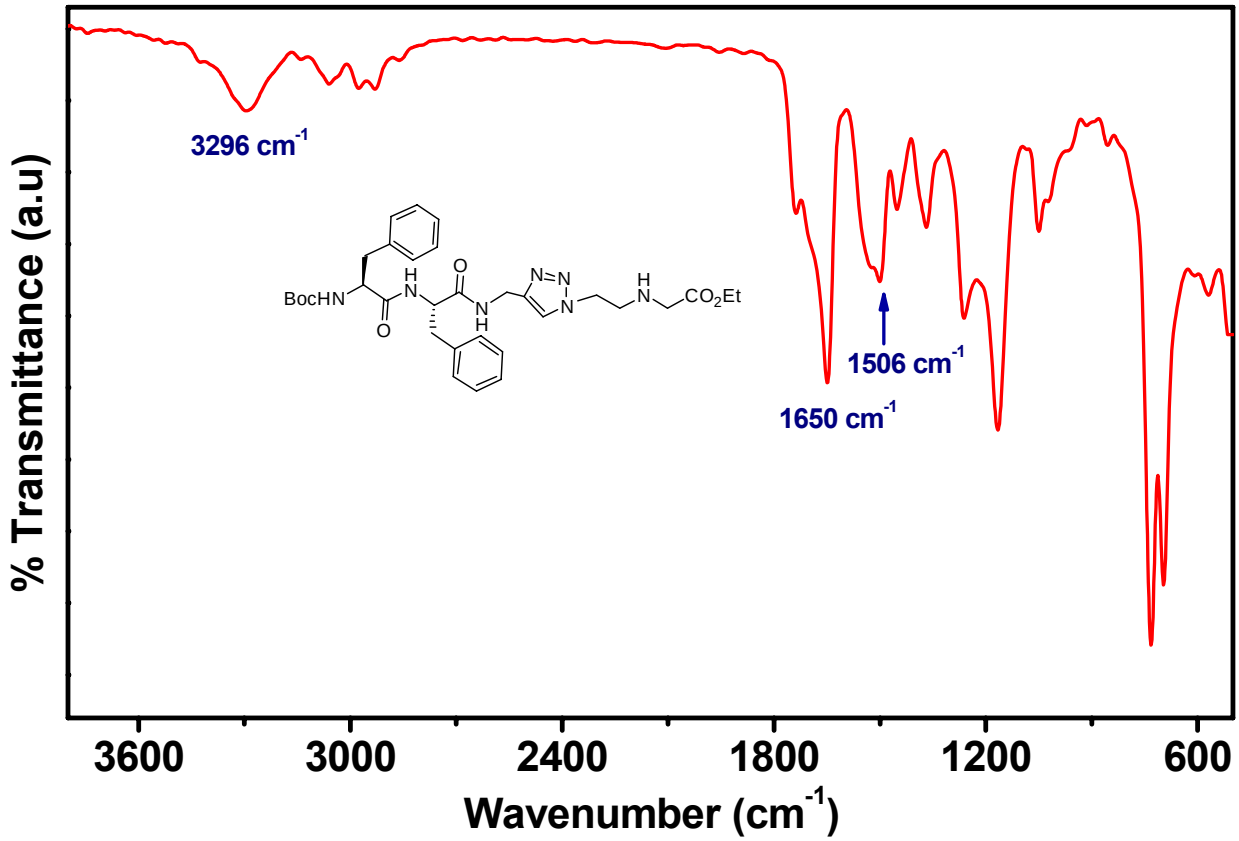

Figure S41: FTIR spectrum of **9**

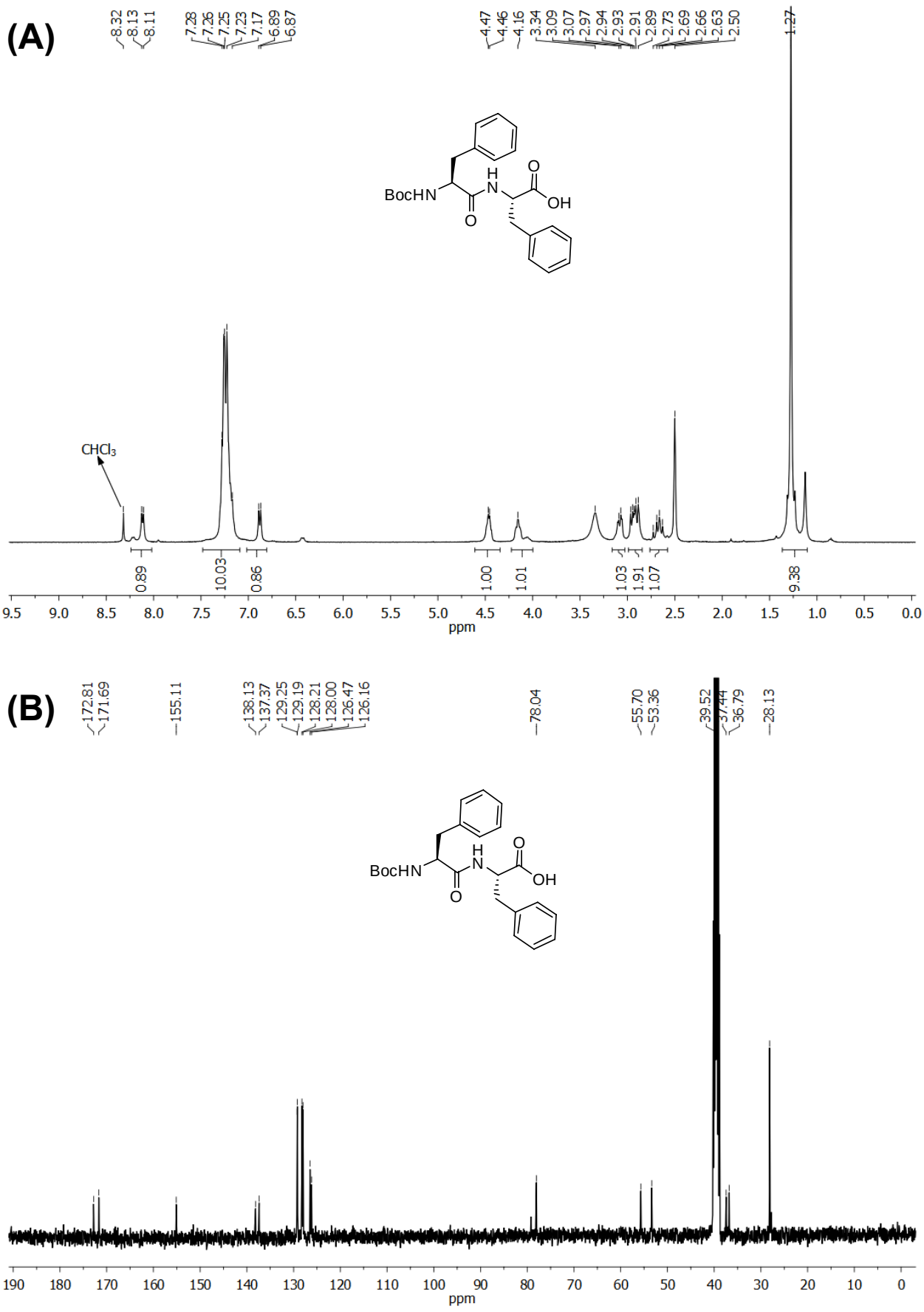

Figure S42: (A) ^{1}H-NMR and (B) ^{13}C NMR of **Boc-Phe-Phe-OH** (in DMSO-d_6)

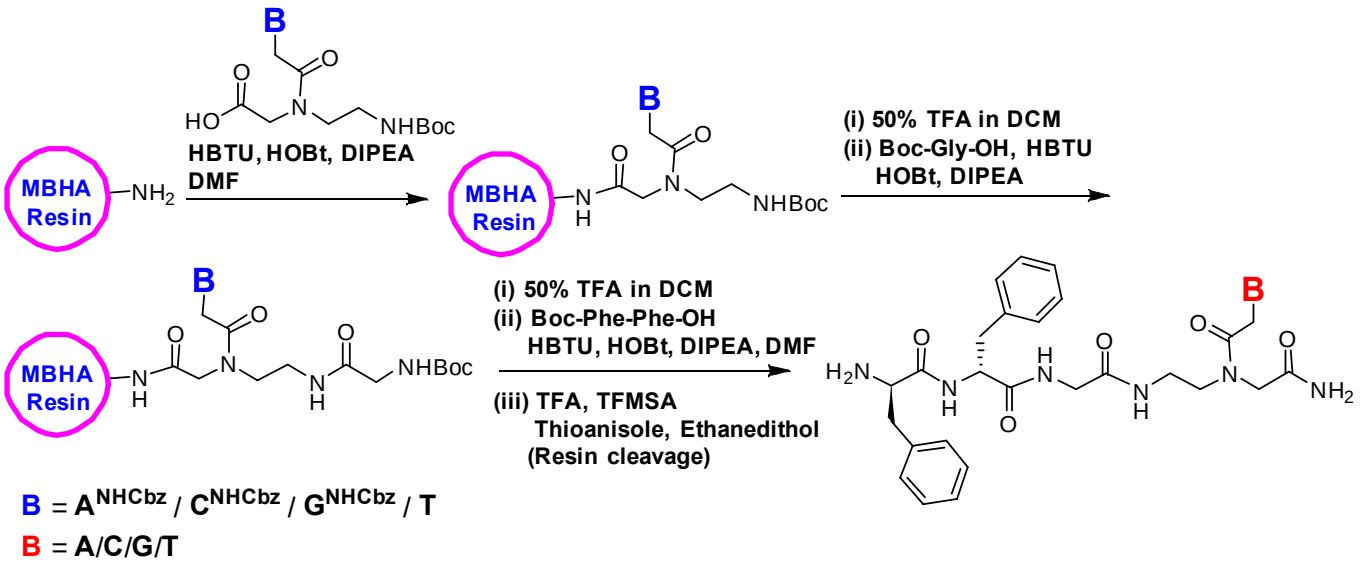

Scheme S3: Synthesis of nucleopeptides through solid support.

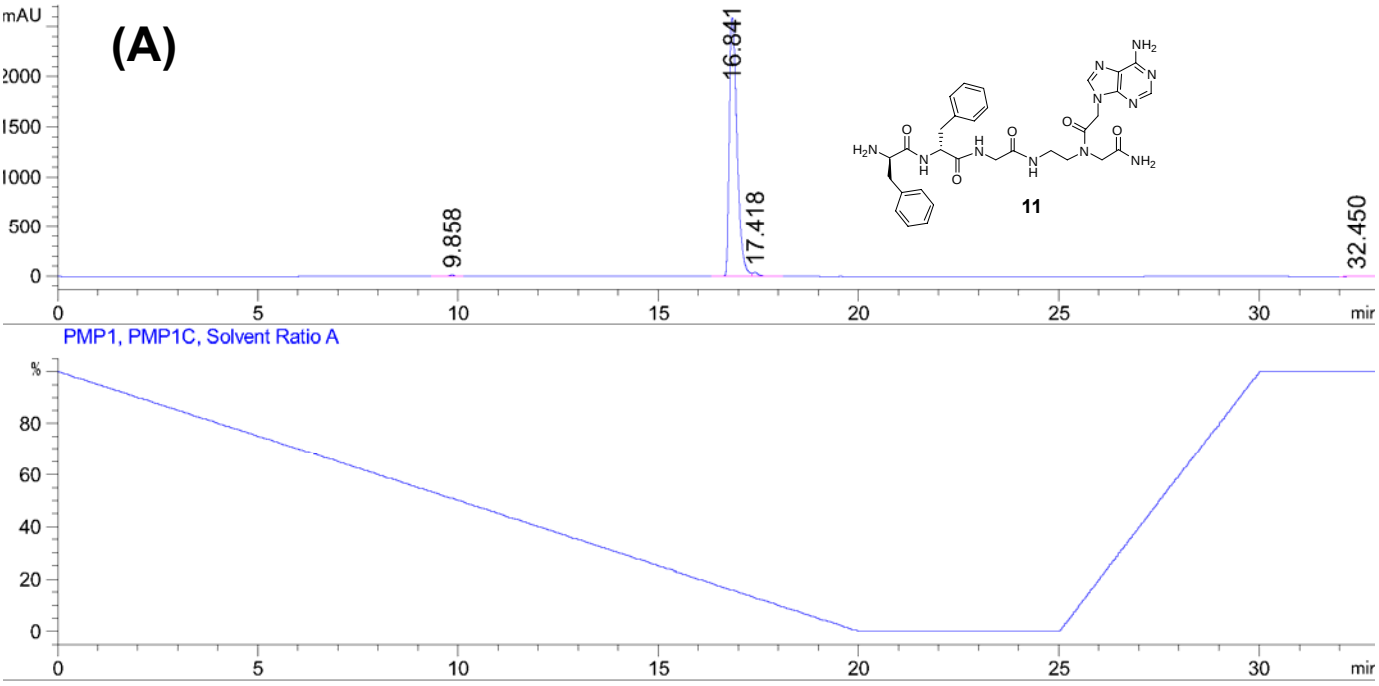

Solvent gradient with respect to **solvent A**

[**Solvent A:** 95% water, 4.5% acetonitrile, 0.5% TFA; **Solvent B:** 49.5% water, 50% acetonitrile, 0.5% TFA]

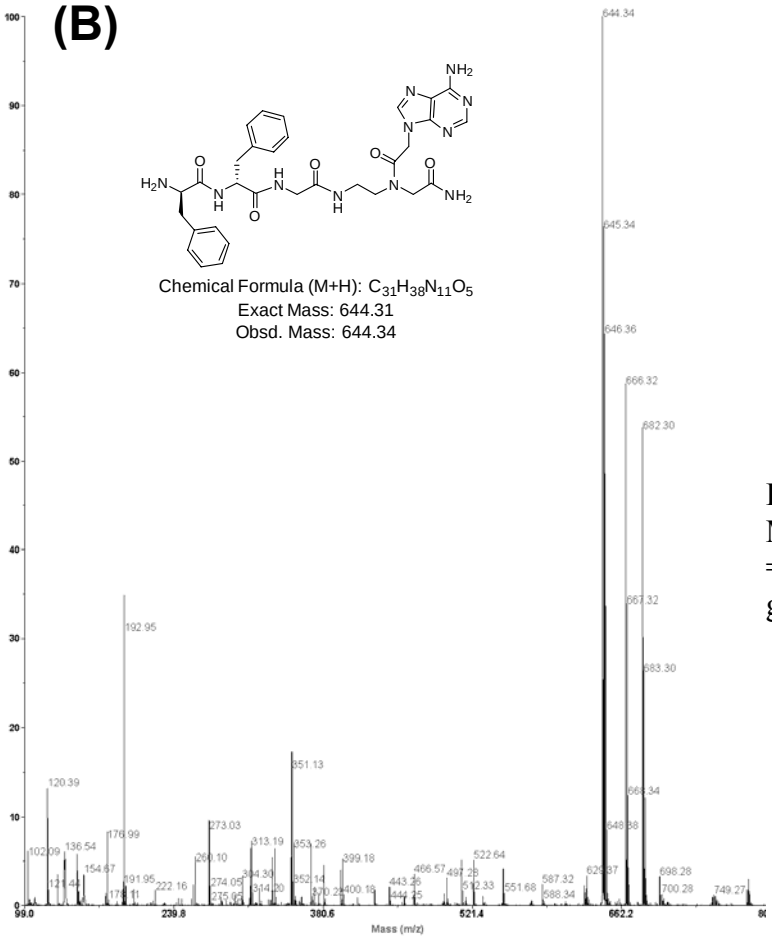

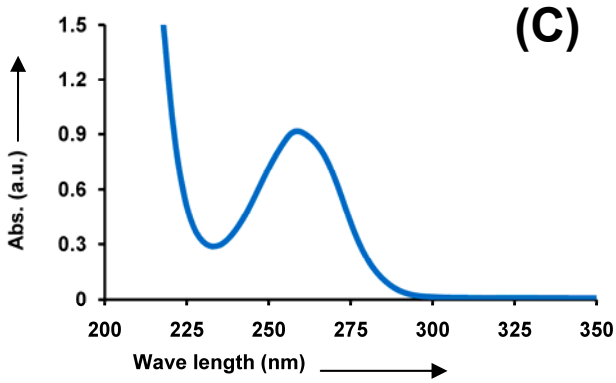

Figure S43: (A) HPLC trace (λ = 260 nm), (B) MALDI Mass and (C) UV spectrum (concentration = 1.34 mM) after purification of **NP1** (H-Phe-Phe-gly-A-*aeg*-NH_2).

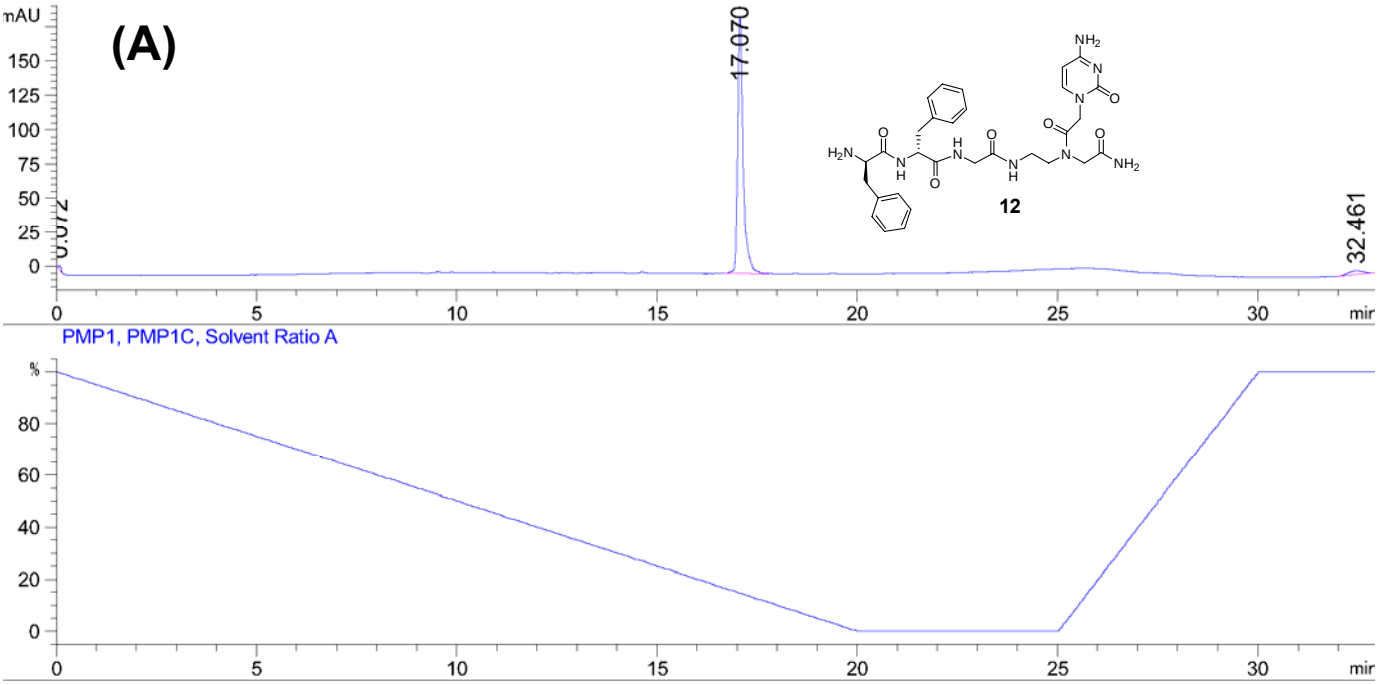

Solvent gradient with respect to **solvent A**

[**Solvent A:** 95% water, 4.5% acetonitrile, 0.5% TFA; **Solvent B:** 49.5% water, 50% acetonitrile, 0.5% TFA]

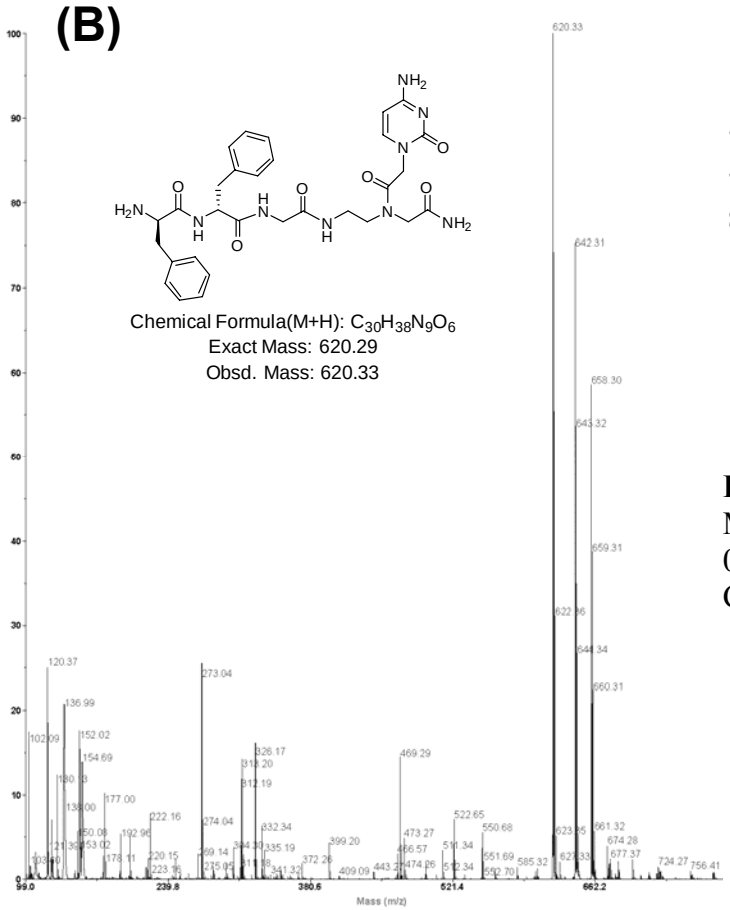

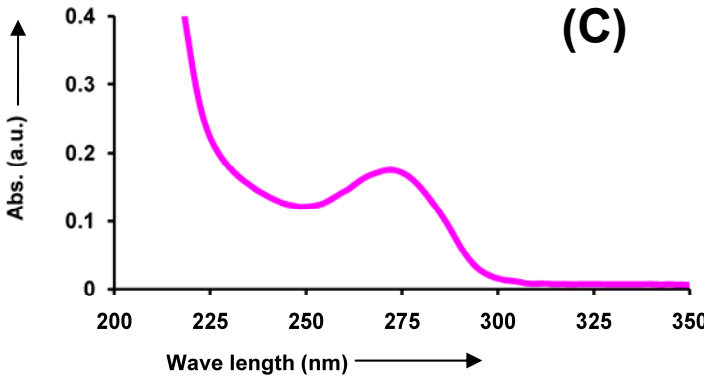

Figure S44: (A) HPLC trace (λ = 260 nm), (B) MALDI Mass and (C) UV spectrum (concentration = 0.23 mM) after purification of **NP2** (H-Phe-Phe-gly-C-*aeg*-NH_2).

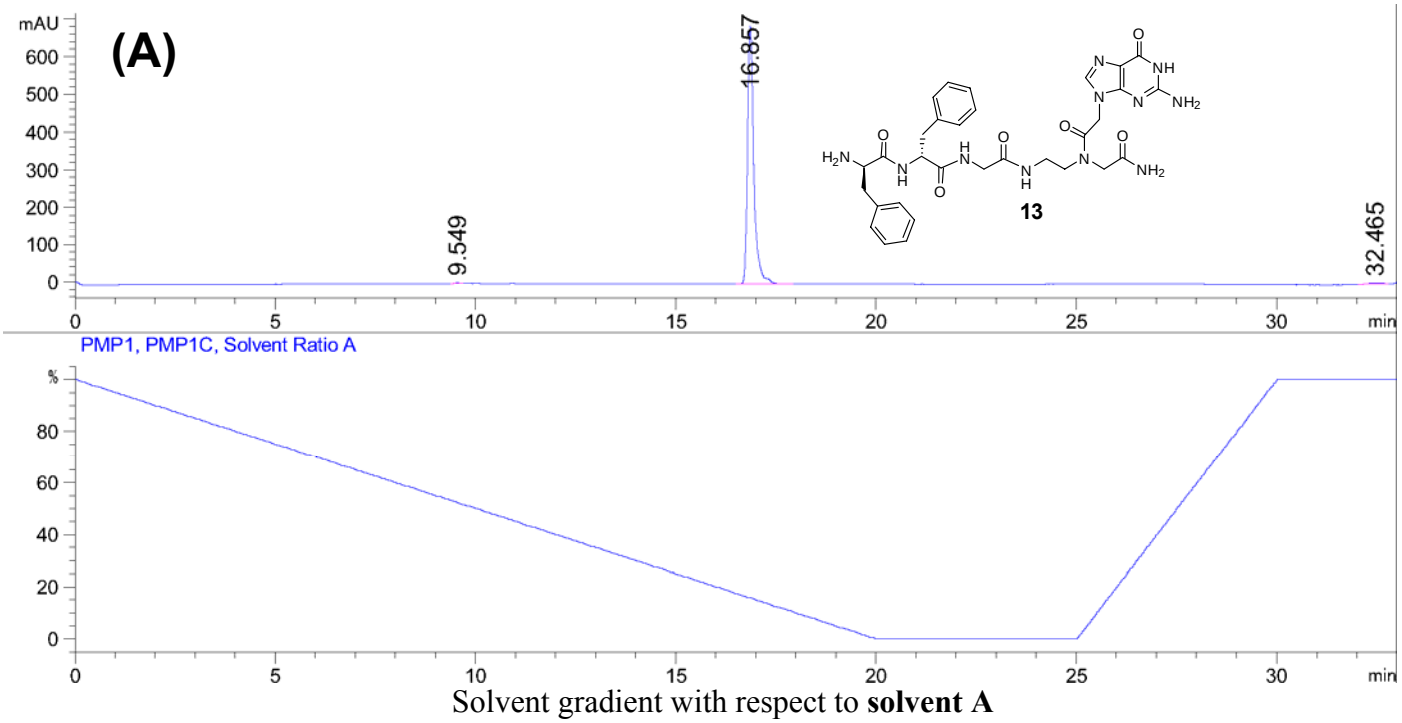

Solvent gradient with respect to **solvent A**

[**Solvent A:** 95% water, 4.5% acetonitrile, 0.5% TFA; **Solvent B:** 49.5% water, 50% acetonitrile, 0.5% TFA]

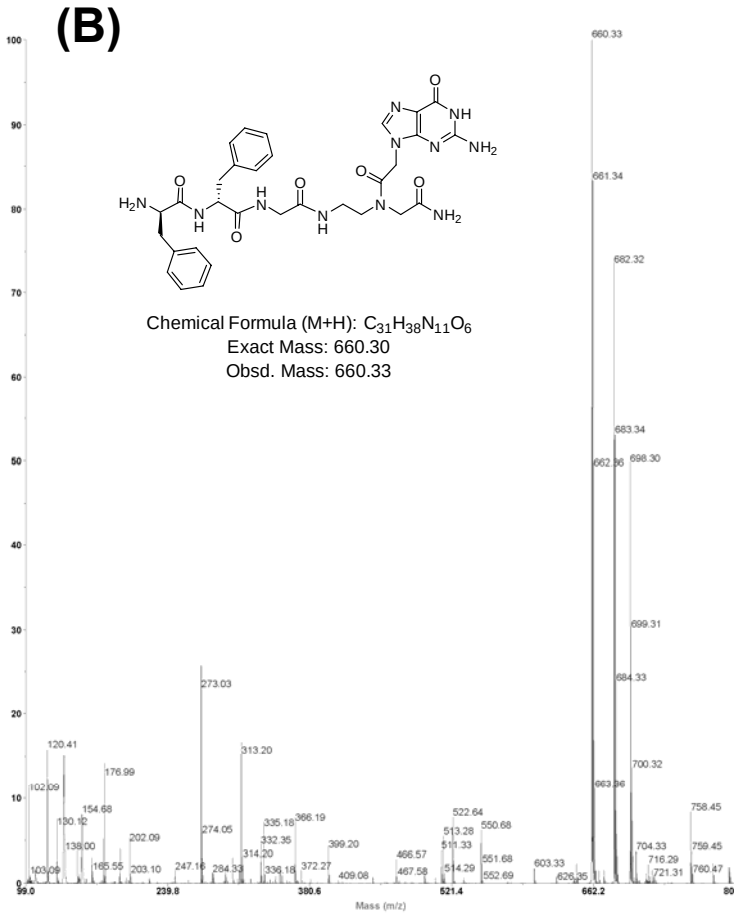

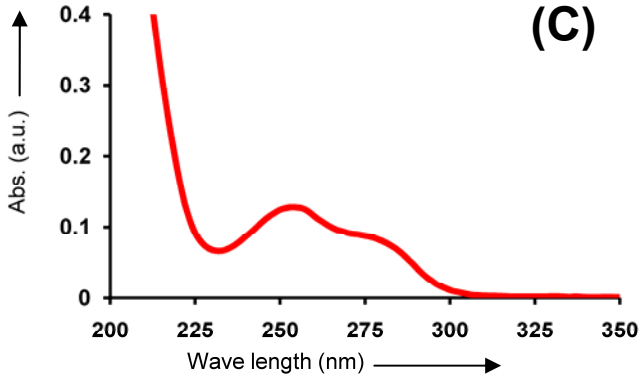

Figure S45: (A) HPLC trace (λ = 260 nm), (B) MALDI Mass and (C) UV spectrum (concentration = 0.44 mM) after purification of **NP3** (H-Phe-Phe-gly-G-*aeg*-NH_2).

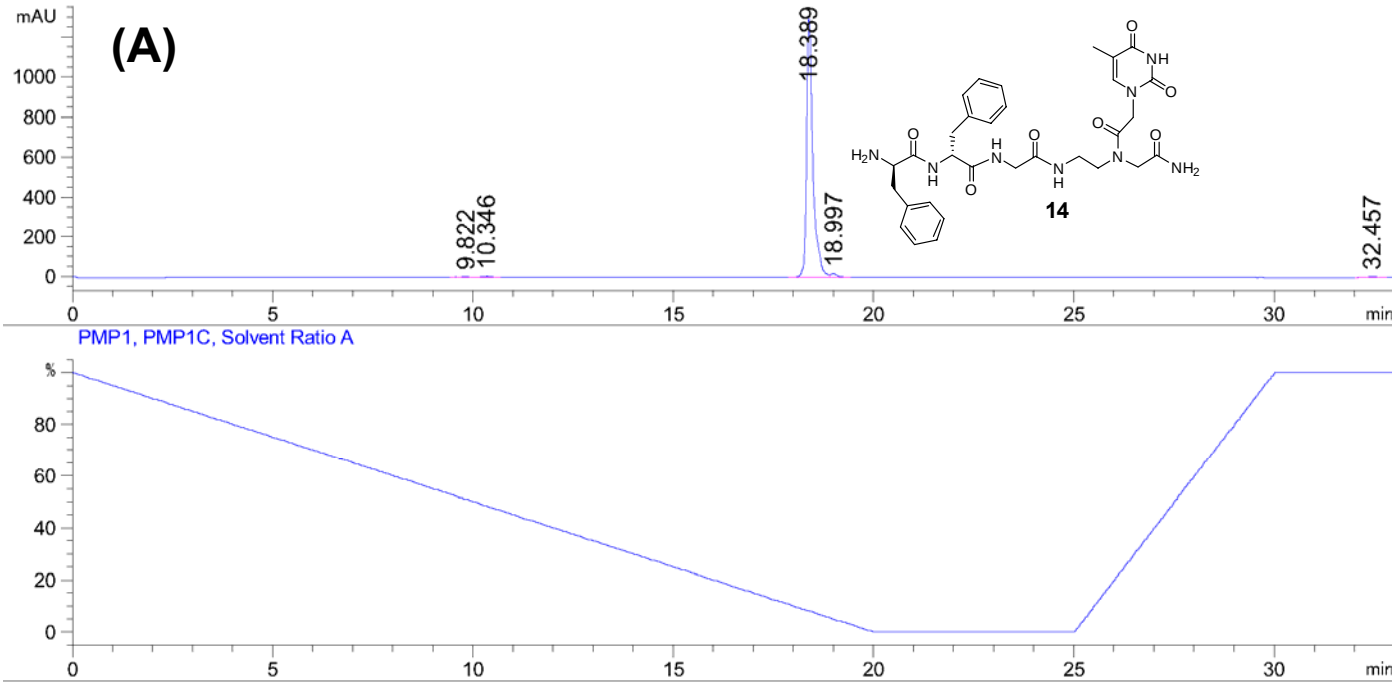

Solvent gradient with respect to **solvent A**

[**Solvent A:** 95% water, 4.5% acetonitrile, 0.5% TFA; **Solvent B:** 49.5% water, 50% acetonitrile, 0.5% TFA]

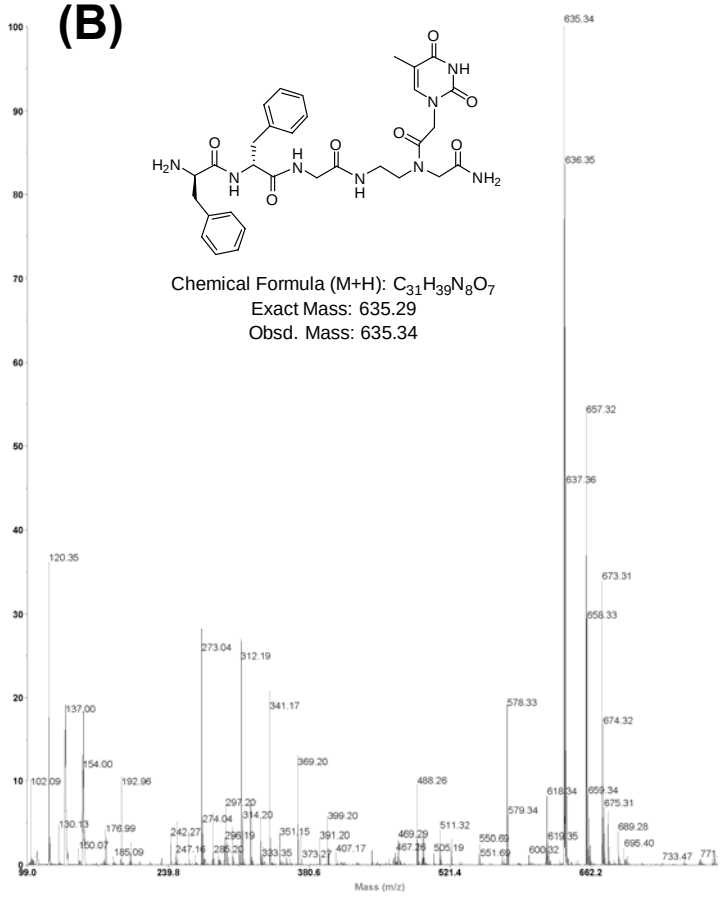

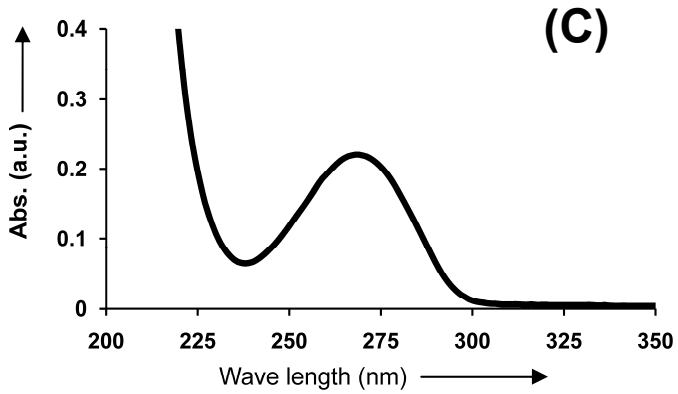

Figure S46: (A) HPLC trace (λ = 260 nm), (B) MALDI Mass and (C) UV spectrum (concentration = 0.92 mM) after purification of **NP4** (H-Phe-Phe-gly-T-*aeg*-NH_2).

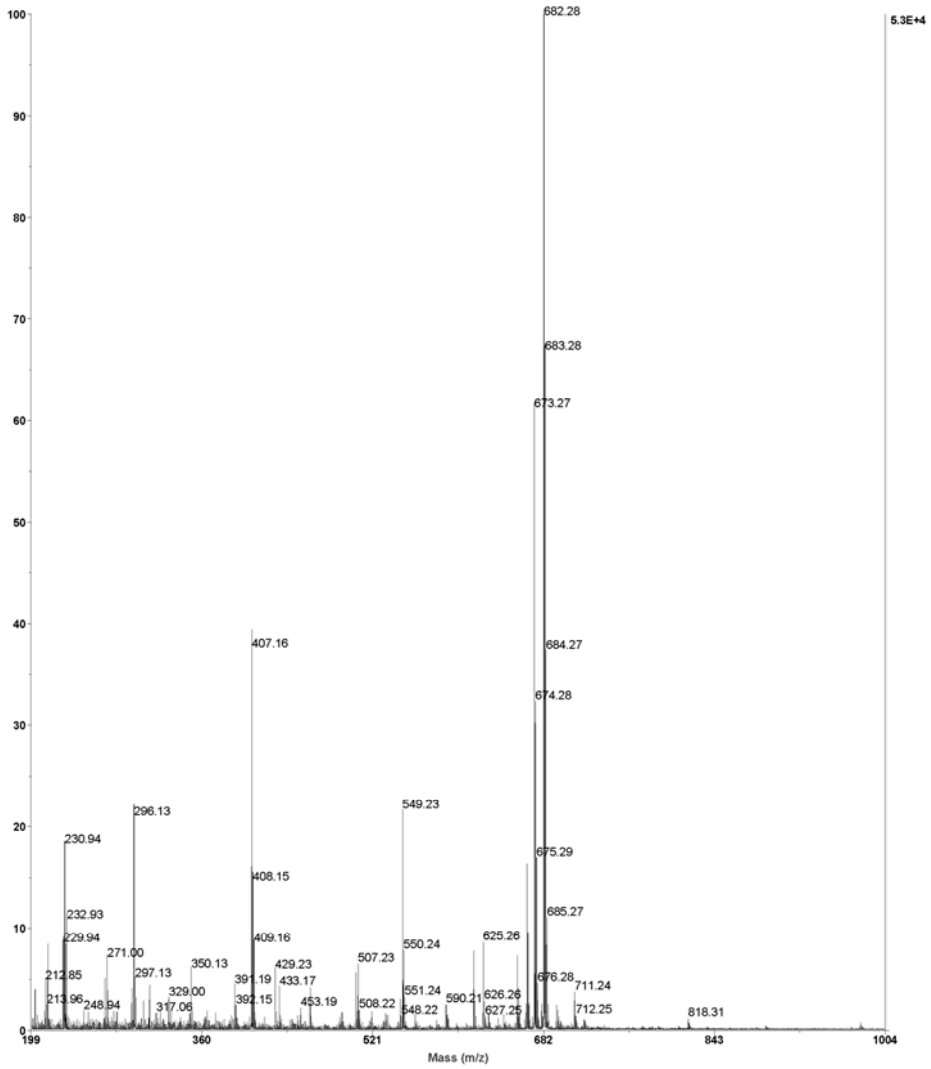

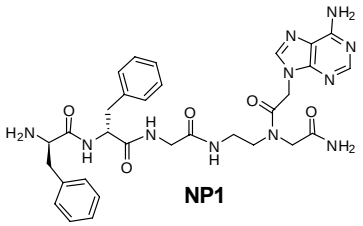

NP1

Chemical Formula (M+K): $C_{31}H_{37}N_{11}O_5K$
Exact Mass: 682.26
Obsd. Mass: 682.28

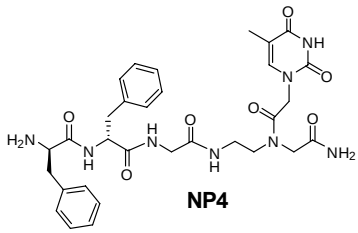

NP4

Chemical Formula (M+K): $C_{31}H_{37}N_8O_7K$
Exact Mass: 673.25
Obsd. Mass: 673.27

Figure S47: MALDI-Tof data of **NP1** and **NP4** duplex

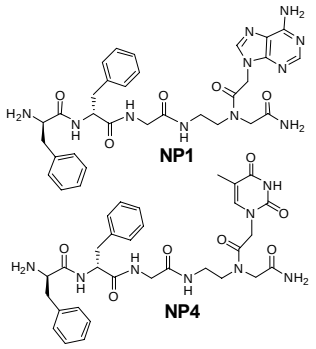

Chemical Formula of Duplex (M+H): $C_{62}H_{76}N_{19}O_{12}$
Calcd. Duplex Mass: 1278.5921
Obsd. Mass: 1278.5879
Error: -3.3 ppm

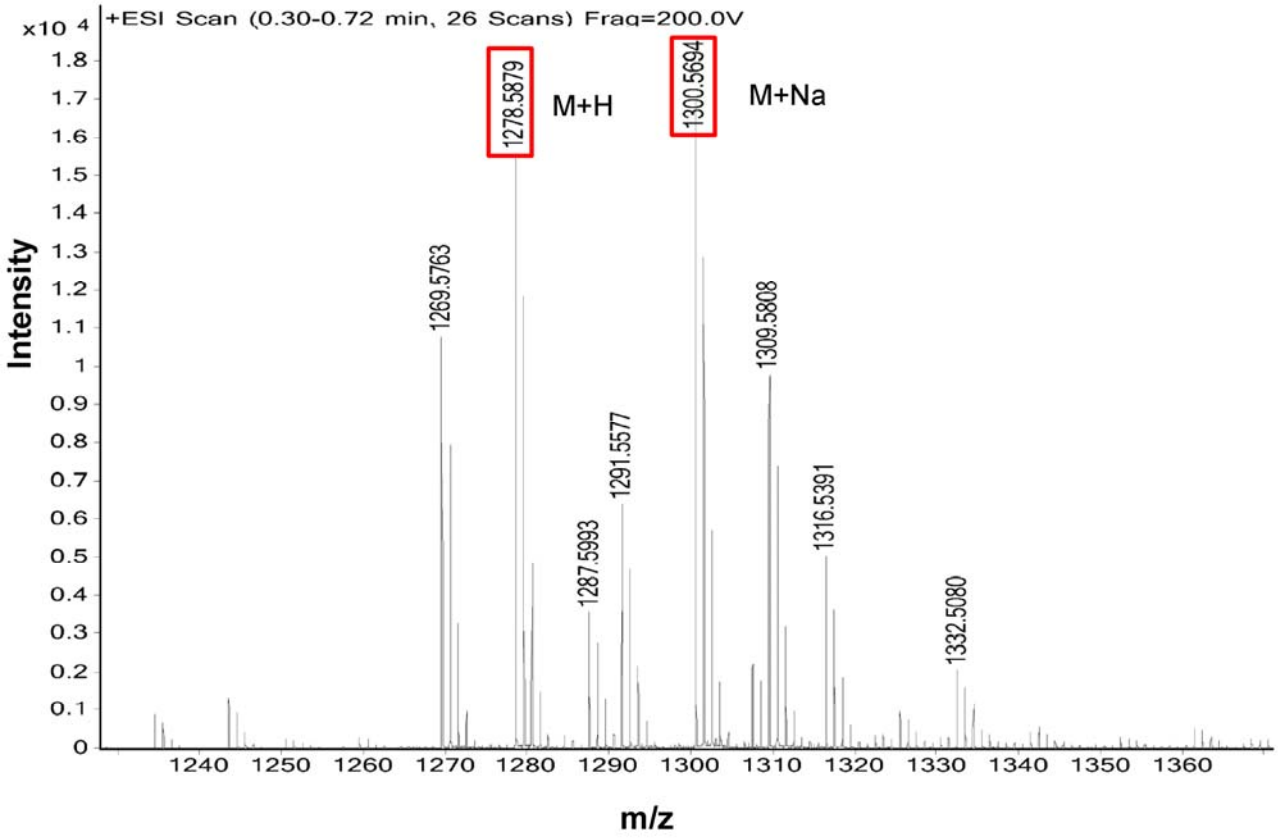

Figure S48: ESI mass data of **NP1** and **NP4** duplex

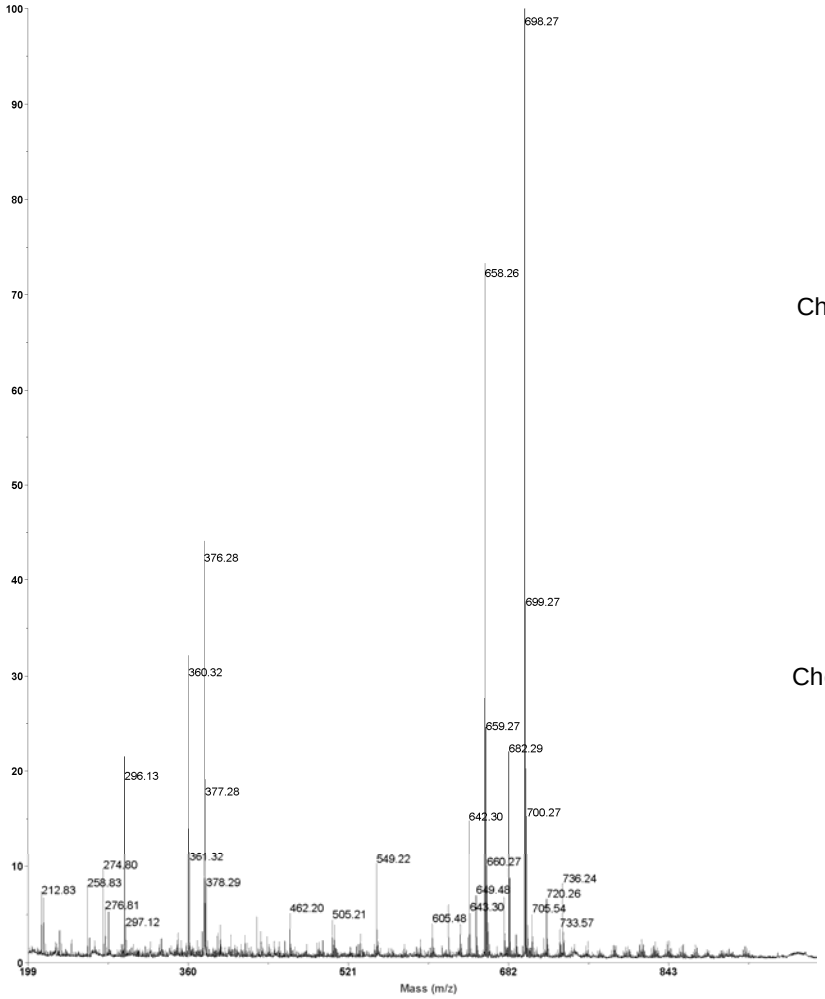

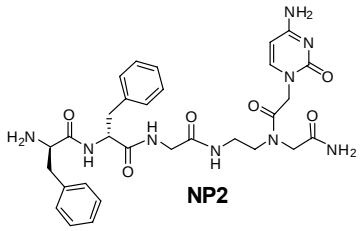

NP2

Chemical Formula(M+K): $C_{30}H_{37}N_9O_6K$
Exact Mass: 658.25
Obsd. Mass: 658.26

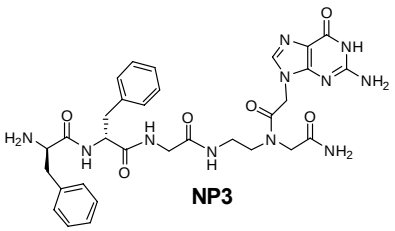

NP3

Chemical Formula (M+K): $C_{31}H_{37}N_{11}O_6K$
Exact Mass: 698.26
Obsd. Mass: 698.27

Figure S49: MALDI-Tof data of **NP2** and **NP3** duplex

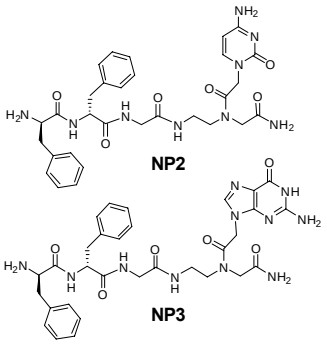

Chemical Formula of Duplex (M+H): $C_{61}H_{75}N_{20}O_{12}$
Calcd. Duplex Mass: 1279.5873
Obsd. Mass: 1279.5886
Error: -1.3 ppm

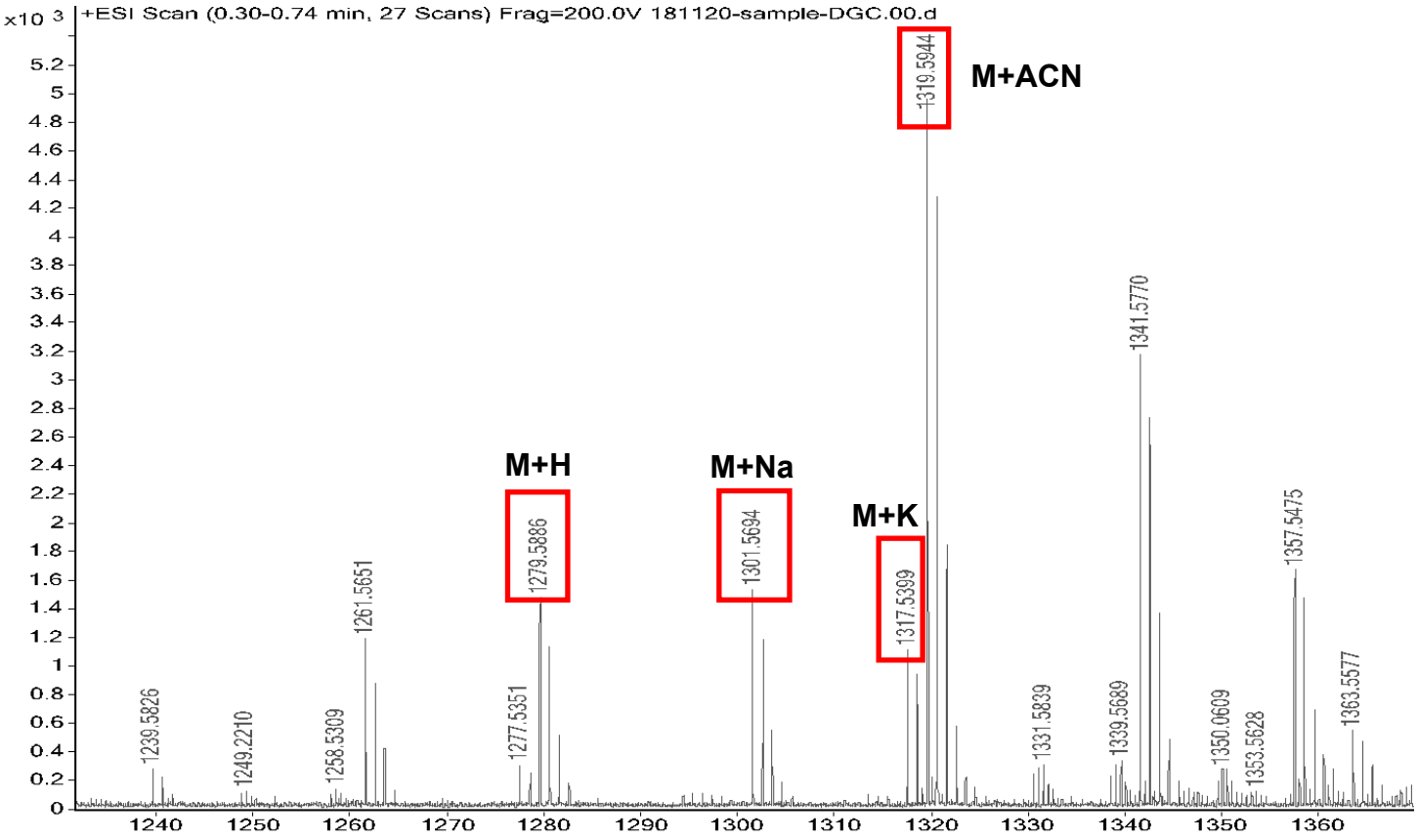

Figure S50: ESI mass data of **NP2** and **NP3** duplex

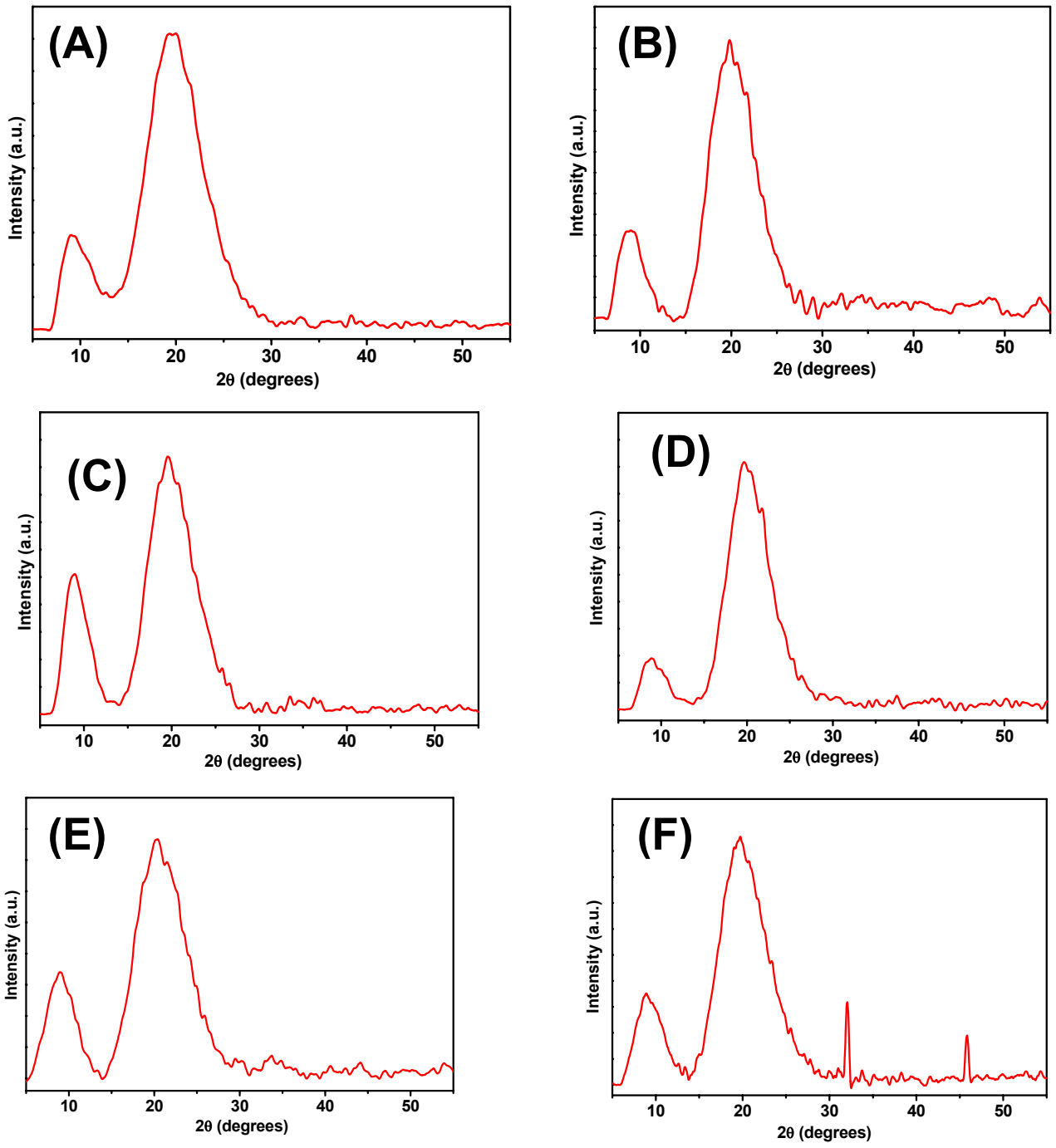

Figure S51: PXRD patterns of representative nucleopeptides (A) **3b** (Boc-Phe-Phe-*am*-6-Cl-G^{NHiBu}-*aeg*-OEt), (B) **3c** (Boc-Phe-Phe-*am*-G^{NHiBu}-*aeg*-OEt), (C) **3d** (Boc-Phe-Phe-*am*-T-*aeg*-OEt), (D) **6c** (Boc-Phe-Phe-*tz*-G^{NHiBu}-*aeg*-OEt), (E) **7d** (H-Phe-Phe-*tz*-T-*aeg*-OEt) and (F) **8d** (Boc-Phe-Phe-*tz*-T-*aeg*-OH).

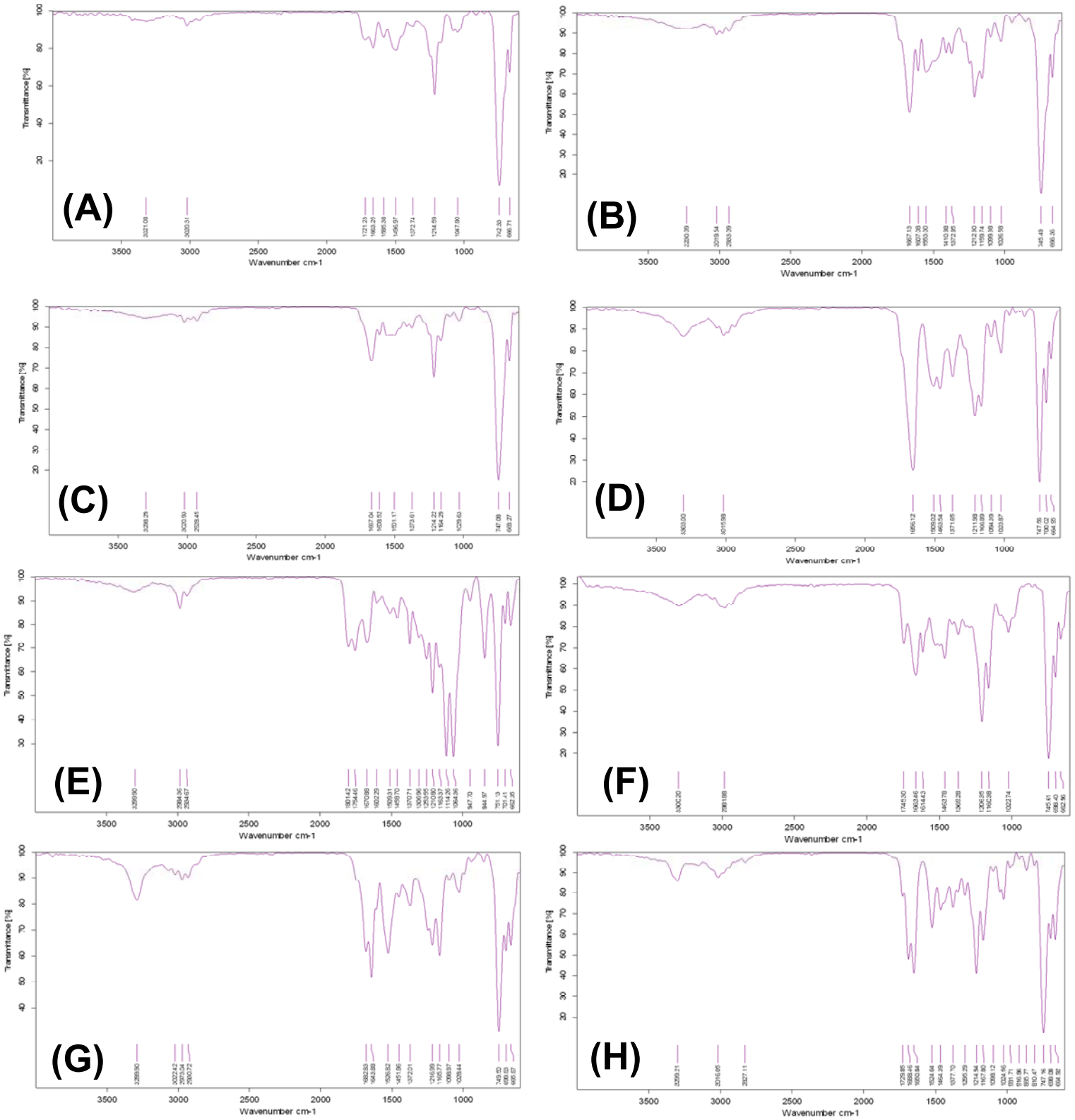

Figure S52: FTIR spectra of peptide (A) **3a** (Boc-Phe-Phe-*am*-A^{NHCbz}-*aeg*-OEt), (B) **3b** (Boc-Phe-Phe-*am*-6-Cl-G^{NHiBu}-*aeg*-OEt), (C) **3c** (Boc-Phe-Phe-*am*-G^{NHiBu}-*aeg*-OEt), (D) **3d** (Boc-Phe-Phe-*am*-T-*aeg*-OEt), (E) **6a** (Boc-Phe-Phe-*tz*-A$^{N(Boc)2}$-*aeg*-OEt), (F) **6b** (Boc-Phe-Phe-*tz*-A^{NHCbz}-*aeg*-OEt), (G) **6c** (Boc-Phe-Phe-*tz*-G^{NHiBu}-*aeg*-OEt) and (H) **6d** (Boc-Phe-Phe-*tz*-T-*aeg*-OEt).

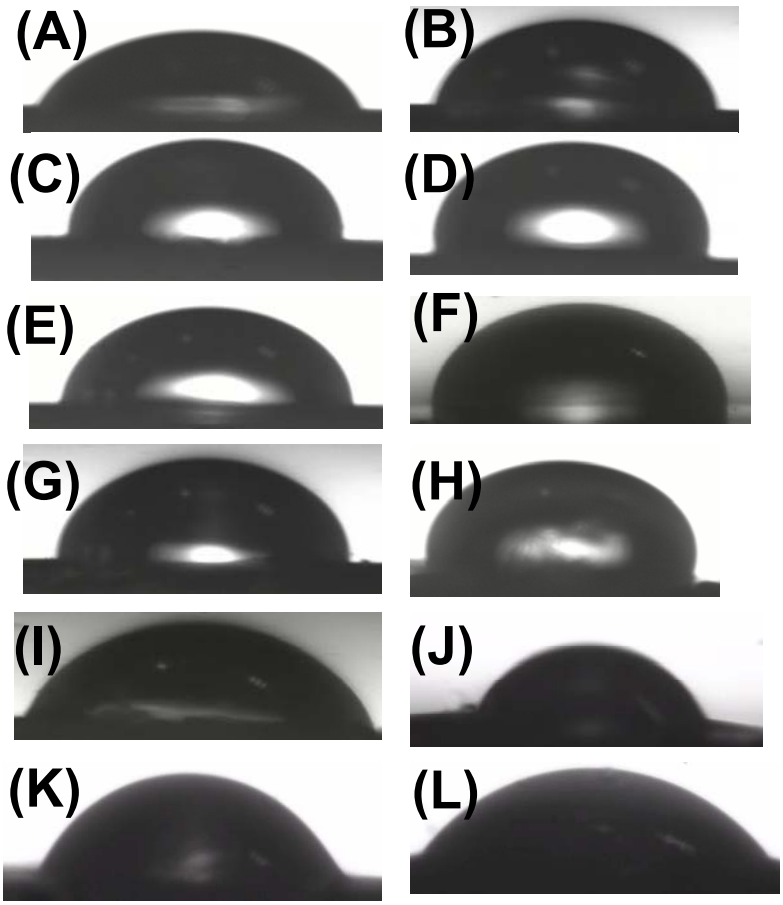

Figure S53: Images captured at 0.5 second for contact angle measurement of (A) bare silicon-wafer, (B) peptide **3a** (Boc-Phe-Phe-*am*-A^{NHCbz}-*aeg*-OEt), (C) peptide **3b** (Boc-Phe-Phe-*am*-6-Cl-G^{NHiBu}-*aeg*-OEt), (D) peptide **3c** (Boc-Phe-Phe-*am*-G^{NHiBu}-*aeg*-OEt), (E) peptide **3d** (Boc-Phe-Phe-*am*-T-*aeg*-OEt), (F) peptide **6a** (Boc-Phe-Phe-*tz*-$A^{N(Boc)_2}$-*aeg*-OEt), (G) peptide **6b** (Boc-Phe-Phe-*tz*-A^{NHCbz}-*aeg*-OEt), (H) peptide **6c** (Boc-Phe-Phe-*tz*-G^{NHiBu}-*aeg*-OEt), (I) peptide **6d** (Boc-Phe-Phe-*tz*-T-*aeg*-OEt), (J) peptide **7d** (H-Phe-Phe-*tz*-T-*aeg*-OEt), (K) peptide **8d** (Boc-Phe-Phe-*tz*-T-*aeg*-OH) and (L) peptide **9** (Boc-Phe-Phe-*tz*-*aeg*-OEt).

Table S1: Contact angle (CA) measured for peptides on glass surface

Sample/Surface	CA (in degree)[a]	ΔCA (in degree)
Bare silicon-wafer	62 ± 1	-
Peptide **3a** Boc-Phe-Phe-*am*-A^{NHCbz}-*aeg*-OEt	73 ± 2	+11
Peptide **3b** Boc-Phe-Phe-*am*-6-Cl-G^{NHiBu}-*aeg*-OEt	84 ± 2	+22
Peptide **3c** Boc-Phe-Phe-*am*-G^{NHiBu}-*aeg*-OEt	95 ± 3	+33
Peptide **3d** Boc-Phe-Phe-*am*-T-*aeg*-OEt	74 ± 2	+12
Peptide **6a** Boc-Phe-Phe-*tz*-$A^{N(Boc)_2}$-*aeg*-OEt	88 ± 2	+16
Peptide **6b** Boc-Phe-Phe-*tz*-A^{NHCbz}-*aeg*-OEt	77 ± 2	+15
Peptide **6c** Boc-Phe-Phe-*tz*-G^{NHiBu}-*aeg*-OEt	94 ± 3	+32
Peptide **6d** Boc-Phe-Phe-*tz*-T-*aeg*-OEt	75 ± 1	+13
Peptide **7d** H-Phe-Phe-*tz*-T-*aeg*-OEt	70 ± 2	+8
Peptide **8d** Boc-Phe-Phe-*tz*-T-*aeg*-OH	81 ± 1	+19
Peptide **9** Boc-Phe-Phe-*tz*-*aeg*-OEt	71 ± 2	+9

[a]Data are the mean ± SD (n=4)

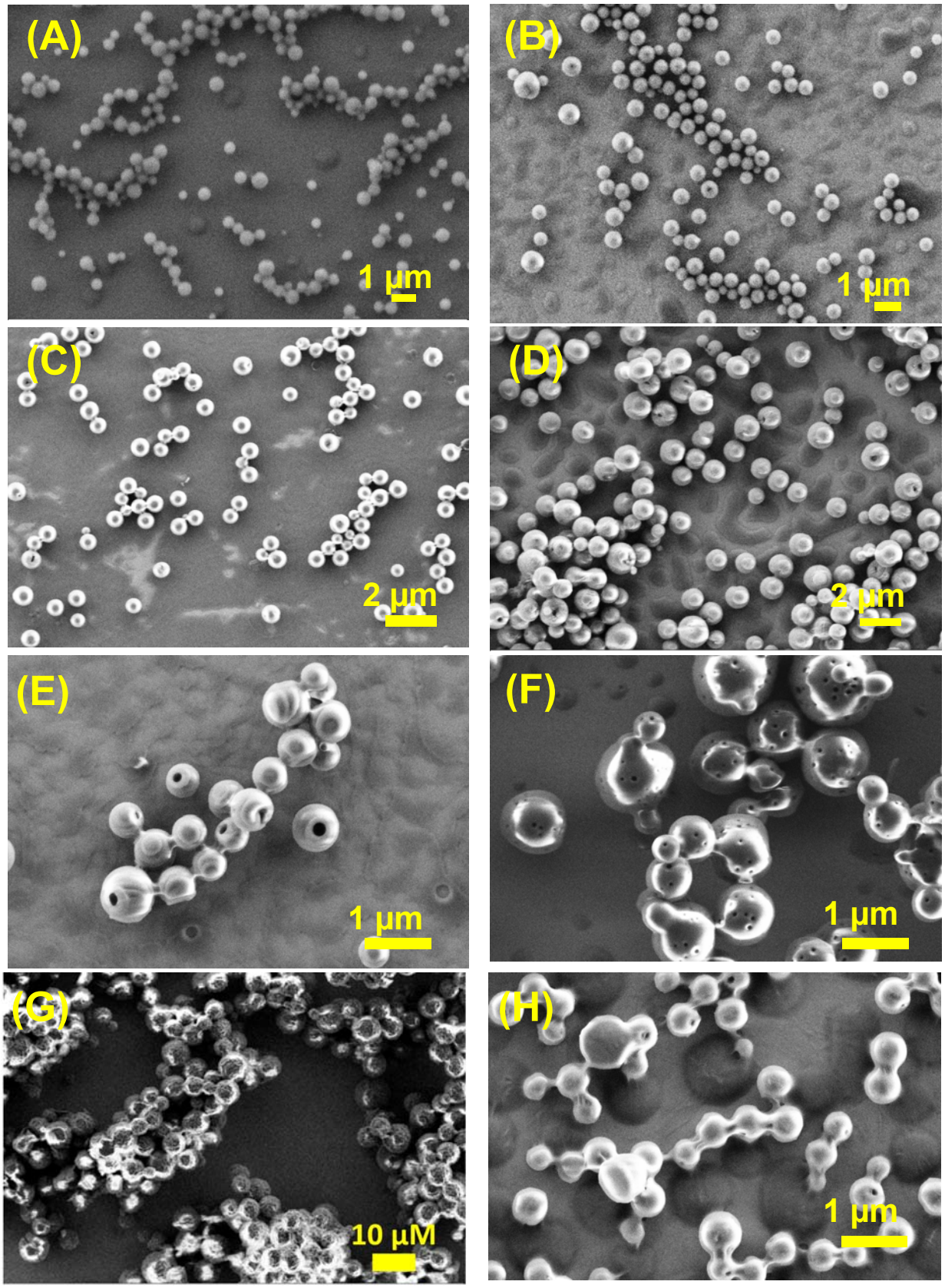

Figure S54: SEM images of peptide (A) **3a** (Boc-Phe-Phe-*am*-A^{NHCbz}-*aeg*-OEt), (B) **3b** (Boc-Phe-Phe-*am*-6-Cl-G^{NHiBu}-*aeg*-OEt), (C) **3c** (Boc-Phe-Phe-*am*-G^{NHiBu}-*aeg*-OEt), (D) **3d** (Boc-Phe-Phe-*am*-T-*aeg*-OEt). (E) **6a** (Boc-Phe-Phe-*tz*-A$^{N(Boc)_2}$-*aeg*-OEt), (F) **6b** (Boc-Phe-Phe-*tz*-A^{NHCbz}-*aeg*-OEt), (G) **6c** (Boc-Phe-Phe-*tz*-G^{NHiBu}-*aeg*-OEt) and (H) **6d** (Boc-Phe-Phe-*tz*-T-*aeg*-OEt).

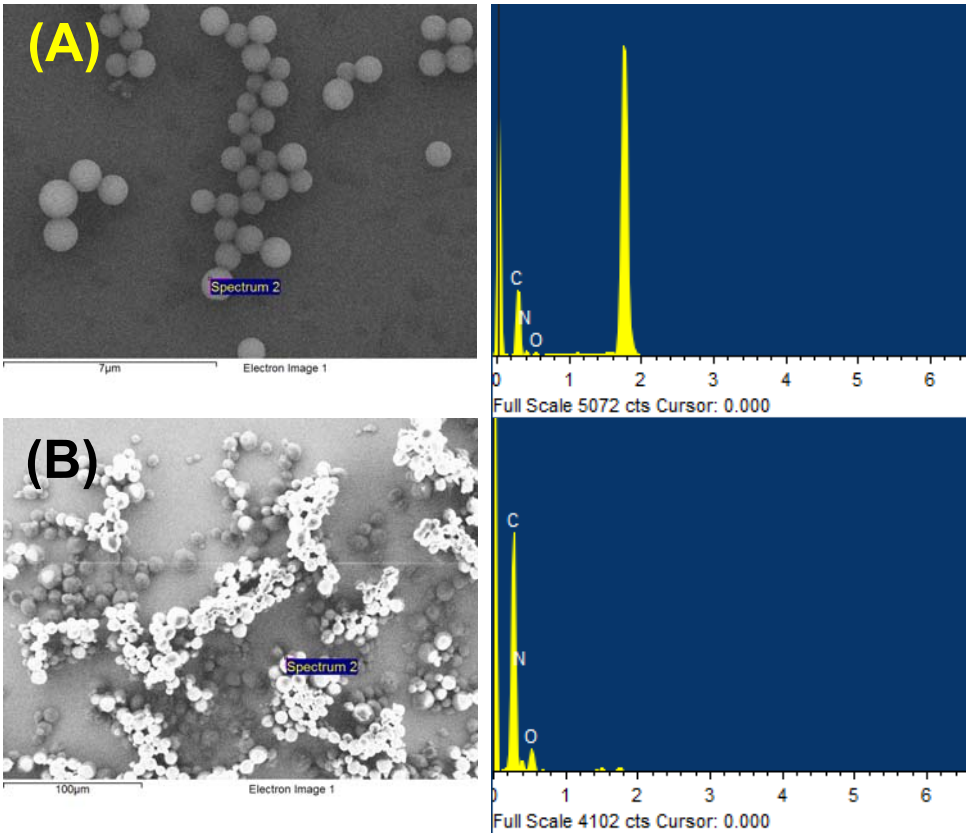

Element	Weight%	Atomic%
C K	52.48	57.05
N K	35.97	33.53
O K	11.55	9.42
Totals	100.00	

Element	Weight%	Atomic%
C K	57.58	62.73
N K	22.03	20.58
O K	20.40	16.68
Totals	100.00	

Figure S55: EDX images of (A) peptide **6b** (Boc-Phe-Phe-*tz*-A^{NHCbz}-*aeg*-OEt), and (B) peptide **6c** (Boc-Phe-Phe-*tz*-G^{NHiBu}-*aeg*-OEt).

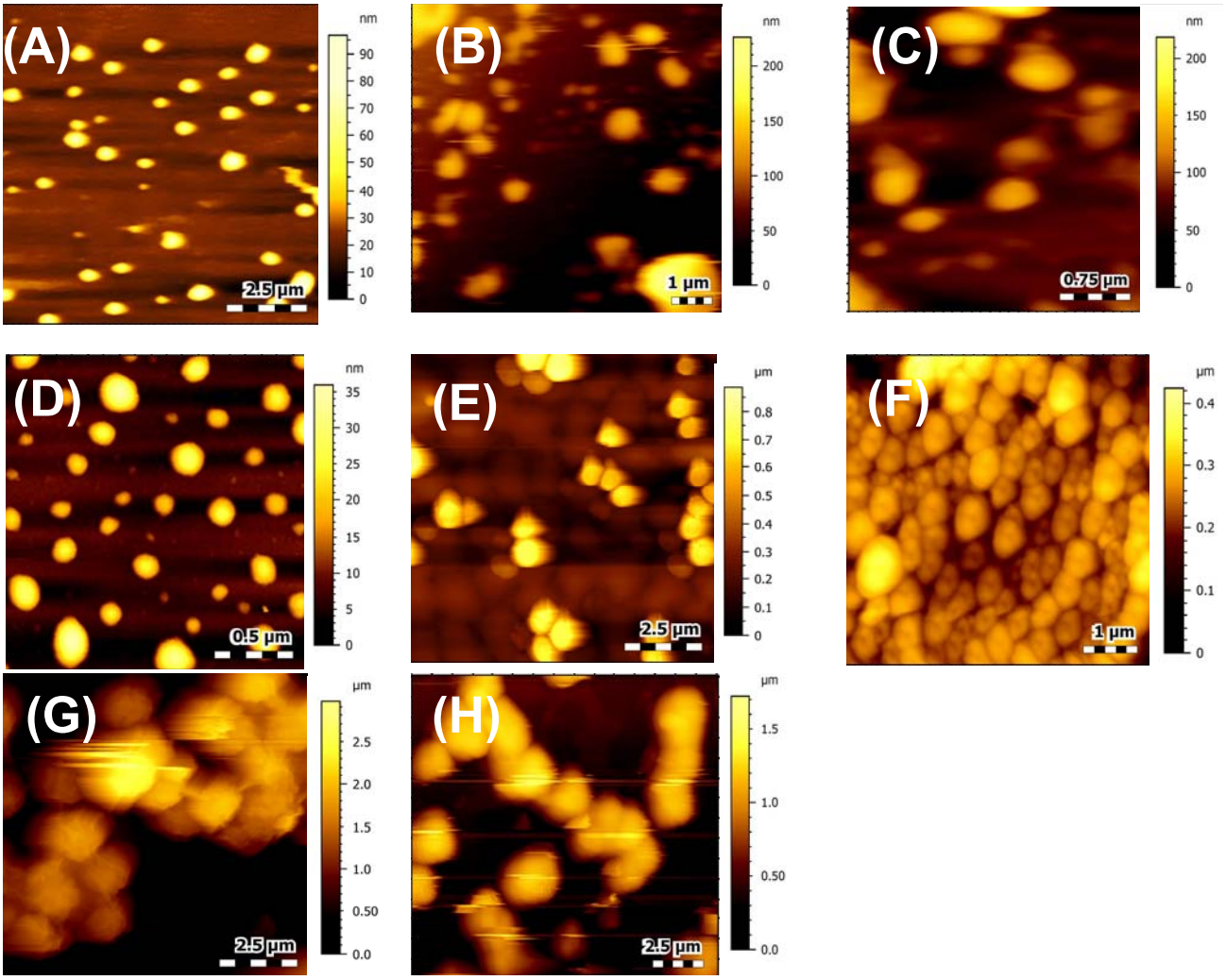

Figure S56: AFM topography images of (A) **3a** (Boc-Phe-Phe-*am*-A^{NHCbz}-*aeg*-OEt), (B) **3b** (Boc-Phe-Phe-*am*-6-Cl-G^{NHiBu}-*aeg*-OEt), (C) **3c** (Boc-Phe-Phe-*am*-G^{NHiBu}-*aeg*-OEt), (D) **3d** (Boc-Phe-Phe-*am*-T-*aeg*-OEt). (E) **6a** (Boc-Phe-Phe-*tz*-A$^{N(Boc)_2}$-*aeg*-OEt), (F) **6b** (Boc-Phe-Phe-*tz*-A^{NHCbz}-*aeg*-OEt), (G) **6c** (Boc-Phe-Phe-*tz*-G^{NHiBu}-*aeg*-OEt), (H) **6d** (Boc-Phe-Phe-*tz*-T-*aeg*-OEt).

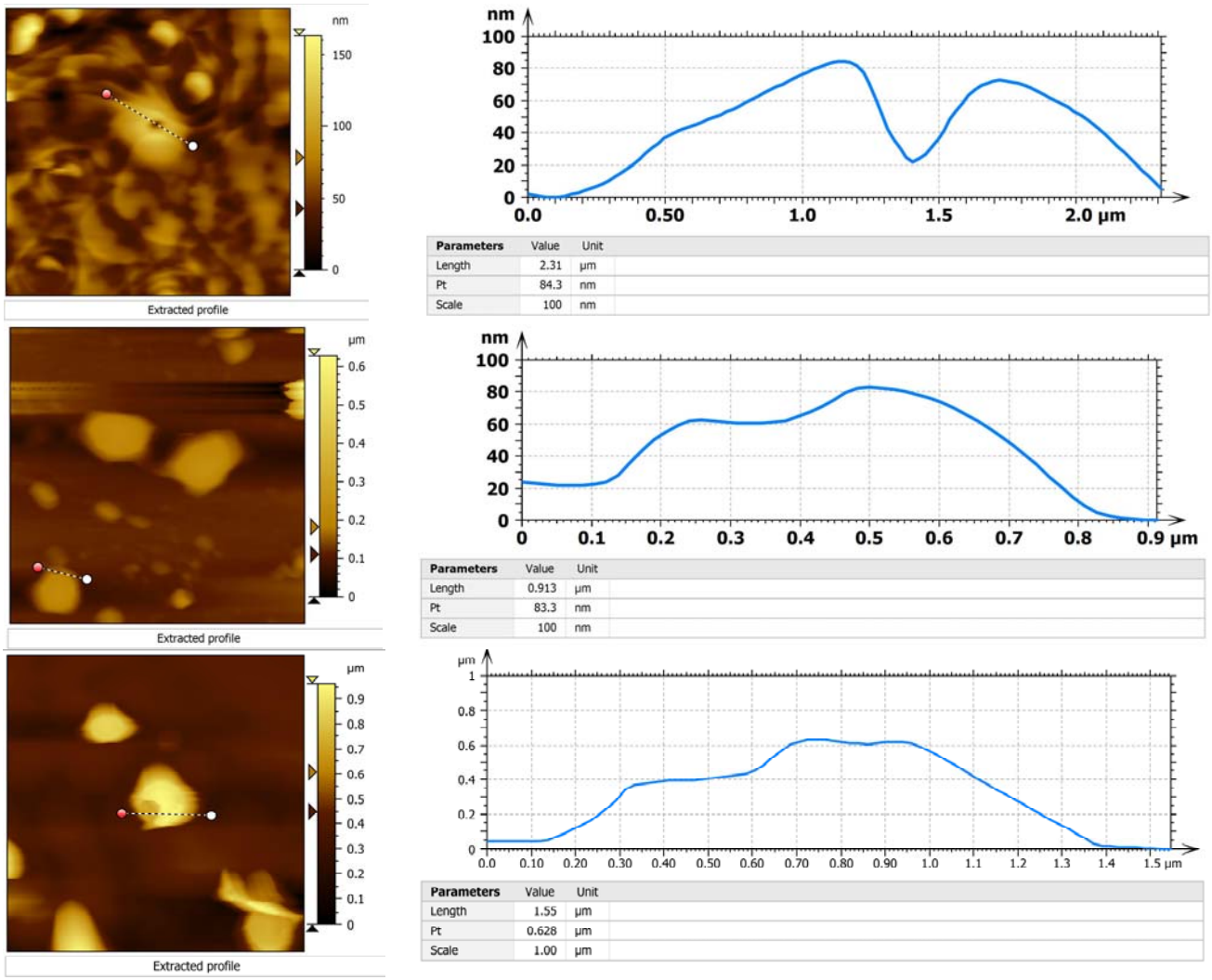

Figure S57: Height profiles diagrams of peptide **6a** (Boc-Phe-Phe-*tz*-A$^{N(Boc)_2}$-*aeg*-OEt) at different places of nanoparticles obtained from AFM.

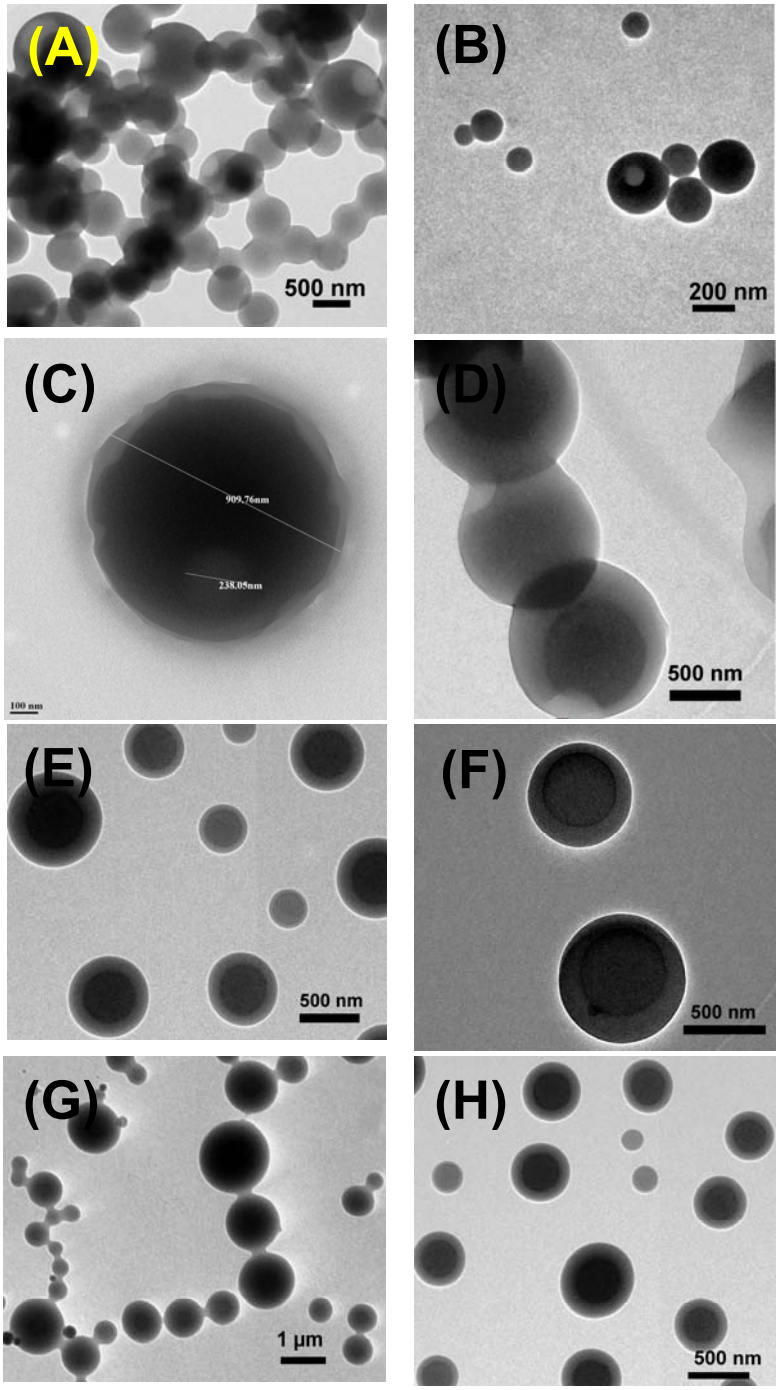

Figure S58: HRTEM images of (A) **6a** (Boc-Phe-Phe-*tz*-A$^{N(Boc)_2}$-*aeg*-OEt), (B) **6b** (Boc-Phe-Phe-*tz*-A^{NHCbz}-*aeg*-OEt), (C) **6c** (Boc-Phe-Phe-*tz*-G^{NHiBu}-*aeg*-OEt), (D) **6d** (Boc-Phe-Phe-*tz*-T-*aeg*-OEt), (E) **3a** (Boc-Phe-Phe-*am*-A^{NHCbz}-*aeg*-OEt), (F) **3b** (Boc-Phe-Phe-*am*-6-Cl-G^{NHiBu}-*aeg*-OEt), (G) **3c** (Boc-Phe-Phe-*am*-G^{NHiBu}-*aeg*-OEt) and (H) **3d** (Boc-Phe-Phe-*am*-T-*aeg*-OEt).

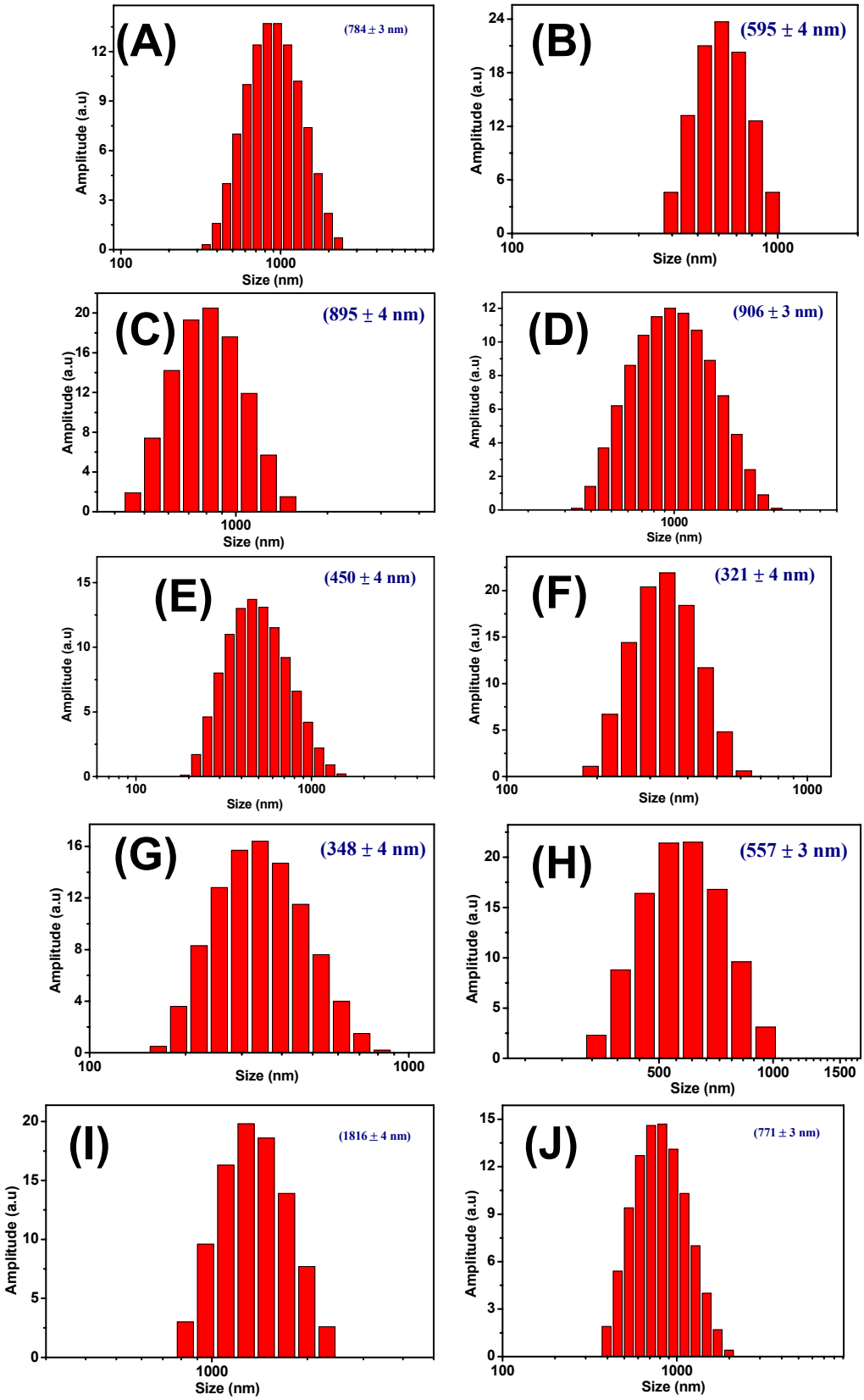

Figure S59: DLS spectra of fresh peptide solution of (A) **3a** (Boc-Phe-Phe-*am*-A^{NHCbz}-*aeg*-OEt), (B) **3b** (Boc-Phe-Phe-*am*-6-Cl-G^{NHiBu}-*aeg*-OEt), (C) **3c** (Boc-Phe-Phe-*am*-G^{NHiBu}-*aeg*-OEt), (D) **3d** (Boc-Phe-Phe-*am*-T-*aeg*-OEt). (E) **6a** (Boc-Phe-Phe-*tz*-A$^{N(Boc)2}$-*aeg*-OEt) (PDI = 0.03), (F) **6b** (Boc-Phe-Phe-*tz*-A^{NHCbz}-*aeg*-OEt) (PDI = 0.07), (G) **6c** (Boc-Phe-Phe-*tz*-G^{NHiBu}-*aeg*-OEt), (H) **6d** (Boc-Phe-Phe-*tz*-T-*aeg*-OEt) and after 10 days incubation of (I) **6a** (PDI = 0.34), (J) **6b** (PDI = 0.57).

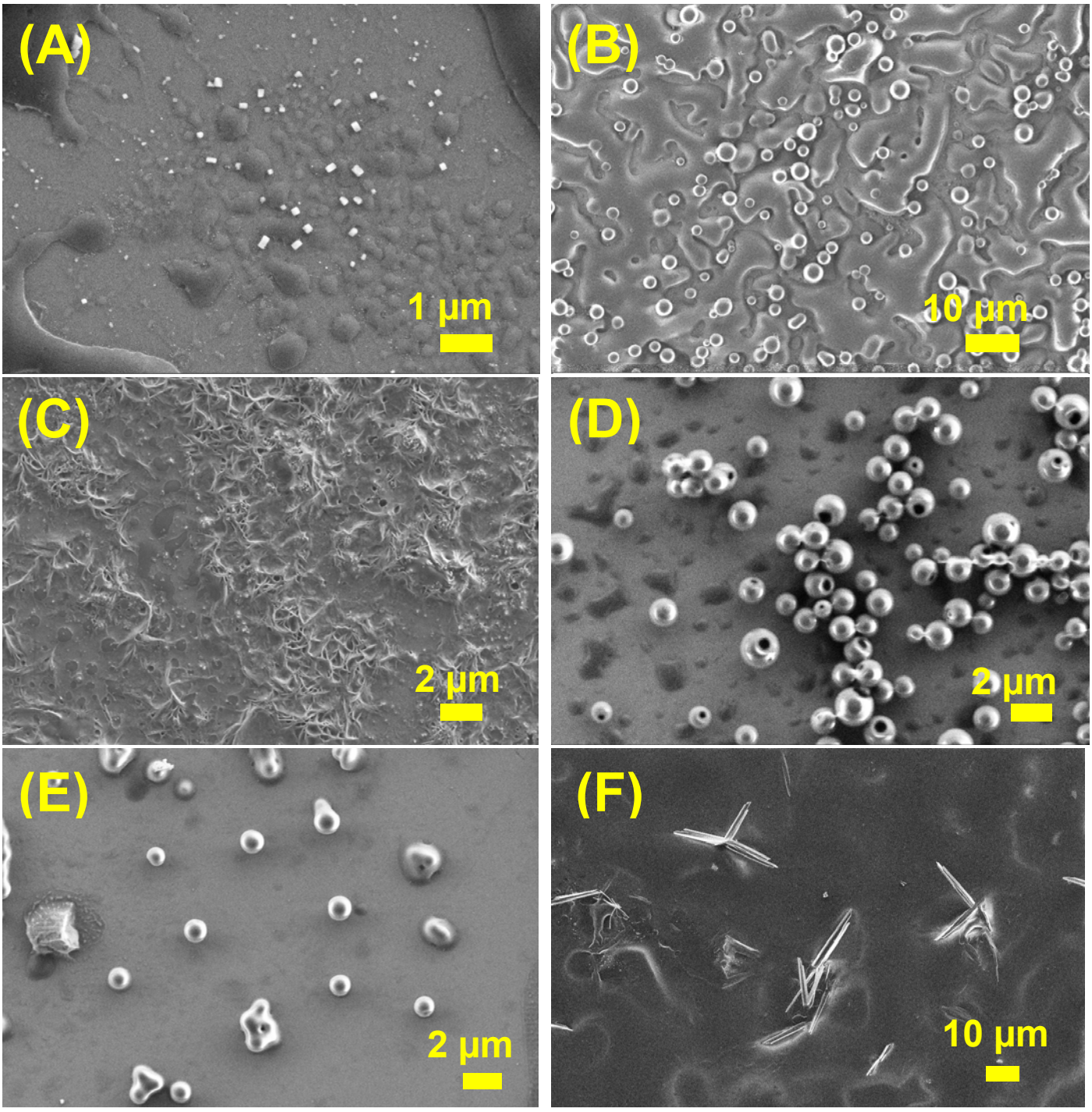

Figure S60: SEM images of peptide **6a** (Boc-Phe-Phe-*tz*-A$^{N(Boc)_2}$-*aeg*-OEt) (A) at pH 2, (B) at pH 7, (C) at pH 10, (D) after heating at 100 ^{o}C for 4 h, (E) after incubation with proteinase K and (F) SEM image of proteinase K.

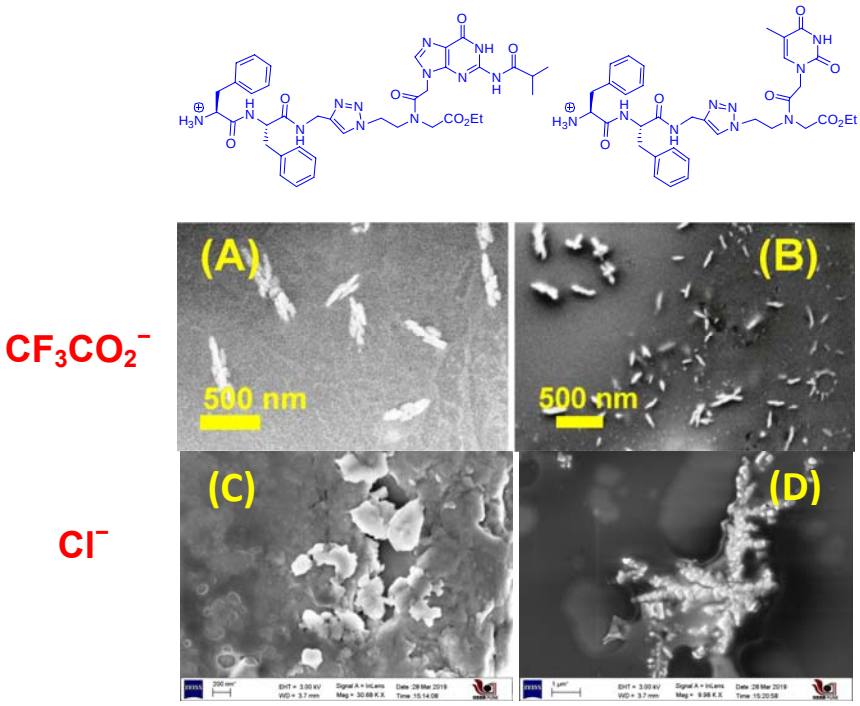

Figure S61: Effect of counter anion on self-assembled morphologies for nucleopeptide **7c** and **7d** in presence of trifluoroacetate (A, B) and chloride (C, D) respectively through SEM images.

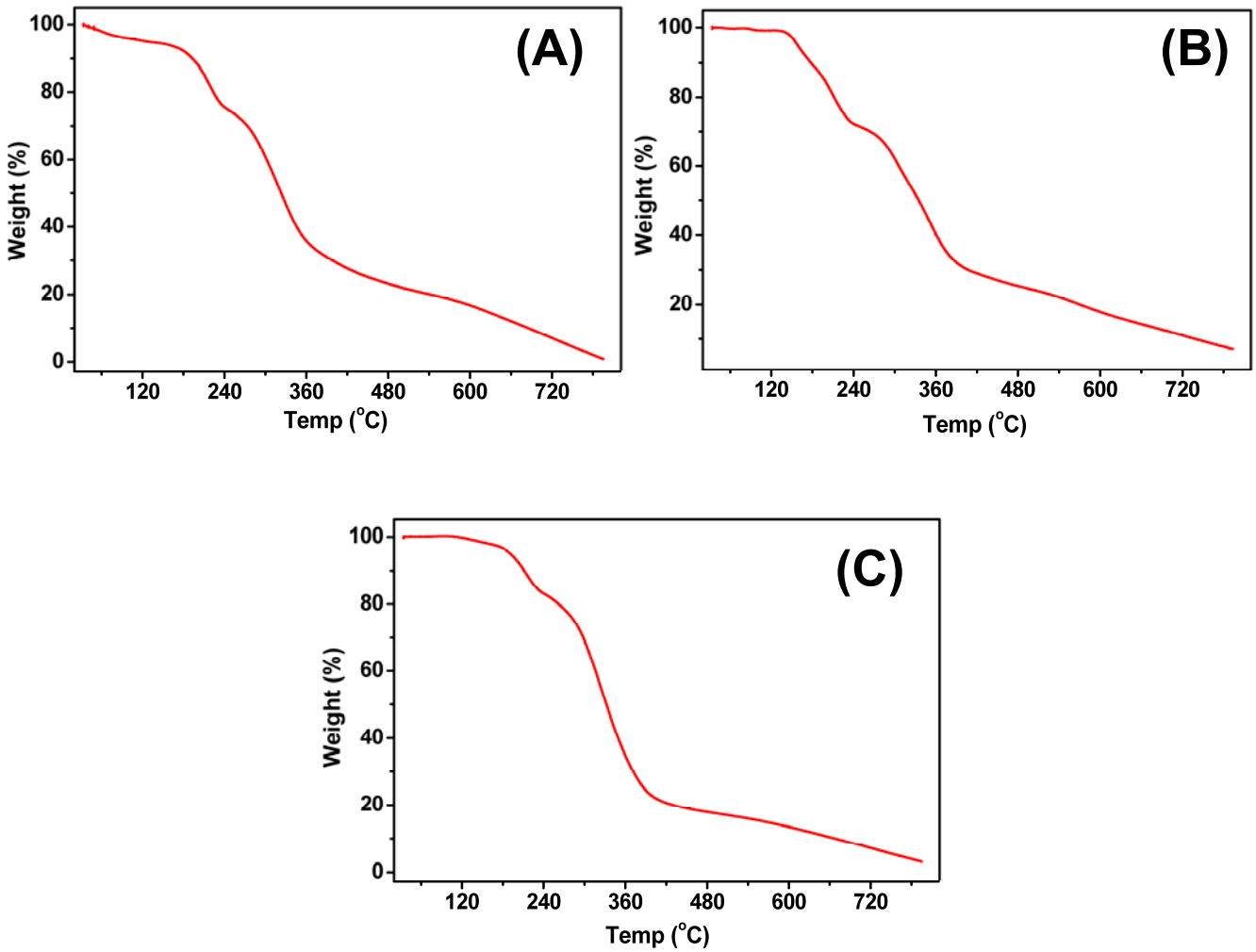

Figure S62: TGA of (A) peptide **3b** Boc-Phe-Phe-*am*-6-Cl-G^{NHiBu}-*aeg*-OEt, (B) peptide **6b** Boc-Phe-Phe-*tz*-A^{NHCbz}-*aeg*-OEt, and (C) peptide **6d** Boc-Phe-Phe-*tz*-T-*aeg*-OEt.

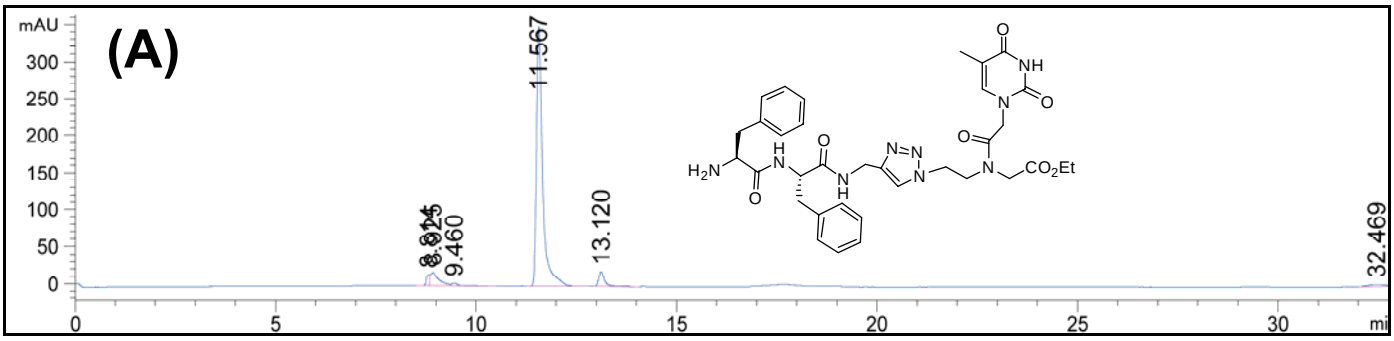

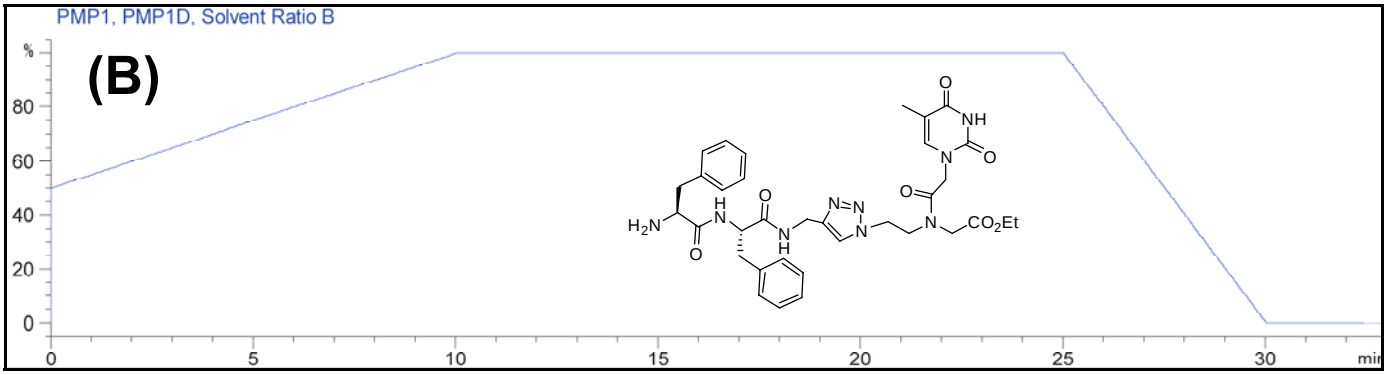

Solvent gradient with respect to **solvent B**

[**Solvent A:** 95% water, 4.5% acetonitrile, 0.5% TFA; **Solvent B:** 49.5% water, 50% acetonitrile, 0.5% TFA]

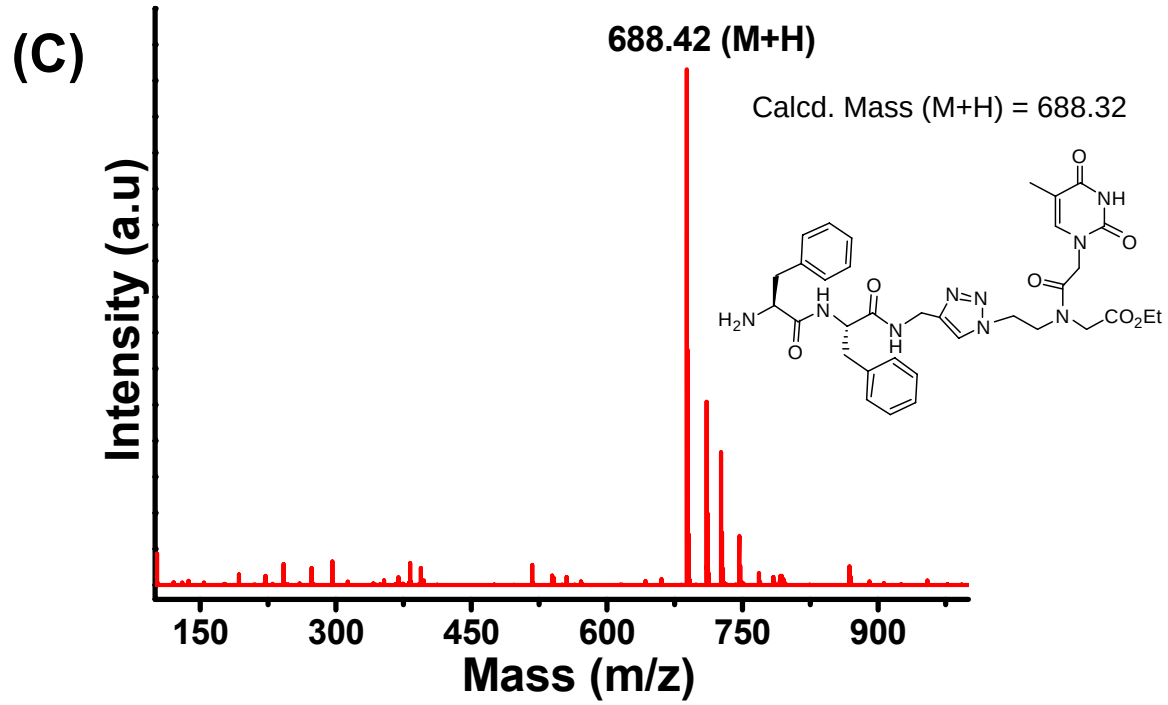

Figure S63: (A) HPLC Trace; (B) solvent gradient and (C) MALDI Mass for purified peptide **7d**.

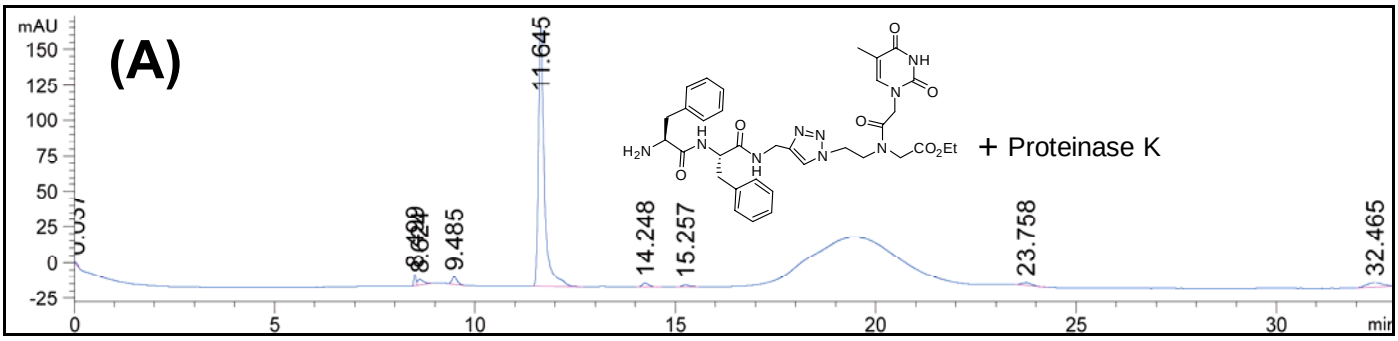

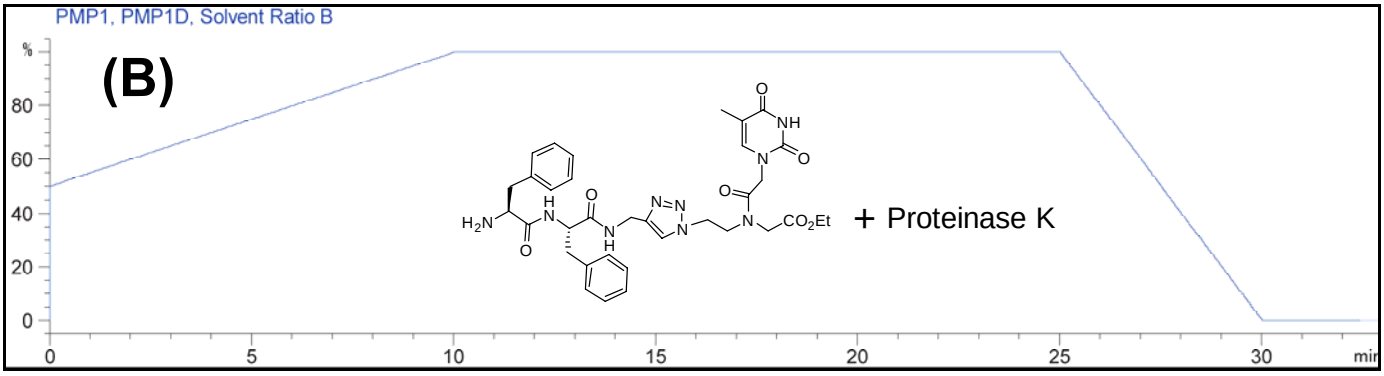

Solvent gradient with respect to **solvent B**

[**Solvent A:** 95% water, 4.5% acetonitrile, 0.5% TFA; **Solvent B:** 49.5% water, 50% acetonitrile, 0.5% TFA]

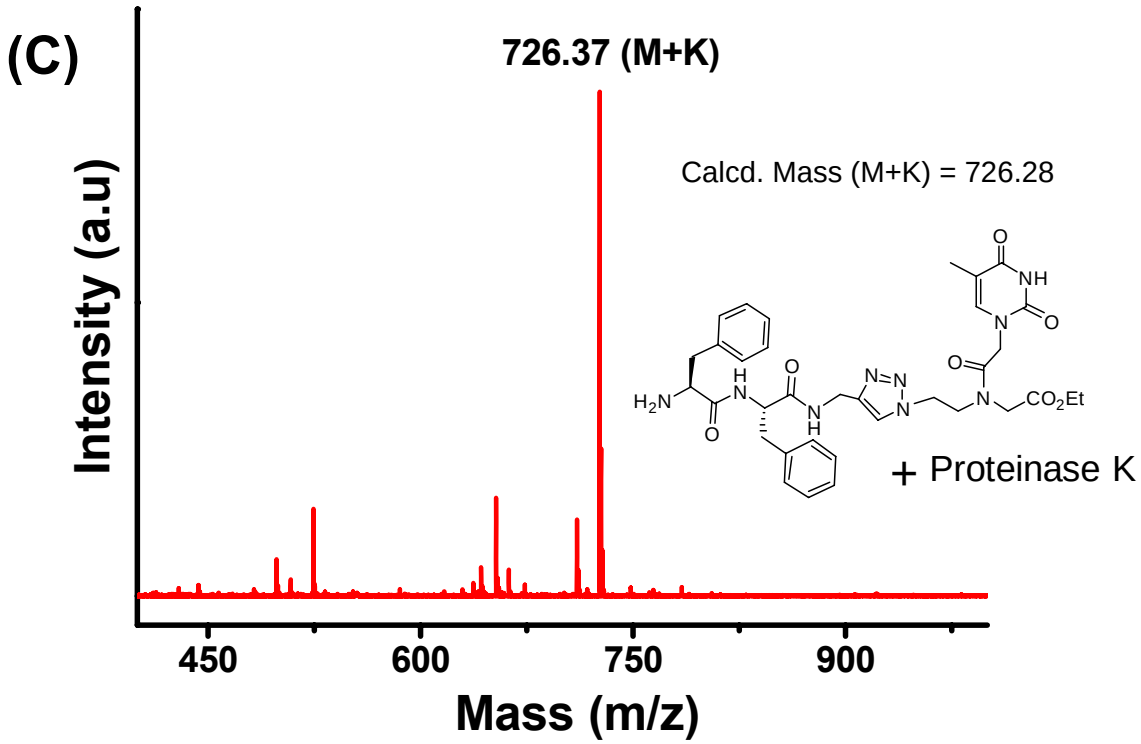

Figure S64: (A) HPLC Trace; (B) solvent gradient and (C) MALDI Mass for proteinase K incubated peptide **7d**

To examine the proteolytic stability, nucleopeptides **3c** (Boc-Phe-Phe-*am*-G^{NHiBu}-*aeg*-OEt) and **6c** (Boc-Phe-Phe-*tz*-G^{NHiBu}-*aeg*-OEt) were incubated with another proteolytic enzyme Chymotrypsin in HEPES buffer at physiological temperature (35 °C) and pH (7.5) following the literature procedure[5]. Then, mass spectra were taken at different time intervals to monitor if there is any change in the mass spectrum. No change of the mass spectrum was observed even after 24 h of incubation.

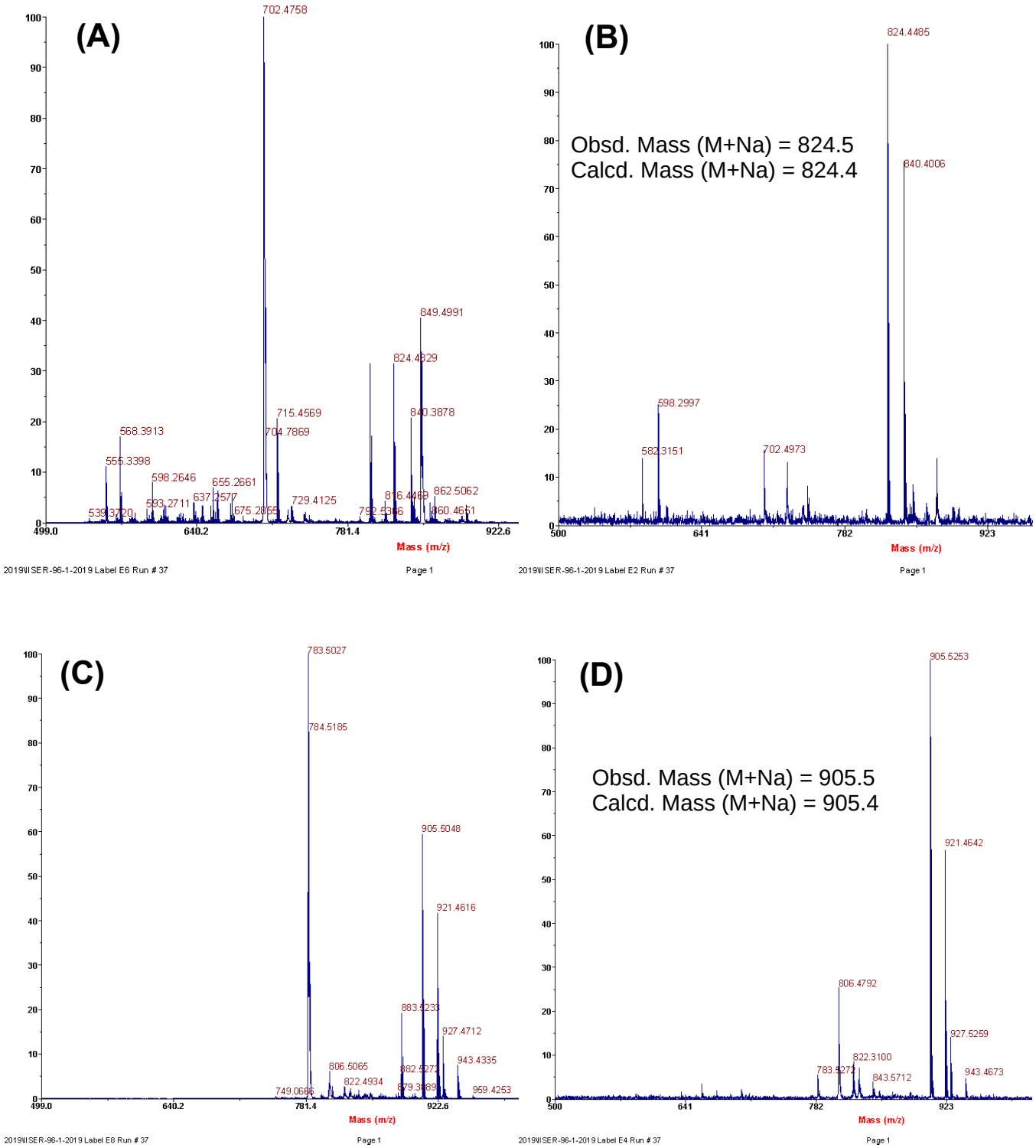

Figure S65: MALDI Mass for Chymotrypsin incubated peptide **3c** (A, B) and **6c** (C, D) after 12 h and 24 h respectively.

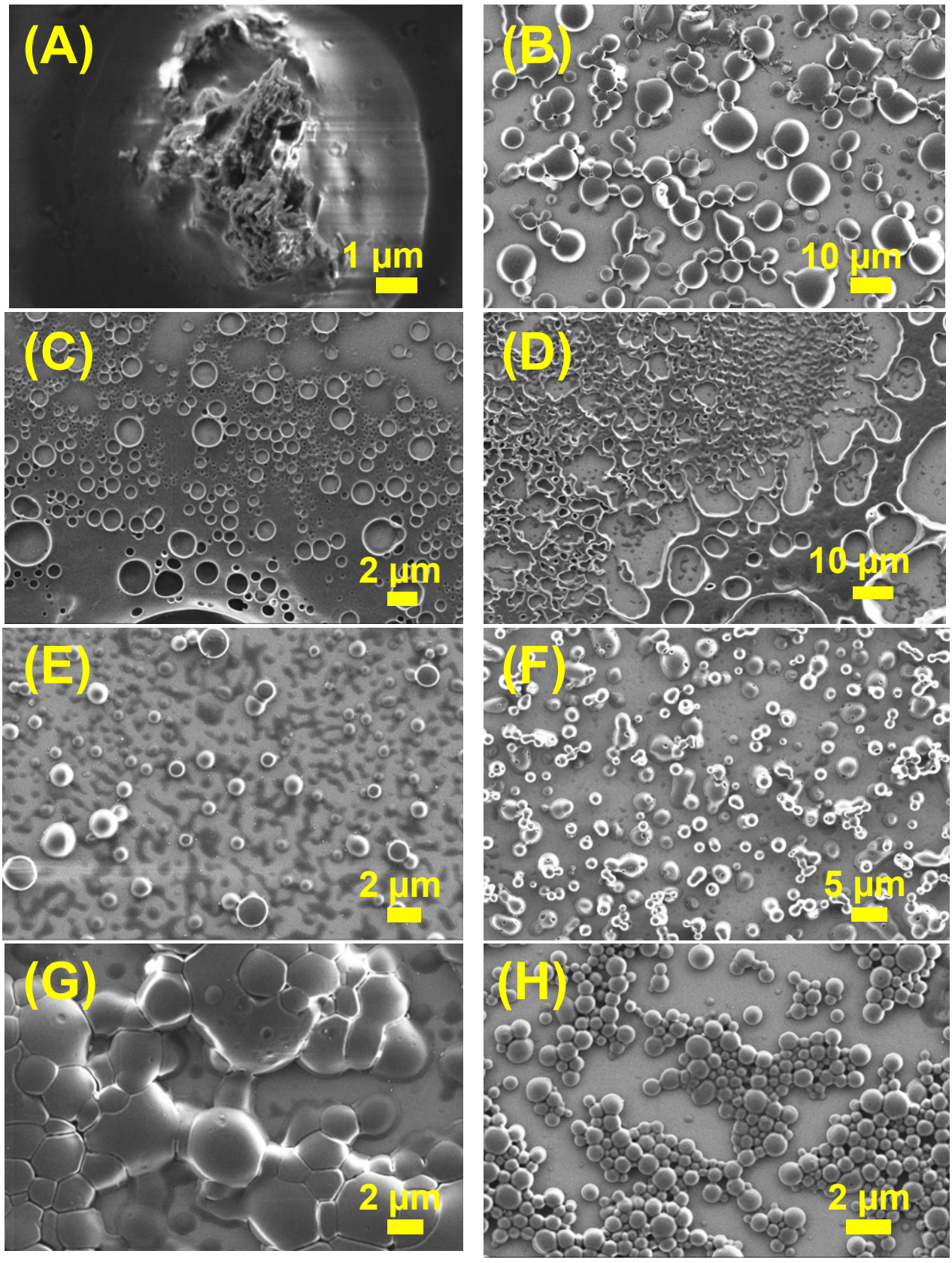

Figure S66: Solvent dependent morphology in SEM images of peptide **6a** (Boc-Phe-Phe-*tz*-$A^{N(Boc)_2}$-*aeg*-OEt): (A) in THF, (B) in MeOH, (C) in $CHCl_3$, (D) in DCM, (E) in 1:1 HFIP and water, (F) in 1:1 MeOH and water, (G) in 1:1 $CHCl_3$ and MeOH, and (H) in 1:1 THF and water.

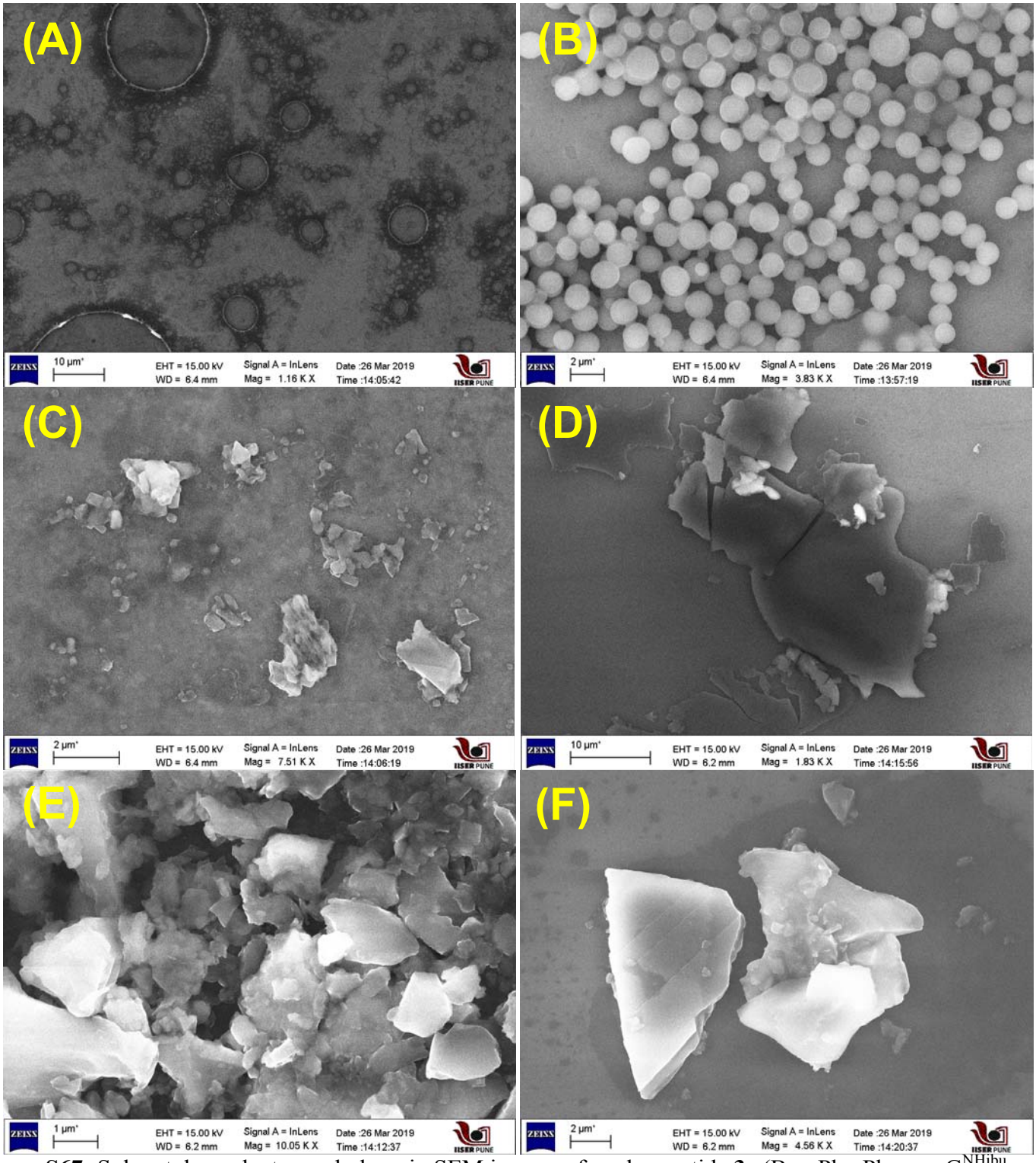

Figure S67: Solvent dependent morphology in SEM images of nucleopeptide **3c** (Boc-Phe-Phe-*am*-G^{NHibu}-*aeg*-OEt) in (A) THF, (B) MeOH, (C) $CHCl_3$, and **7d** (Boc-Phe-Phe-*am*-G^{NHibu}-*aeg*-OEt) in (D) THF, (E) MeOH and (F) $CHCl_3$.

- *SEM images clearly shows that only in presence of MeOH (which was not anhydrous) ordered spherical morphology was exhibited by nucleopeptide* **3c**. *Other neat solvents failed to produce good self-assembled morphologies*

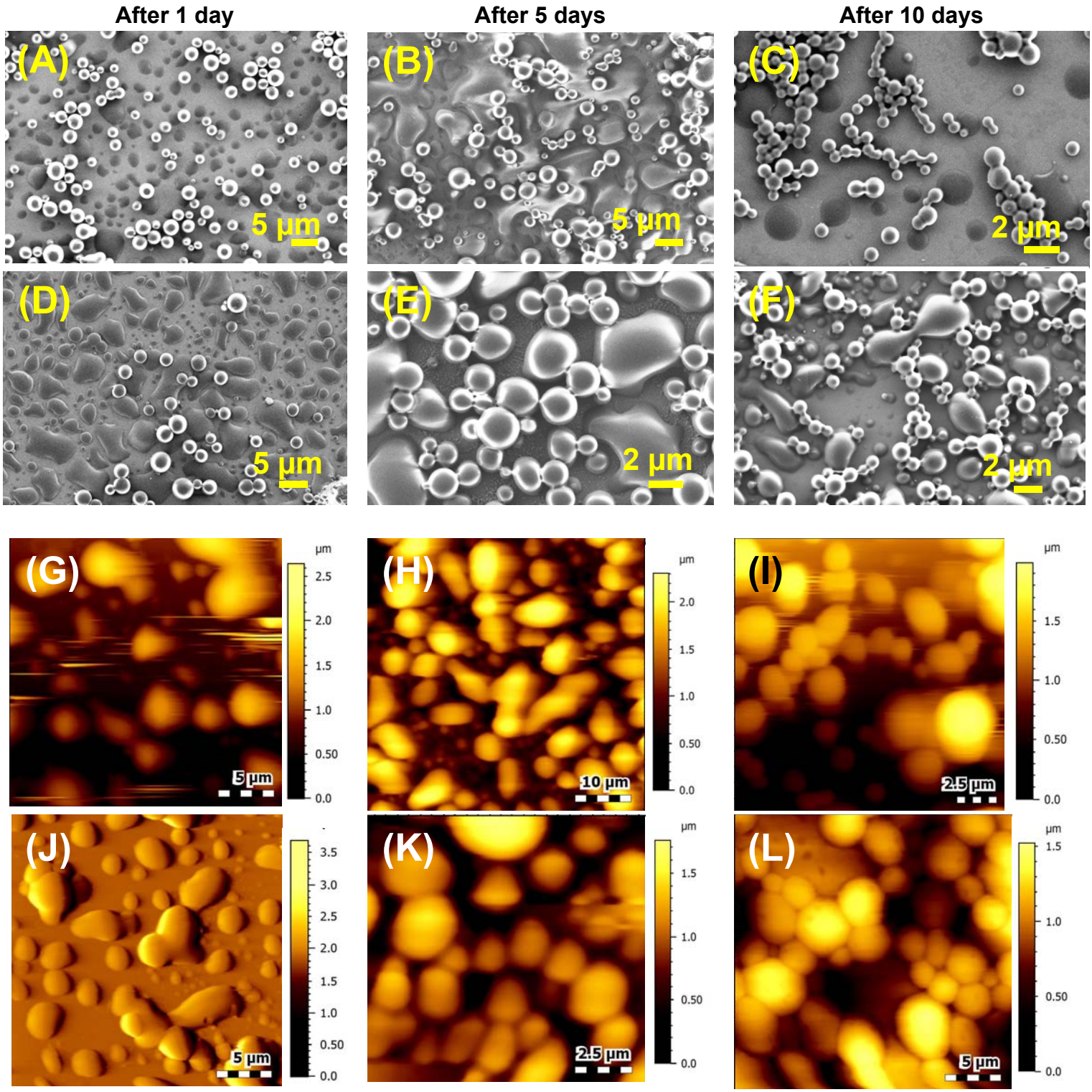

Figure S68: Time dependent morphologies observed through SEM for nucleopeptide **6a** (Boc-Phe-Phe-*tz*-$A^{N(Boc)_2}$-*aeg*-OEt) (FigA-C), **6b** (Boc-Phe-Phe-*tz*-A^{NHCbz}-*aeg*-OEt) (FigD-F) and AFM for nucleopeptide **6a** (Boc-Phe-Phe-*tz*-$A^{N(Boc)_2}$-*aeg*-OEt) (FigG-I), **6b** (Boc-Phe-Phe-*tz*-A^{NHCbz}-*aeg*-OEt) (FigJ-L) respectively.

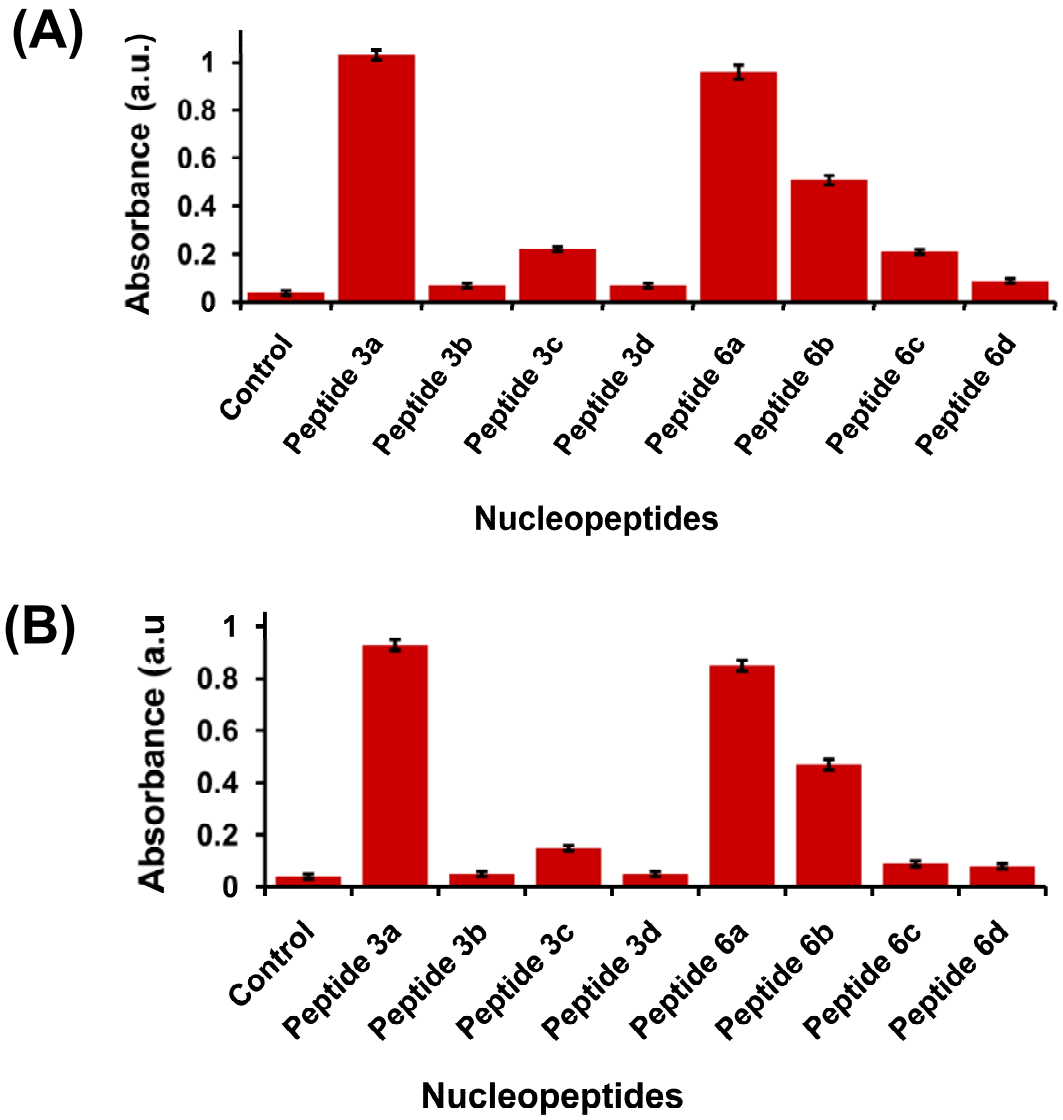

Figure S69: Absorbance values measured from turbidity assay of nucleopeptides at (A) 405 nm and (B) 570 nm.

Table S2: Absorbance of nucleopeptides observed in turbidity assay at 405 and 570 nm

Nucleopeptides	Abs. in turbidity assay at 405 nm[a]	Abs. in turbidity assay at 570 nm[a]
Peptide **3a** Boc-Phe-Phe-*am*-A^{NHCbz}-*aeg*-OEt	1.03 ± 0.02	0.93 ± 0.02
Peptide **3b** Boc-Phe-Phe-*am*-6-Cl-G^{NHiBu}-*aeg*-OEt	0.07 ± 0.01	0.05 ± 0.01
Peptide **3c** Boc-Phe-Phe-*am*-G^{NHiBu}-*aeg*-OEt	0.22 ± 0.01	0.15 ± 0.01
Peptide **3d** Boc-Phe-Phe-*am*-T-*aeg*-OEt	0.07 ± 0.01	0.05 ± 0.01
Peptide **6a** Boc-Phe-Phe-*tz*-A$^{N(Boc)_2}$-*aeg*-OEt	0.96 ± 0.03	0.85 ± 0.02
Peptide **6b** Boc-Phe-Phe-*tz*-A^{NHCbz}-*aeg*-OEt	0.51 ± 0.02	0.47 ± 0.02
Peptide **6c** Boc-Phe-Phe-*tz*-G^{NHiBu}-*aeg*-OEt	0.21 ± 0.01	0.09 ± 0.01
Peptide **6d** Boc-Phe-Phe-*tz*-T-*aeg*-OEt	0.09 ± 0.01	0.08 ± 0.01
Control	0.04 ± 0.01	0.04 ± 0.01

[a]Data are the mean ± SD (n=4)

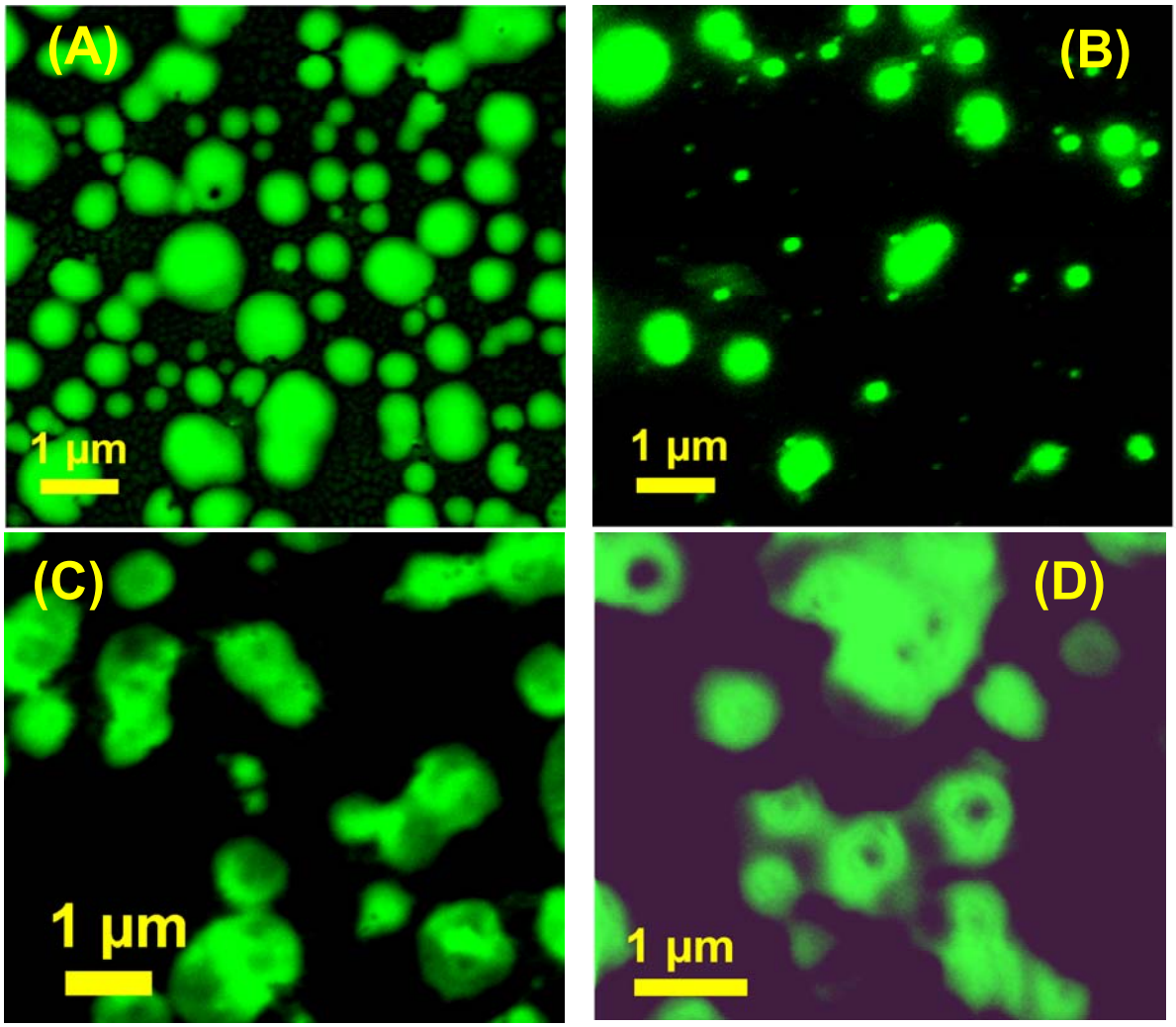

Figure S70: Confocal microscope images of fluorescent dye encapsulated nucleopeptide (A) **6a** (Boc-Phe-Phe-*tz*-$A^{N(Boc)_2}$-*aeg*-OEt), (B) **6b** (Boc-Phe-Phe-*tz*-A^{NHCbz}-*aeg*-OEt), (C) **6c** (Boc-Phe-Phe-*tz*-G^{NHiBu}-*aeg*-OEt) and (D) **6d** (Boc-Phe-Phe-*tz*-T-*aeg*-OEt).

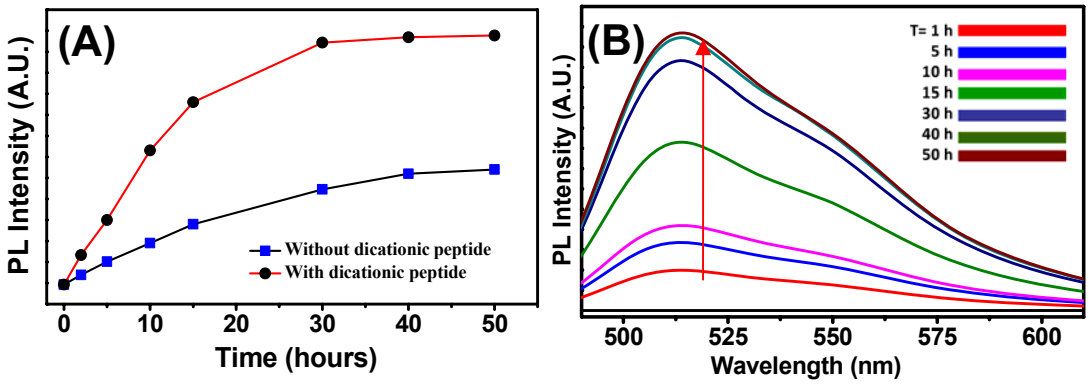

Figure S71: The increasing fluorescence intensity of the solution outside the dialysis tube containing **CF** encapsulated peptide **6a** (Boc-Phe-Phe-*tz*-$A^{N(Boc)_2}$-*aeg*-OEt), after the addition of 3 eq. of (A) dicationic peptide (Boc-Lys-Lys-OMe) into dialysis tube. (B) Fluorescence emission spectra of carboxyfluorescein showing increasing intensity after the addition of dicationic peptide into **CF** encapsulated peptide **6a** (Boc-Phe-Phe-*tz*-$A^{N(Boc)_2}$-*aeg*-OEt) (at 517 nm, $\lambda_{ex} = 417$nm).

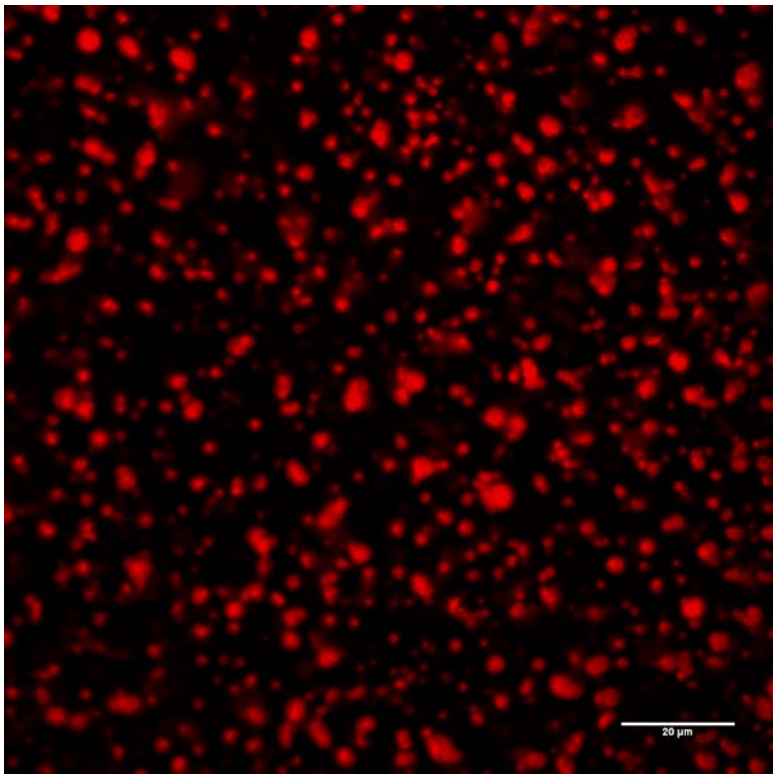

Figure S72: Confocal microscope images of fluorescent drug doxorubicin encapsulated nucleopeptide **6a** (Boc-Phe-Phe-*tz*-A$^{N(Boc)_2}$-*aeg*-OEt) (emission at 590 nm, λex = 485 nm).

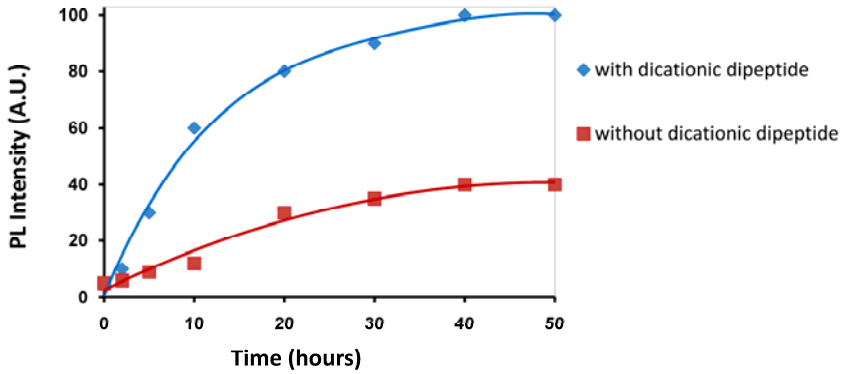

Figure S73: The increasing fluorescence intensity of the solution outside the dialysis tube containing Doxorubicin encapsulated peptide **6a** (Boc-Phe-Phe-*tz*-A$^{N(Boc)_2}$-*aeg*-OEt), after the addition of 3 eq. of dicationic peptide (Boc-Lys-Lys-OMe) into dialysis tube (emission at 595 nm, λex = 480 nm).

Cyclic voltammetry:

Electrochemical Analysis was done in the Biologic VMP3 multichannel potentiostat. A standard three-electrode cell consisting of a Toray carbon Paper having 1 cm^2 as the working electrode, Ag/AgCl (sat. KCl) as the reference electrode and a Pt foil as the counter electrode were used for electrochemical measurements. The solution were purged with Ar during the experiments. The potential values are in volt (V) vs. Ag/AgCl scale. The electrolyte was a standard inorganic solution of 0.1M Potassium Phosphate Buffer electrolytes at pH=7.4 and 0.1M KCl. All working electrodes had an identical geometric area of 1.00 cm^2. The capacitance was evaluated from experimental cyclic voltammetric profile, according to the following equation:

$$C = \frac{A_T / 2}{\Delta V \times V_{SR} \times A_e}$$

C = Total capacitance in millifarad per cm^2(or in mF / cm^2)
A_T = Total area under the curve of cyclic voltammetry in milliampere (or in mA)
V_{SR} = Scan rate (50 mV/s)
A_e = Area of the toray carbon paper electrode (1 cm^2)
ΔV = Potential window (-0.300 V to 0.900 V *i.e.* [0.900 + 0.300] V = 1.2 V)

All solutions were prepared using triply distilled water and the cell temperature was maintained at 27 °C. Currents are normalized with respect to geometric area (1 cm^2). All the electrolytic solutions were prepared by 0.1M Potassium Phosphate Buffer electrolytes at pH=7.4 and 0.1M KCl. Working electrodes were made by drop casting a suspension of those peptides (2 mg/400 µL in a 10 wt% aqueous dispersion of PTFE) on a Toray carbon paper electrode.

Table S3: Capacitance values of peptide modified Torey carbon electrodes

Peptides used for electrode modification	Capacitance (µF/cm^2)
Boc-Phe-Phe-*tz*-$A^{N(Boc)_2}$-aeg-OEt (**6a**)	260.0
Boc-Phe-Phe-*tz*-A^{NHCbz}-aeg-OEt (**6b**)	205.8
Boc-Phe-Phe-*tz*-G^{NHiBu}-aeg-OEt (**6c**)	617.0
Boc-Phe-Phe-*tz*-T-aeg-OEt (**6d**)	342.0
Boc-Phe-Phe-*tz*-aeg-OEt (**9**)	500.0
None (unmodified electrode)	90.0

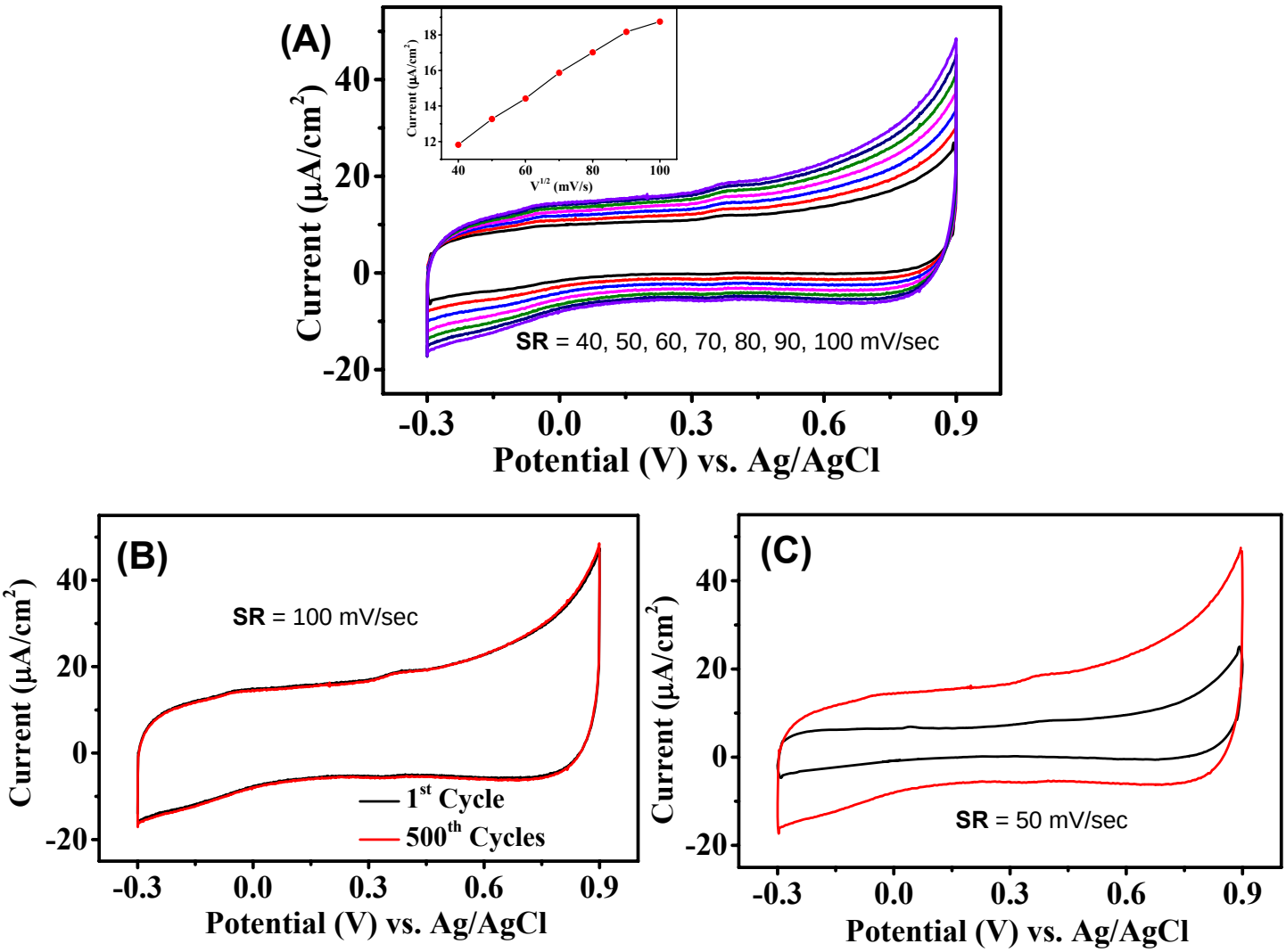

Figure S74: Cyclic voltammograms of peptide **6a** (Boc-Phe-Phe-*tz*-$A^{N(Boc)_2}$-aeg-OEt) supported Toray Carbon electrode in 0.1M potassium phosphate buffer electrolytes at pH=7.4 and 0.1M KCl (A) at different scan rate from 40 mV/s to 100mV/s; **Inset:** Scan rate effect at different scan rate from 40 mV/s to 100mV/s; (B) at a scan rate of 50mV/s of 1st and 500th cycles; (C) at a scan rate of 50 mV/s compared to bare electrode.

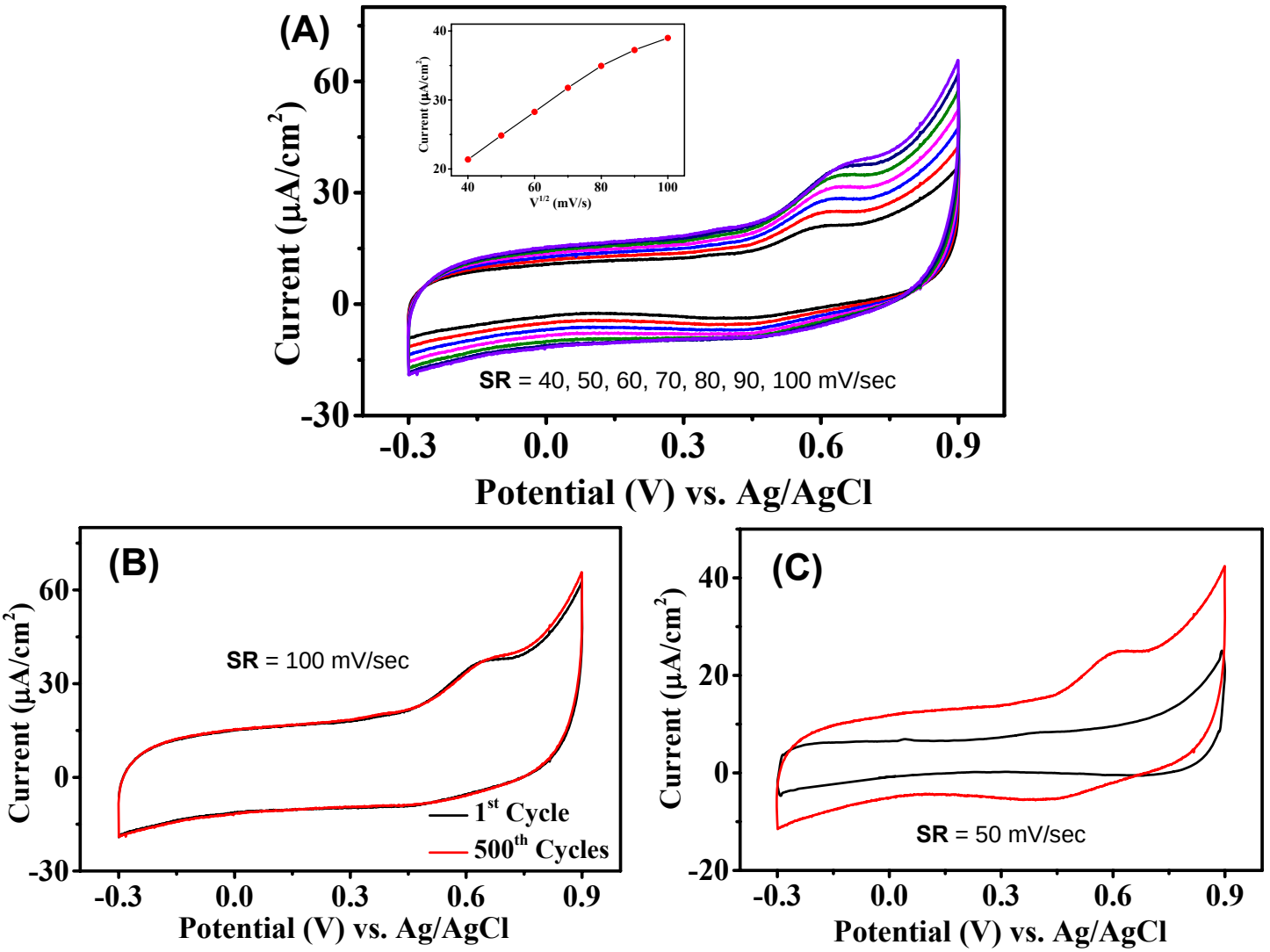

Figure S75: Cyclic voltammograms of peptide **6b** (Boc-Phe-Phe-*tz*-A^{NHCbz}-aeg-OEt) supported Toray Carbon electrode in 0.1M potassium phosphate buffer electrolytes at pH=7.4 and 0.1M KCl (A) at different scan rate from 40 mV/s to 100mV/s; **Inset:** Scan rate effect at different scan rate from 40 mV/s to 100mV/s; (B) at a scan rate of 50mV/s of 1st and 500th cycles; (C) at a scan rate (SR) of 50 mV/s compared to bare electrode.

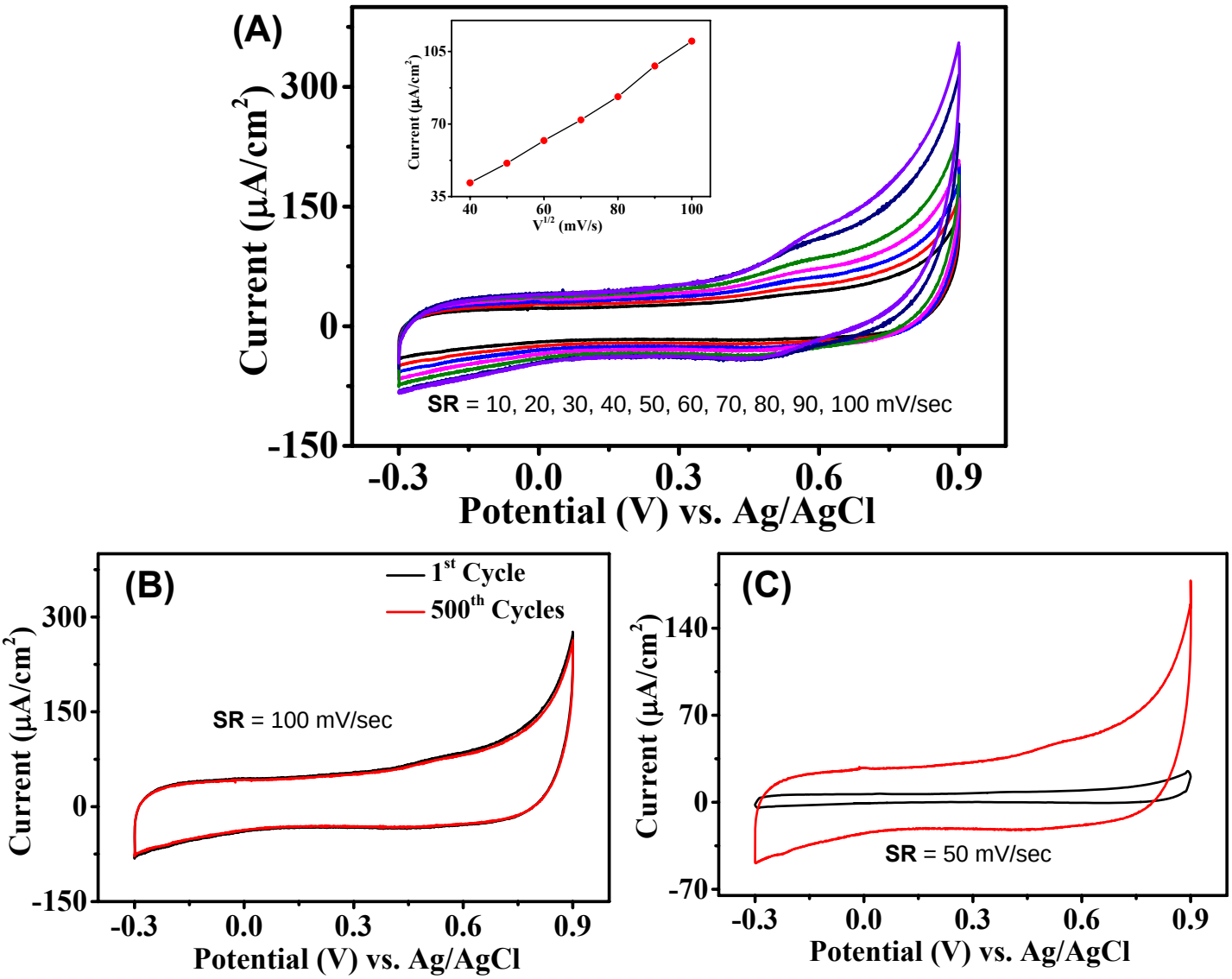

Figure S76: Cyclic voltammograms of peptide **6c** (Boc-Phe-Phe-*tz*-G^{NHiBu}-aeg-OEt) supported Toray Carbon electrode in 0.1M potassium phosphate buffer electrolytes at pH=7.4 and 0.1M KCl (A) at different scan rate from 10 mV/s to 100mV/s; **Inset:** Scan rate effect at different scan rate from 10 mV/s to 100mV/s; (B) at a scan rate of 50mV/s of 1st and 500th cycles; (C) at a scan rate of 50 mV/s compared to bare electrode.

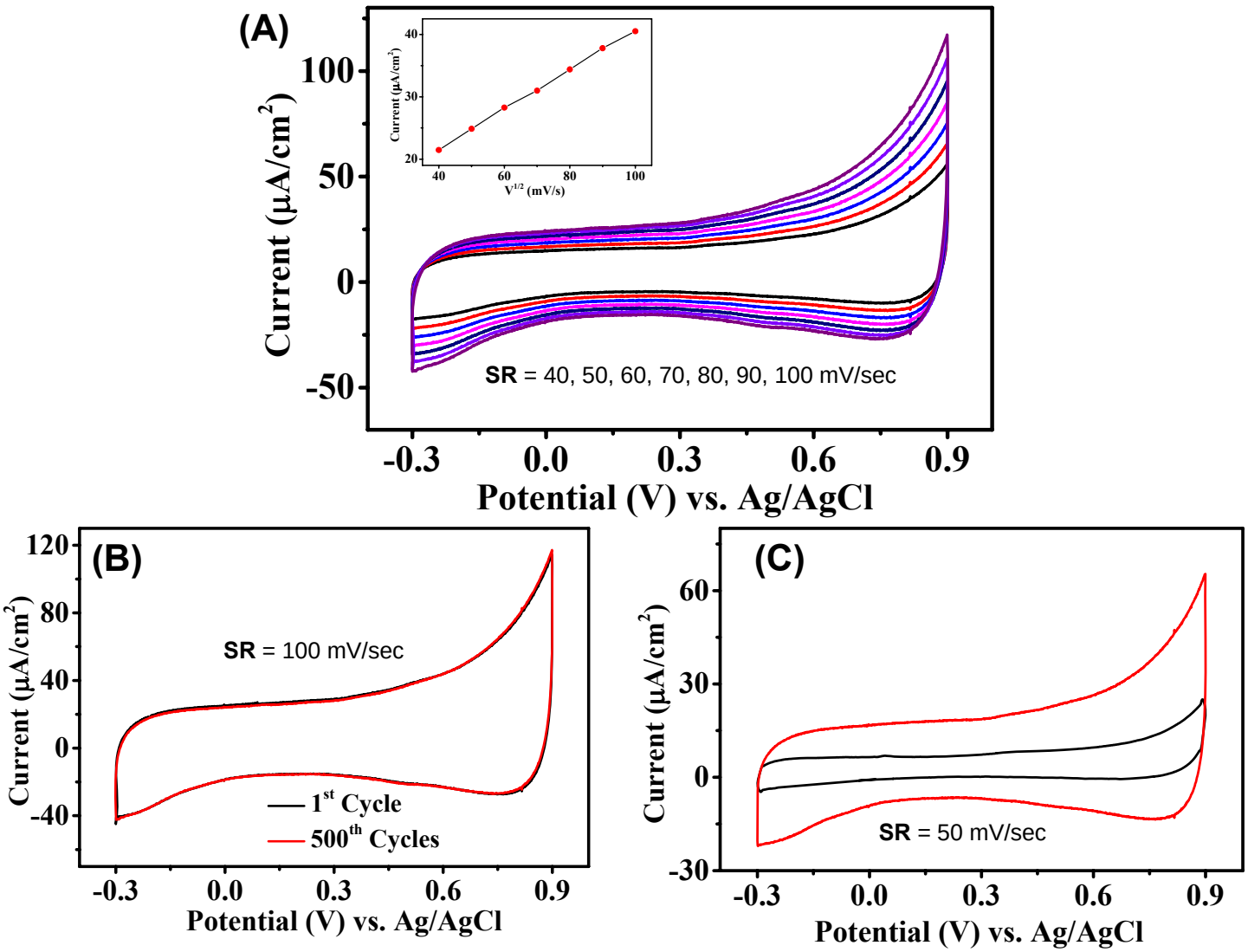

Figure S77: Cyclic voltammograms of peptide **6d** (Boc-Phe-Phe-*tz*-T-aeg-OEt) supported Toray Carbon electrode in 0.1M potassium phosphate buffer electrolytes at pH=7.4 and 0.1M KCl (A) at different scan rate from 40 mV/s to 100mV/s; **Inset:** Scan rate effect at different scan rate from 40 mV/s to 100mV/s; (B) at a scan rate of 50mV/s of 1st and 500th cycles; (C) at a scan rate of 50 mV/s compared to bare electrode.

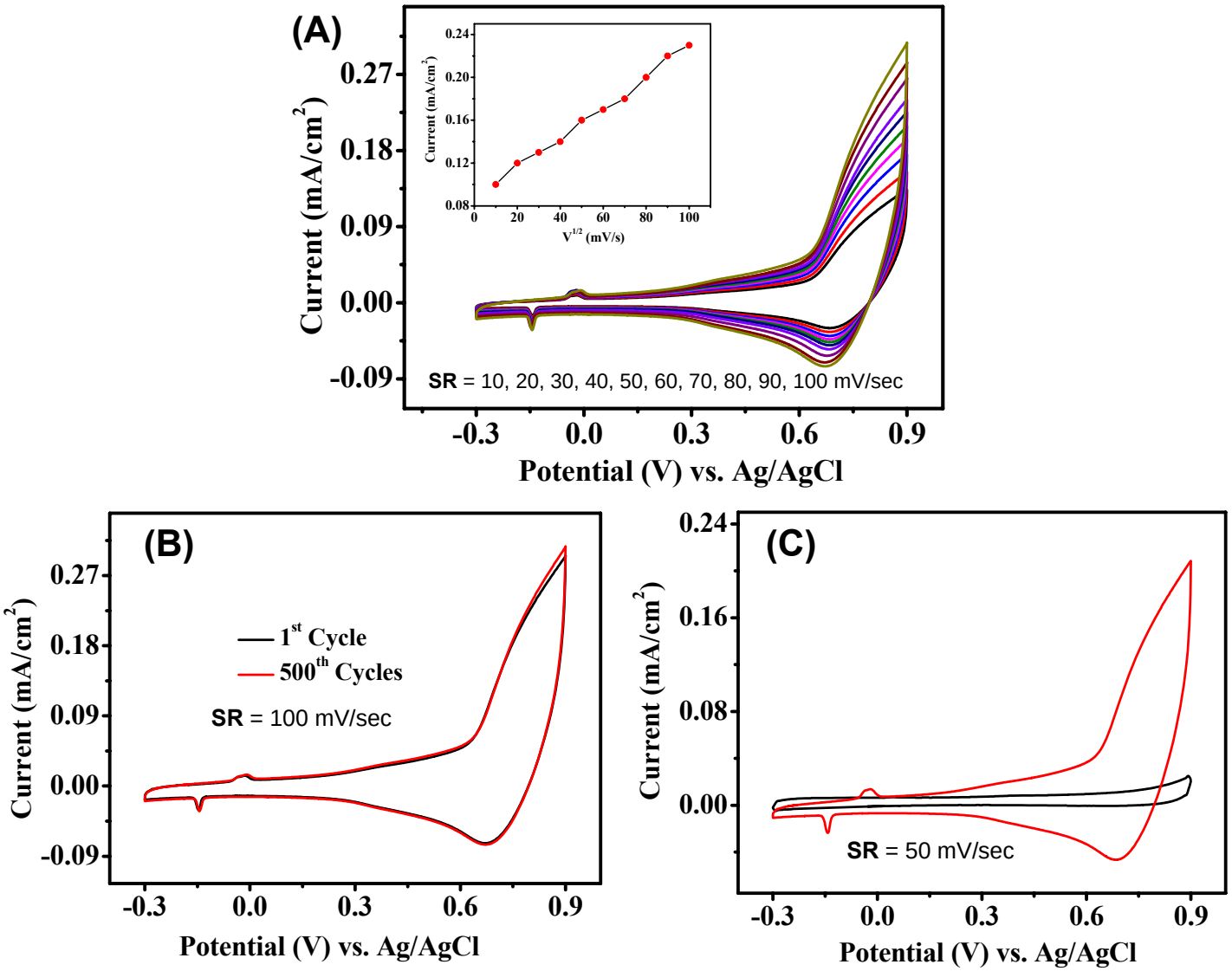

Figure S78: Cyclic voltammograms of peptide **9** (Boc-Phe-Phe-*tz*-aeg-OEt) supported Toray Carbon electrode in 0.1M potassium phosphate buffer electrolytes at pH=7.4 and 0.1M KCl (A) at different scan rate from 10 mV/s to 100mV/s; **Inset:** Scan rate effect at different scan rate from 10 mV/s to 100mV/s; (B) at a scan rate of 50mV/s of 1st and 500th cycles; (C) at a scan rate of 50 mV/s compared to bare electrode.

References:

1. Meltzer, P. C.; Liang A. Y.; Matsudaira, P. Peptide Nucleic Acids: Synthesis of Thymine, Adenine, Guanine, and Cytosine Nucleobases. *J. Org. Chem.* **1995**, *60*, 4305-4308.

2. Efthymiou, T. C.; Desaulniers, J-P. Synthesis and properties of oligonucleotides that contain a triazole-linked nucleic acid dimer. *J. Heterocyclic Chem*. **2011**, *48*, 533-539.

3. Englund, E. A.; Xu, Q.; Witschi, M. A.; Appella, D. H. PNA-DNA Duplexes, Triplexes, and Quadruplexes Are Stabilized with trans-Cyclopentane Units. *J. Am. Chem. Soc*. **2006**, *128*, 16456-16457.

4. Datta, D.; Tiwari, O.; Ganesh, K. N. New archetypes in self-assembled Phe-Phe motif induced nanostructures from nucleoside conjugated-diphenylalanines. *Nanoscale* **2018**, *10*, 3212-3224.

5. Baral, A.; Roy, S.; Ghosh, S.; Hermida-Merino, D.; Hamley, I. W.; Banerjee, A. A Peptide-Based Mechanosensitive, Proteolytically Stable Hydrogel with Remarkable Antibacterial Properties. *Langmuir* **2016**, *32*, 1836-1845.